

UNCLASSIFIED

AD NUMBER
AD901844
NEW LIMITATION CHANGE
TO Approved for public release, distribution unlimited
FROM Distribution authorized to U.S. Gov't. agencies only; Test and Evaluation; MAY 1972. Other requests shall be referred to Air Force Avionics Lab., Wright-Patterson AFB, OH 45433.
AUTHORITY
AFAL ltr, 6 Mar 1975

THIS PAGE IS UNCLASSIFIED

THIS REPORT HAS BEEN DELIMITED
AND CLEARED FOR PUBLIC RELEASE
UNDER DOD DIRECTIVE 5200.20 AND
NO RESTRICTIONS ARE IMPOSED UPON
ITS USE AND DISCLOSURE.

DISTRIBUTION STATEMENT A

APPROVED FOR PUBLIC RELEASE;
DISTRIBUTION UNLIMITED.

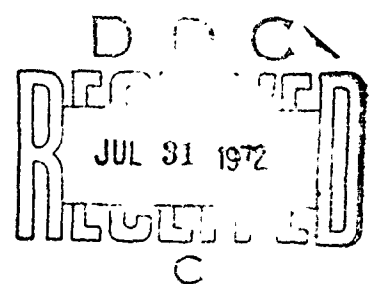
DICHROIC PARAMETRIC MIRROR TECHNIQUES

E. O. Ammann

GTE Sylvania Inc.

TECHNICAL REPORT AFAL-TR-72-177

May 1972



Distribution limited to U. S. Government agencies only: test and evaluation; May 1972. Other requests for this document must be referred to AFAL/TEO, Wright-Patterson AFB, Ohio 45433.

Air Force Avionics Laboratory

Air Force Systems Command

Wright-Patterson Air Force Base, Ohio 45433

AD901844

NOTICE

When Government drawings, specifications, or other data are used for any purpose other than in connection with a definitely related Government procurement operation, the United States Government thereby incurs no responsibility nor any obligation whatsoever; and the fact that the government may have formulated, furnished, or in any way supplied the said drawings, specifications, or other data, is not to be regarded by implication or otherwise as in any manner licensing the holder or any other person or corporation, or conveying any rights or permission to manufacture, use, or sell any patented invention that may in any way be related thereto.

Copies of this report should not be returned unless return is required by security considerations, contractual obligations, or notice on a specific document.

DICHROIC PARAMETRIC MIRROR TECHNIQUES

E. O. Ammann

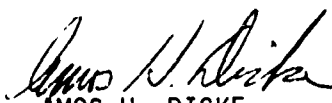
Distribution limited to U. S. Government agencies only; test and evaluation; May 1972. Other requests for this document must be referred to AFAL/TEO, Wright-Patterson AFB, Ohio 45433.

FOREWORD

N/k
This report summarizes the twelve months of work performed on Air Force Contract F33615-71-C-1403 entitled "Dichroic Parametric Mirror Techniques". This work was done on Project Number 6100 under Task number 03. The goal of this work has been to develop and test mirrors which are suitable for use with optical parametric oscillators operating in the region from 1.5 to 4.5 microns. The work which is summarized in this report covers the period from 1 April 1971 through 31 March 1972. This report was prepared by the Electro-Optics Organization of GTE Sylvania Inc., Electronic Systems Group - Western Division, Mountain View, California, and describes work performed in the Research and Development Department headed by Dr. L. M. Osterink. Dr. E. O. Ammann was the principal technical investigator on this program; other contributors include Mr. J. D. Wintemute and Dr. J. M. Yarborough. Technical assistance was provided by Mr. J. D. Wintemute.

The work performed under this contract is administered by the Air Force Avionics Laboratory, Air Force Systems Command, Wright-Patterson Air Force Base, Ohio. Mr. Elgene R. Nichols (AFAL/TEO) is the technical representative on this program for the Avionics Laboratory. This report was submitted by the author in May 1972.

This technical report has been reviewed and is approved for publication.



AMOS H. DICKE
CHIEF, Electro Optics Device Branch
Electronic Technology Division
AF Avionics Laboratory

ABSTRACT

This report summarizes the results of a twelve-month program whose goal was to develop mirrors which are suitable for use with optical parametric oscillators having outputs in the 1.5 to 4.5 micron region. The properties which such mirrors must have are: (1) low scatter; (2) the correct spectral reflectances at signal, idler, and pump wavelengths; and (3) high resistance to optical damage. The mirrors which were studied on this program were designed for use with a lithium niobate parametric oscillator which is pumped by 1.08 microns. Several different types of multilayer coatings were fabricated and tested. These were ZnS-ThF₄, ZnS-ThF₄ overcoated with Al₂O₃, ZnS-cryolite, ZnS-cryolite overcoated with Al₂O₃, ZnS-ThF₄ undercoated and overcoated with Al₂O₃, and a "hard coating" of unknown composition. The tests which were performed on each coating included (1) microscopic inspection to determine scatter properties, (2) spectrophotometer traces to determine spectral transmittance, (3) 1.08 micron damage threshold tests, and (4) operation of an optical parametric oscillator using the coatings. Best overall results were obtained with mirrors composed of ZnS-ThF₄ undercoated and overcoated with Al₂O₃. Measurements were also performed to determine the surface-damage thresholds of uncoated and coated lithium niobate; it was found that both soft (e.g. ZnS, ThF₄, cryolite, etc.) and hard (e.g. Al₂O₃) coatings raise this threshold, with the greatest improvement effected by the Al₂O₃ coating.

Table of Contents

<u>Section</u>	<u>Title</u>	<u>Page</u>
I	INTRODUCTION	1
II	COATING MATERIALS AND MIRROR DESIGNS EMPLOYED	9
	2.1 COATING MATERIALS	9
	2.1.1 ZnS-ThF ₄	9
	2.1.2 ZnS-Cryolite	10
	2.1.3 Mirrors with Al ₂ O ₃ Overcoatings	10
	2.1.4 Mirrors with Al ₂ O ₃ Undercoatings and Overcoatings	11
	2.1.5 Spectrum Systems Coatings	11
	2.2 MIRROR SUBSTRATES	12
	2.2.1 Fused Quartz Mirror Substrates	12
	2.2.2 Lithium Niobate Disks	13
	2.2.3 Lithium Niobate Oscillator Crystals	13
	2.3 MIRROR DESIGNS	15
	2.3.1 Mirror Coating Type #1	16
	2.3.2 Mirror Coating Type #2	17
	2.3.3 Mirror Coating Type #3	18
III	COATING AND TESTING PROCEDURES	21
	3.1 COATING TECHNIQUES AND APPARATUS	21
	3.2 SCATTER EVALUATION	21
	3.3 SPECTRAL TRANSMITTANCE EVALUATION	24
	3.4 DAMAGE THRESHOLD EVALUATION	25
IV	SCATTER CHARACTERISTICS OF FABRICATED MIRRORS	31
	4.1 TECHNIQUES USED TO OBTAIN LOW-SCATTER COATINGS	31
	4.2 RESULTS OF SCATTER TESTS	33
	4.3 COATING SCATTER CAUSED BY THE PYROELECTRIC EFFECT	38
V	SPECTRAL TRANSMITTANCES OF FABRICATED MIRRORS	49
	5.1 MIRROR COATING TYPES #1 AND #2	49
	5.1.1 ZnS-ThF ₄ Mirrors	49
	5.1.2 ZnS-ThF ₄ Overcoated with Al ₂ O ₃	54
	5.1.3 ZnS-Cryolite Mirrors	54
	5.1.4 ZnS-Cryolite Overcoated with Al ₂ O ₃	54
	5.1.5 ZnS-ThF ₄ Undercoated and Overcoated with Al ₂ O ₃	67
	5.1.6 Spectrum Systems Coatings	67

<u>Section</u>	<u>Title</u>	<u>Page</u>
	5.2 MIRROR COATING TYPE #3	67
	5.3 GENERAL OBSERVATIONS	76
VI	DAMAGE MEASUREMENTS ON FABRICATED MIRRORS	81
	6.1 TYPES OF DAMAGE ENCOUNTERED	81
	6.2 LITHIUM NIOBATE DAMAGE LEVELS	83
	6.3 THE CAUSE OF SMALL-SPOT DAMAGE	86
	6.4 COATING DAMAGE LEVELS	89
VII	OPTICAL PARAMETRIC OSCILLATOR EXPERIMENTS	93
	7.1 2.16 MICRON OSCILLATOR EXPERIMENTS	93
	7.2 3 TO 4 MICRON OSCILLATOR EXPERIMENTS	98
VIII	SUMMARY AND RECOMMENDATIONS FOR FURTHER WORK	103
REFERENCES		109

LIST OF ILLUSTRATIONS

<u>Figure No.</u>	<u>Caption</u>	<u>Page</u>
1	External Optical Parametric Oscillator	5
2	Internal Optical Parametric Oscillator	7
3	Lithium niobate and fused quartz substrates used on this program.	14
4	Parametric oscillator resonators for (a) external oscillator and (b) internal oscillator	15
5	Design used for ZnS-ThF ₄ highly reflecting mirrors	17
6	Design used for ZnS-ThF ₄ partially transmitting mirrors	17
7	Design used for doubly-resonant ZnS-ThF ₄ mirrors	20
8	Evaporator used for low-temperature materials such as ZnS, ThF ₄ , and cryolite	22
9	Evaporator with electron-gun source for evaporating high- temperature materials	22
10	Leitz Ortholux Polarizing Microscope	23
11	Technique for Determining Scatter Losses from Coated Crystals and Substrates	25
12	Perkin-Elmer Model 137G Spectrophotometer	26
13	Test setup used for coating-damage threshold measurements	27
14	Specimen holder for coating damage tests	29
15	Scatter characteristics (magnification 20) of 2 micron HR mirrors fabricated by (a) Lambda (ZnS-ThF ₄), (b) Lambda (ZnS-ThF ₄ overcoated), (c) Lambda (ZnS-cryolite), (d) Lambda (ZnS-cryolite overcoated), (e) ZnS-ThF ₄ undercoated and overcoated, (f) Spectrum Systems, (g) Laser Optics, and (h) Valpey. All coatings are on fused quartz sub- strates.	34
16	Scatter characteristics (magnification 28) of Lambda 3.5 micron doubly-resonant ZnS-ThF ₄ mirrors.	36
17	Thick layer of (a) ZnS and (b) ThF ₄ on fused quartz substrates. Both layers are about 10 microns thick.	39

<u>Figure No.</u>	<u>Caption</u>	<u>Page</u>
18	Scatter present in ZnS-ThF ₄ coatings deposited on (a) fused quartz substrate, and (b) lithium niobate substrate	41
19	Scatter present in Spectrum Systems coatings deposited on (a) fused quartz substrate, and (b) lithium niobate substrate	42
20	Pyroelectric induced polarizations for lithium niobate crystals having (a) $\theta = 44^\circ$, and (b) $\theta = 90^\circ$	44
21	Pyroelectric induced polarizations for (a) lithium niobate with $\theta = 44^\circ$, and (b) fused quartz substrate	45
22	Pyroelectric induced polarizations for lithium niobate having $\theta = 44^\circ$ for three different mountings: (a) electrically insulating oven, (b) copper oven, but with the crystal protruding 1/8" beyond the end, and (c) copper oven with crystal flush to end.	46
23	Pyroelectric induced polarizations for lithium niobate having $\theta = 90^\circ$ for three different mountings: (a) electrically insulating oven, (b) copper oven, but with the crystal protruding 1/8" beyond the end, and (c) copper oven with crystal flush to end.	47
24 (a)	Measured spectral transmittance of ZnS-ThF ₄ mirror which is HR at 2.16 microns	50
24 (b)	Measured spectral transmittance of ZnS-ThF ₄ mirror which is HR at 2.16 microns	51
25 (a)	Measured spectral transmittance of ZnS-ThF ₄ mirror which is slightly transmitting at 2.16 microns	52
25 (b)	Measured spectral transmittance of ZnS-ThF ₄ mirror which is slightly transmitting at 2.16 microns	53
26 (a)	Comparison of spectral transmittances of ZnS-ThF ₄ mirrors with and without Al ₂ O ₃ overcoatings which are HR at 2.16 microns	55
26 (b)	Comparison of spectral transmittances of ZnS-ThF ₄ mirrors with and without Al ₂ O ₃ overcoatings which are HR at 2.16 microns.	56
27 (a)	Comparison of spectral transmittances of ZnS-ThF ₄ mirrors with and without Al ₂ O ₃ overcoatings which are slightly transmitting at 2.16 microns.	57

<u>Figure No.</u>	<u>Caption</u>	<u>Page</u>
27 (b)	Comparison of spectral transmittances of ZnS-ThF ₄ mirrors with and without Al ₂ O ₃ overcoatings which are slightly transmitting at 2.16 microns	58
28 (a)	Measured spectral transmittance of ZnS-cryolite mirror which is HR at 2.16 microns	59
28 (b)	Measured spectral transmittance of ZnS-cryolite mirror which is HR at 2.16 microns	60
29 (a)	Measured spectral transmittance of ZnS-cryolite mirror which is slightly transmitting at 2.16 microns	61
29 (b)	Measured spectral transmittance of ZnS-cryolite mirror which is slightly transmitting at 2.16 microns	62
30 (a)	Comparison of spectral transmittances of ZnS-cryolite mirrors with and without Al ₂ O ₃ overcoating which are HR at 2.16 microns	63
30 (l)	Comparison of spectral transmittances of ZnS-cryolite mirrors with and without Al ₂ O ₃ overcoating which are HR at 2.16 microns	64
31 (a)	Comparison of spectral transmittances of ZnS-cryolite mirrors with and without Al ₂ O ₃ overcoating which are slightly transmitting at 2.16 microns	65
31 (b)	Comparison of spectral transmittances of ZnS-cryolite mirrors with and without Al ₂ O ₃ overcoating which are slightly transmitting at 2.16 microns	66
32 (a)	Measured spectral transmittance of ZnS-ThF ₄ mirror undercoated and overcoated with Al ₂ O ₃ which is HR at 2.16 microns	68
32 (b)	Measured spectral transmittance of ZnS-ThF ₄ mirror undercoated and overcoated with Al ₂ O ₃ which is HR at 2.16 microns	69
33 (a)	Measured spectral transmittance of ZnS-ThF ₄ mirror undercoated and overcoated with Al ₂ O ₃ which is slightly transmitting at 2.16 microns	70
33 (b)	Measured spectral transmittance of ZnS-ThF ₄ mirror undercoated and overcoated with Al ₂ O ₃ which is slightly transmitting at 2.16 microns	71

<u>Figure No.</u>	<u>Caption</u>	<u>Page</u>
34 (a)	Measured spectral transmittance of Spectrum Systems mirror which is HR at 2.16 microns	72
34 (b)	Measured spectral transmittance of Spectrum Systems mirror which is HR at 2.16 microns	73
35 (a)	Measured spectral transmittance of Spectrum Systems mirror which is slightly transmitting at 2.16 microns	74
35 (b)	Measured spectral transmittance of Spectrum Systems mirror which is slightly transmitting at 2.16 microns	75
36 (a)	Measured spectral transmittance of 3.5 micron doubly-resonant ZnS-ThF ₄ mirror	77
36 (b)	Measured spectral transmittance of 3.5 micron doubly-resonant ZnS-ThF ₄ mirror	78
37	Dependence of spectral transmittance upon substrate	79
38	Variation from substrate to substrate of spectral transmittance	80
39	Types of coating and substrate damage encountered on this program: (a) crater (coating) damage; (b) lithium niobate (substrate) damage; (c) small-spot (coating) damage; and (d) dust damage.	82
40	Damage tests performed in order to understand the behavior and cause of small-spot damage	87
41	Typical result obtained from coating damage tests. The coating shown here was ZnS-cryolite on a fused quartz substrate. The magnification of this photograph is 28.	90
42	Internal Optical Parametric Oscillator	94
43 (a & b)	"Before" and "After" Damage photographs for 2-micron HR coatings of (a) ZnS-ThF ₄ ; (b) ZnS-ThF ₄ overcoated with Al ₂ O ₃	97
43 (c & d)	"Before" and "After" Damage photographs for 2-micron HR coatings of (c) ZnS-cryolite; and (d) ZnS-ThF ₄ undercoated and overcoated with Al ₂ O ₃	98
44	"Before" and "After" Damage photographs of ZnS-ThF ₄ coating for 3-micron singly resonant oscillator	101
Table 1	Mirror reflectivity as a function of the number of coating layers used. Odd-numbered layers are ThF ₄ and even-numbered layers are ZnS.	19
Table 2	Insertion loss tests on coated lithium niobate crystals	37

		<u>Page</u>
Table 3	1.08 Micron Damage Thresholds for Lithium Niobate with Various Coatings	84
Table 4	Damage Levels of Multilayer Dielectric Coatings	91
Table 5	Average 2-Micron Oscillator Output Powers Obtained Using Crystals with Various Types of Coatings	95

Section I

INTRODUCTION

The object of this program has been to study means of improving the characteristics of mirrors which are used with optical parametric oscillators. This work was motivated by the realization that better oscillator mirrors would produce improved parametric oscillator performance. GTE Sylvania was the prime contractor on this program with overall technical responsibility for specifying and evaluating the oscillator mirrors. Lambda Optics and Coating, Inc. performed the mirror fabrication as a subcontractor. This final report summarizes the results obtained on this program covering the period from 1 April 1971 to 1 April 1972.

Optical parametric oscillation is obtained by "pumping" a nonlinear crystal with an intense laser beam¹. Signal and idler waves originate in the crystal from noise and interact parametrically with the pump to produce two outputs at new frequencies. The nonlinear crystal is placed in an optical cavity that is resonant at either one (singly-resonant oscillator) or both (doubly-resonant oscillator) the signal and idler wavelengths. Parametric oscillator mirrors must therefore have specified reflectances at three different wavelengths - the signal, idler, and pump. This is a much more difficult problem² than the situation encountered with laser mirrors where only a single wavelength is involved.

Correct spectral reflectance is just one of several criteria which parametric oscillator mirrors must meet, however. On this program, we have sought to develop mirrors which (1) have the correct reflectances at signal, idler, and pump wavelengths; (2) have very little scatter; and (3) have high resistance to optical damage. Let us briefly consider each of these below.

(1) Spectral Reflectance: In a doubly-resonant parametric oscillator, the coatings should be highly reflecting (or at most, slightly transmitting) at both the signal and idler wavelengths. The coatings should also be transmissive (80% or more) at the pump wavelength. The need for high reflectivity (HR) at two different wavelengths will, in general, require two HR stacks to

be placed one on top of the other. Thus substantially more coating material than usual will be needed for oscillator mirrors, and this can lead to such problems as stress (and subsequent crazing) in the coatings³ or excessive scatter. We see already that the three desired mirror properties mentioned above are not independent, but rather are interrelated to a considerable degree.

In a singly-resonant oscillator, the coatings need be HR at the signal wavelength and transmitting at the idler and pump wavelengths. This is an easier situation to achieve, and does not require as many layers of dielectric material in the stack as do doubly-resonant coatings.

Fairly standard mirror design techniques⁴ were employed in this work. The difficulties encountered in realizing suitable mirrors are often practical ones, such as the presence of large numbers of layers in the coating, or the utilization of materials which do not behave in a completely predictable fashion during deposition.

(2) Scatter Properties: The main failing of oscillator mirrors which were previously commercially available is that they contained excessive numbers of scatter centers. Scatter centers in coatings are caused by the presence of discrete particles in the thin-film layers that compose the mirror. The reasons for the presence of these particles has not been clearly understood. Suspected sources have included dust particles in the coating chamber, fine particles in the vapor stream, and the polycrystalline nature of the deposited film layers. Very few investigators have previously addressed themselves to this problem. Perry⁵ has suggested and implemented some practical approaches to reducing scatter in zinc sulfide-thorium fluoride laser mirrors. Forbes and Fraser⁶ have studied scatter and stresses in He-Ne laser mirrors using zinc sulfide, cryolite, and magnesium fluoride. We have considered the reduction of coating scatter to be a major goal of this program.

A word should be mentioned here about why the reduction of scatter losses from coatings is important. In a doubly-resonant optical parametric oscillator, threshold is inversely proportional to the single-pass signal and

idler losses of the resonator⁷. In an external oscillator configuration (nonlinear crystal situated outside the pump laser), scatter centers in the mirrors act as losses to the signal and idler waves (because energy is scattered out of the resonant modes of the resonator) thereby raising threshold for the oscillator. In an internal oscillator (nonlinear crystal situated inside the pump laser), scatter losses are detrimental for two reasons, rather than one. As with the external oscillator, threshold is raised due to signal and idler losses. In addition, mirror scatter losses will reduce the available pump power because these mirrors are situated inside the pump laser. The scatter levels were sufficiently bad in some of the mirrors which were commercially available prior to this program that it would often not be possible to reach oscillator threshold with a doubly-resonant oscillator.

There is another reason why it is advantageous to reduce the scatter level in coatings. Scatter particles are, in effect, imperfections in the coating; thus laser damage may occur at a lower level than in a perfect coating. Thus it is possible that there is a relationship between the scatter properties and the laser damage threshold of a coating. Bennett⁸, for example, has found that metallic or dielectric inclusions in laser glass are a prime source of rod damage.

(3) Damage Thresholds: As the average and peak power outputs of parametric oscillators continue to grow, mirror and crystal damage has become more and more of a limitation on oscillator performance. On this program, we have measured damage thresholds for the various types of mirrors which were fabricated. In addition, the selection of coating materials was made with an eye toward achieving high damage thresholds.

Several investigations have previously been carried out on damage thresholds of laser coatings. Steinberg, et al⁹ have studied ruby laser damage thresholds for various combinations of coating materials. They conclude that "soft" coating materials having low residual stresses are most durable. Turner¹⁰ has also studied ruby laser damage in various types of coatings. Turner suggests that absorption and subsequent thermal effects lead to damage. The limited and sometimes conflicting data which exist have prompted us to carry out our own investigations of coating damage. This allows us to duplicate in our damage experiments the exact conditions (wavelength, pulse duration, repetition rate, etc.) which exist during parametric oscillator operation.

The motivation for this mirror program came in large part from optical parametric oscillator work which was sponsored by Wright-Patterson Air Force Base and which was performed by the Electro-Optics Organization of GTE Sylvania in Mountain View, California. This work was performed under contracts No. F33615-69-C-1702 and F33615-71-C-1642 covering the period from May 1969 through the present. The object of these programs was to generate tunable outputs in the 2 to 5 micron region of the spectrum. Lithium niobate crystals were pumped by the 1 micron output of a Nd laser to achieve the desired outputs.

The mirrors which we have studied on this program are appropriate to the above type of optical parametric oscillator and its wavelength range. This does not mean, however, that the results of this program are only of limited use. The techniques and materials which were studied are, in general, useful throughout the entire visible spectrum and the near infrared. However the specific designs which were used, and the tests which were performed were for the 2 to 5 micron oscillator. A more complete description of that oscillator will now be given.

The oscillator can be operated in either of two forms, external or internal. The external configuration is shown in Fig. 1. The 1.08 micron output from a continuously pumped, repetitively Q-switched Nd:YAlO₃ laser is focused (by means of a 10 cm lens) into a lithium niobate crystal. The crystal is cut with its optic axis at an angle of 45 degrees with respect to its end faces in order to achieve phase matching near room temperature. The crystal used is about 4mm long and is antireflection coated. A temperature-controlled copper oven houses the crystal. The external oscillator resonator consists of two mirrors which are highly reflecting at the signal and idler wavelengths. The resonator is near-hemispherical with the flat mirror placed within a millimeter or so of the crystal. The output mirror has a radius of curvature of 5 cm and is placed approximately 5 cm from the flat mirror. In the external oscillator configuration, the mirrors are deposited on fused quartz substrates.

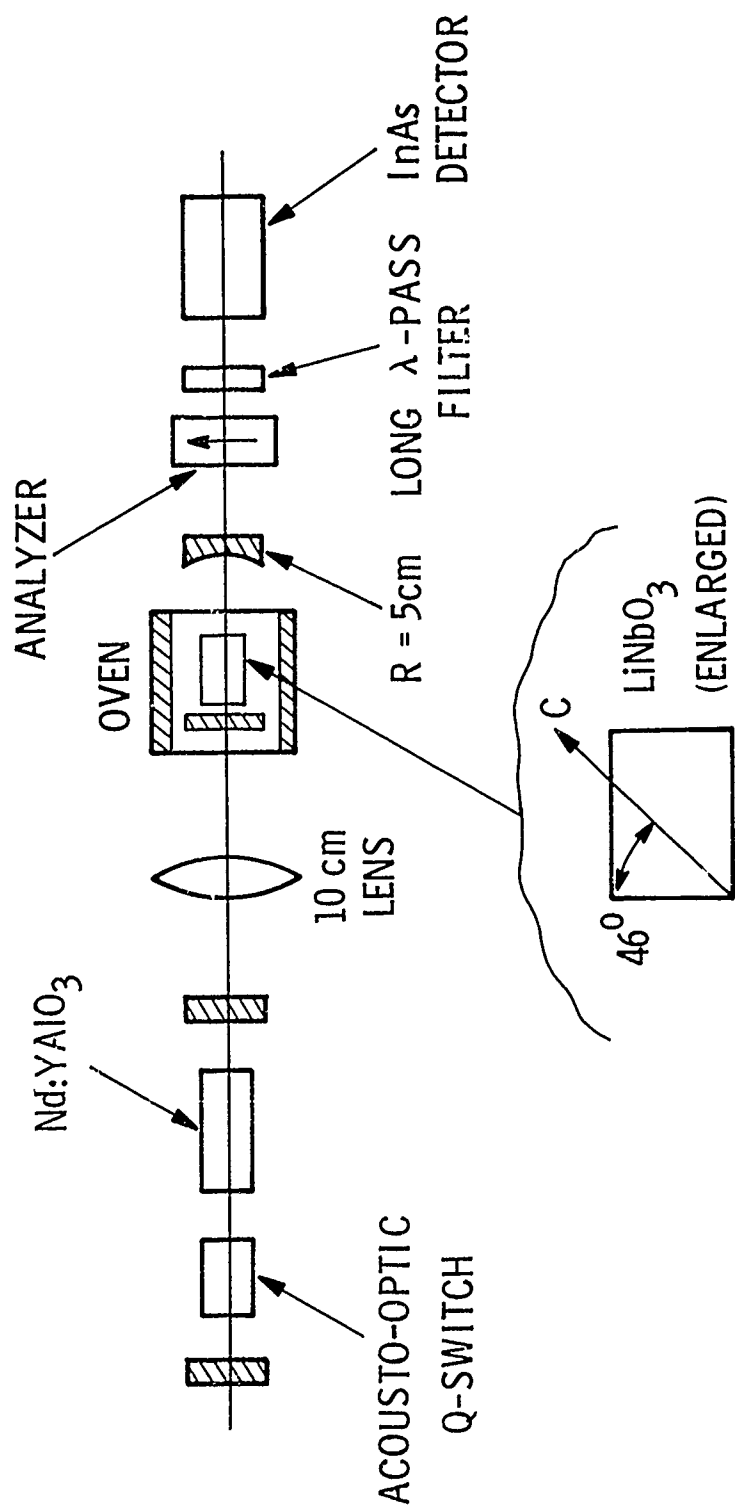


Figure 1 External Optical Parametric Oscillator

The internal oscillator configuration is pictured in Fig. 2. The Nd:YAlO₃ pump laser resonator is formed by two flat mirrors spaced about 45 cm apart. The laser mirrors are highly reflecting at the pump wavelength of 1.08 microns while transmitting about 85% at the signal and idler wavelengths. A lithium niobate crystal, housed in a temperature-controlled oven, is placed within the laser resonator. The oscillator mirrors are coated directly onto the plane-parallel end faces of the crystal. Thus the internal configuration requires mirrors to be coated on lithium niobate whereas the external configuration requires mirrors on fused quartz substrates. For this reason, both lithium niobate and quartz substrates were used with each of the coatings investigated on this program.

The remainder of this report is organized in the following manner. Section II is concerned with the types of mirrors that were investigated. Coating materials which were employed are discussed along with the mirror designs which were used. The coating procedures which were used by Lambda Optics are described in Section III. Also covered in Section III are the techniques used by Sylvania in evaluating and testing the oscillator mirrors. Sections IV, V, and VI give the results of our scatter, spectral transmittance, and damage threshold tests, respectively, for the various types of mirrors. In Section VII, the results of optical parametric oscillator experiments employing these coatings are given. Data on oscillator output power and coating damage under actual operating conditions are given. Conclusions reached on the mirror program are given in Section VIII along with recommendations for further work. Finally, references are listed in Section IX.

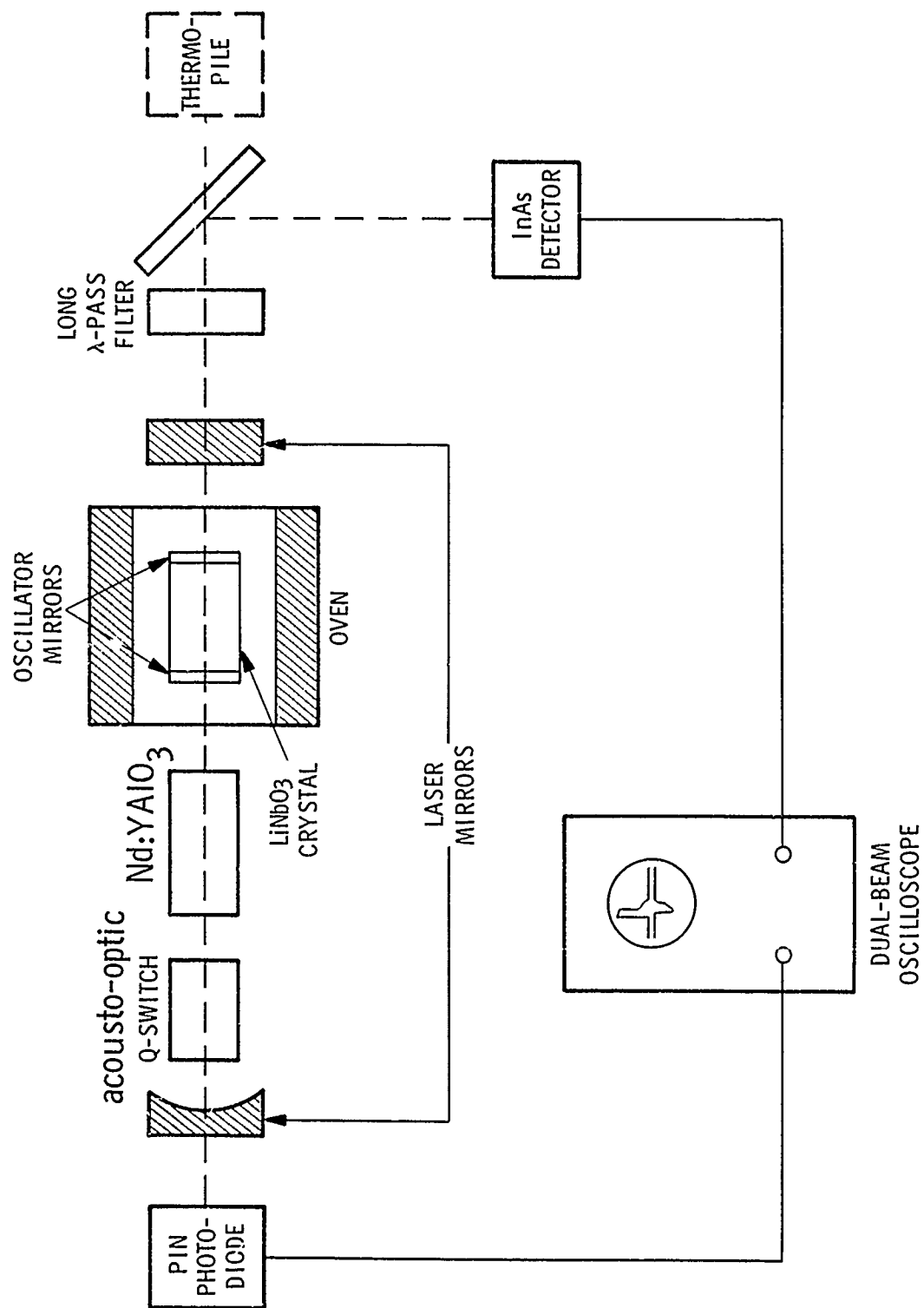


Figure 2 Internal Optical Parametric Oscillator

Section II

COATING MATERIALS AND MIRROR DESIGNS EMPLOYED

Several different combinations of coating materials were investigated on this program in an effort to find an optimum pair for the realization of parametric oscillator mirrors. In this section we discuss the coating materials selected, the substrates used, and the designs used in fabricating the mirrors.

2.1 COATING MATERIALS

A large number of different materials have been used in various optical thin-film applications¹¹. Probably the four materials which have received the most attention as laser mirror coatings in the literature are zinc sulfide (ZnS), zinc selenide (ZnSe), thorium fluoride (ThF_4), and cryolite (Na_3AlF_6). On this program, the materials studies were selected according to our expectation that they would (1) produce a low-scatter coating; (2) have a high damage threshold; and (3) produce the desired spectral reflectances. These priorities are listed in decreasing order of importance.

2.1.1 ZnS - ThF_4

A combination which is presently widely used in the production of laser mirrors is a zinc sulfide (ZnS) and thorium fluoride (ThF_4) quarter-wave stack. This combination is attractive for several reasons. Perry has shown⁵ that scatter losses can be held to a quite low level through the use of appropriate coating techniques. Ennos has determined³ that $\text{ZnS} - \text{ThF}_4$ multilayers contain relatively little net stress; this is because the compressive stress of each ZnS layer almost exactly balances the tensile stress of each ThF_4 layer. The practical significance of this is that large numbers of alternating ZnS and ThF_4 layers can be deposited on a substrate without cracking (or crazing) of the coating occurring. In addition, both ZnS and ThF_4 are moderately durable, are transparent well into the infrared, and are very easy to work with. We now briefly consider each of these materials individually.

ZnS is one of the most widely used of all coating materials. It has a relatively high index of refraction of about 2.2 and is transparent over the

entire range from 0.38 microns to 25 microns. One of the reasons for its wide use is the paucity of other suitable high-index coating materials. Other reasons are its ease of handling and excellent behavior during deposition. Its only drawback is its moderate durability.

ThF_4 coatings are also mechanically and chemically very stable. The index of refraction is approximately 1.51, and thus ThF_4 is used as the low index material in a multilayer stack. ThF_4 is transparent from 0.20 microns through 15 microns, although Heitmann and Ritter¹² have noted a faint water absorption band at 3.0 microns. We have not been able to detect this absorption band from spectrophotometer traces which we have run on $\text{ZnS} - \text{ThF}_4$ mirrors. Heitmann and Ritter¹² also state that ThF_4 coatings are obtained irrespective of whether ThF_4 or ThOF_2 is used as the starting material. ThF_4 films are somewhat more durable than those of ZnS .

2.1.2 ZnS - Cryolite

Another thin-film combination which has been widely used, especially for visible mirrors, is ZnS and cryolite. Neither of these materials is particularly hard, but both are easy to evaporate and both give high optical performance even when condensed on a cold substrate. Ennos³ found that moderate stress build-up occurs in $\text{ZnS} - \text{cryolite}$ multilayers. The buildup is about a factor of five greater than for $\text{ZnS} - \text{ThF}_4$ multilayers.⁹ One reason for trying this particular combination was that Steinberg, et al⁹ found that the use of soft coating materials in multilayers gave high damage thresholds.

ZnS has been discussed already, so we discuss only cryolite here. Cryolite has an index of refraction of 1.35 and is transparent from 0.20 microns to 14 microns. Like ZnS , cryolite sublimes, rather than melts, and can be deposited from a tantalum or molybdenum boat. The scatter properties of cryolite coatings have been studied by Perry⁵ in $\text{ZnS} - \text{cryolite}$ multilayers, and have been found to be excellent.

2.1.3 Mirrors with Al_2O_3 Overcoatings

Because of the somewhat fragile nature of the above coatings, it was decided to try a single-layer overcoating of aluminum oxide (Al_2O_3) for protection of some of the mirrors. A half-wave overcoating of Al_2O_3 was applied

to both $\text{ZnS} - \text{ThF}_4$ and $\text{ZnS} - \text{cryolite}$ mirrors of the types just described in Sections 2.1.1 and 2.1.2. Aluminum oxide has an index of about 1.59 and is transparent from 0.2 microns to about 7 microns. It forms an extremely durable coating and has long been used to protect metal mirrors¹³. It is likely that other materials such as SiO_2 or SiO would also have proven satisfactory as overcoatings for oscillator mirrors. However Lambda Optics has previously had outstanding overcoating success with Al_2O_3 and it was therefore selected for this application.

2.1.4 Mirrors with Al_2O_3 Undercoatings and Overcoatings

As will be described later, the Al_2O_3 overcoatings, in general, proved effective in providing protection to the oscillator mirrors. It was decided to therefore try Al_2O_3 undercoatings as well as overcoatings with $\text{ZnS} - \text{ThF}_4$ and $\text{ZnS} - \text{cryolite}$ mirrors. It was hoped that the undercoating would provide substrate (lithium niobate) protection while the overcoating provided mirror protection. The undercoating and overcoating were each one-half wavelength thick.

2.1.5 Spectrum Systems Coatings

All of the coatings discussed thus far (except for the Al_2O_3 overcoating) are composed of low melting point materials. The rather stable optical properties of these materials enable one to control the optical thickness of individual layers with little difficulty. Thus the spectral response of coatings made with these materials is excellent, but the coatings themselves are not particularly durable. Numerous other materials exist which have much higher melting points and are much sturdier physically, but they are also considerably more difficult to deposit¹⁴. They can be produced by employing electron-beam evaporation technology, rather than the conventional tungsten filament heating method. Many of these materials are oxides such as Al_2O_3 , SiO_2 , TiO_2 , ZrO_2 , etc. which present special difficulties during electron-beam evaporation. These difficulties include:

a) Molecular binding energies of oxides are much smaller than the electron energies needed to evaporate the oxides. Thus during evaporation one tends to disassociate molecules and to produce absorbing films.

b) The index of refraction of these materials tends to change during evaporation. This makes it difficult to control the optical thickness of the film, and hence the spectral reflectance of the coating. For some materials, the change in index can be as great as 50%.

c) These hard materials usually tend to have more scatter centers, and hence result in lossier coatings.

In spite of these difficulties, we elected to try one lot of mirrors which consisted of very durable materials. These mirrors were purchased from Spectrum Systems, Inc. of Waltham, Massachusetts. All other mirrors used on this program were fabricated by Lambda Optics and Coating, Inc., the subcontractor. The dielectric layers used in the Spectrum Systems coatings are actually mixtures of materials,¹⁵⁻¹⁷ rather than pure materials. They have found that better adhesion and durability are obtained with these mixtures than with pure materials. Spectrum Systems would not divulge the materials involved nor the ratios in which they were mixed, considering this information to be company proprietary.

2.2 MIRROR SUBSTRATES

The various coatings that were studied on this program were each deposited on both fused quartz and lithium niobate substrates. As explained in Section I, an external oscillator configuration requires that the parametric oscillator mirrors be deposited on fused quartz substrates; an internal oscillator configuration utilizes parametric oscillator mirrors that are deposited directly on the nonlinear crystal (lithium niobate in this case). It was felt that the scatter, spectral transmittance, and damage properties of the coatings might depend upon the substrate employed, and thus we elected to use both fused quartz and lithium niobate substrates on this program. Details of the substrates which were used are given below.

2.2.1 Fused Quartz Mirror Substrates

Lambda Optics and Coating, Inc. fabricated fused quartz mirror substrates for this program. These substrates, when appropriately coated, were used in making spectral transmittance and coating damage measurements. The substrates were fabricated from infrasil, which transmits out to a wavelength of about 3.5 microns. The substrates were 15 mm in diameter, 11 mm thick

(a standard size for laser mirrors), and were flat. The surfaces were parallel to within 30 seconds or better, flat to within $1/10$ wavelength, and of 0-0 surface quality. An uncoated fused quartz substrate is shown in Fig. 3.

2.2.2 Lithium Niobate Disks

Lithium niobate disks were fabricated by Sylvania and used as substrates on this program. One surface of each disk was coated and the disks used in spectral transmittance and coating damage tests. A c-axis stoichiometric lithium niobate boule of acoustic-grade quality was purchased from Crystal Technology, Inc., of Mountain View, California. This boule was cut into disks 14 mm in diameter and 2.3 mm thick. The surface flatness was approximately 1 wavelength, and the surface parallelism 30 seconds or better. The c-axis (optic axis) of the lithium niobate was perpendicular to the polished faces. One of these disks is shown in Fig. 3.

2.2.3 Lithium Niobate Oscillator Crystals

Lithium niobate crystals which are suitable for use in an optical parametric oscillator were fabricated by Sylvania for this program. Coatings were deposited on both faces of each crystal. The coated crystals were used to measure coating scatter, damage thresholds (qualitatively), and parametric oscillator performance. A stoichiometric a-axis lithium niobate boule of "linobate" (highest) quality was purchased from Crystal Technology, Inc. This boule was cut into crystals approximately 5 mm long and 8.4 by 7.1 mm in cross section. Crystals were oriented with the c-axis at an angle of $48^{\circ}30'$ with respect to the end faces; this orientation resulted in phasematching for parametric oscillation at a temperature of about 100°C . The crystal faces were polished flat to within $1/8$ wavelength and parallel to within 5 seconds. One of these oscillator crystals is pictured in Fig. 3.

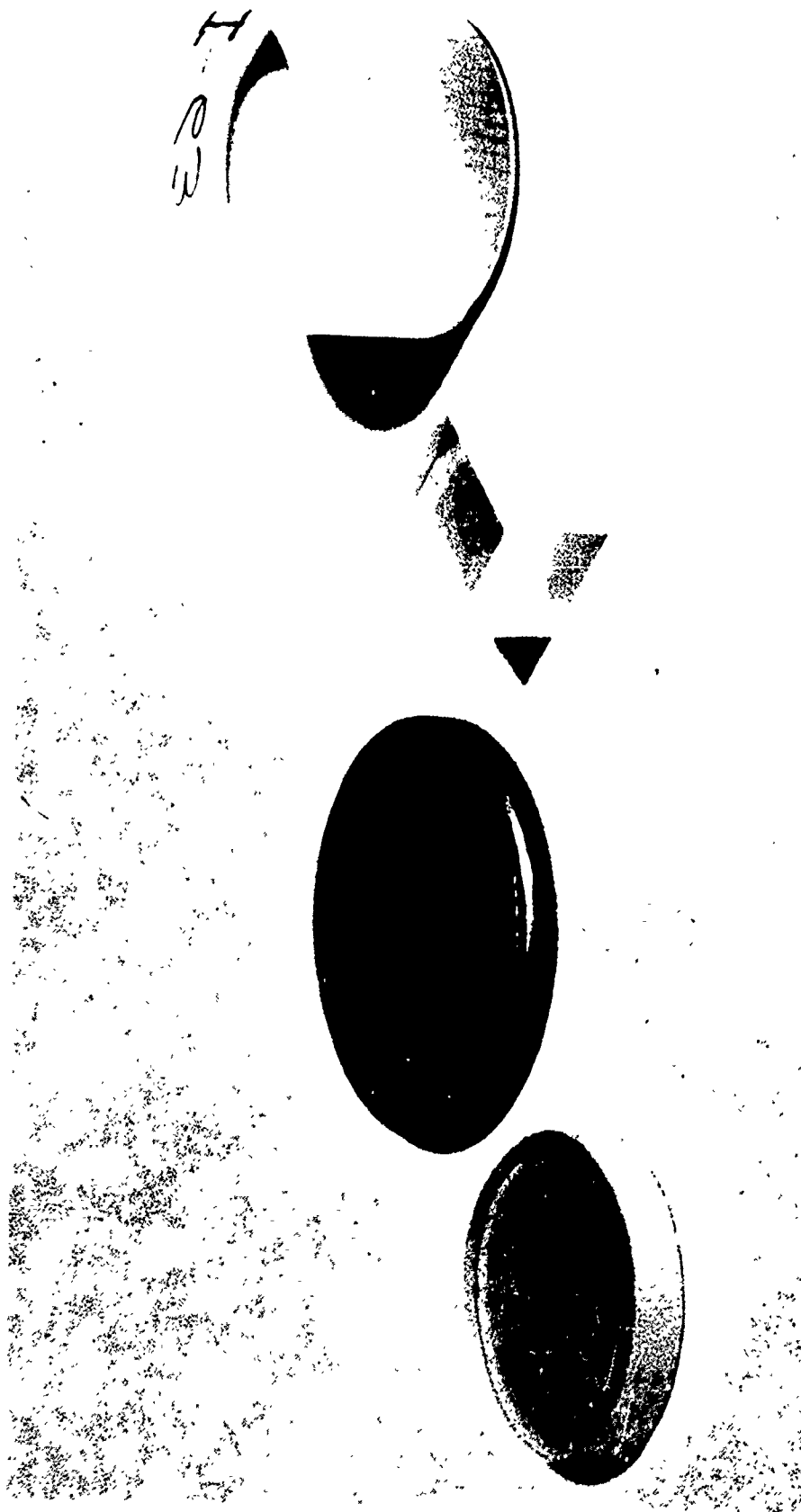


Figure 3 Lithium niobate and fused quartz substrates used on this program

2.3 MIRROR DESIGNS

Mirrors with several different spectral transmittances were designed and fabricated on this program. In this section, we discuss the designs which were employed. In order to clarify our list of mirror types, we have schematically shown external and internal oscillators in Figs. 4a and 4b, respectively.

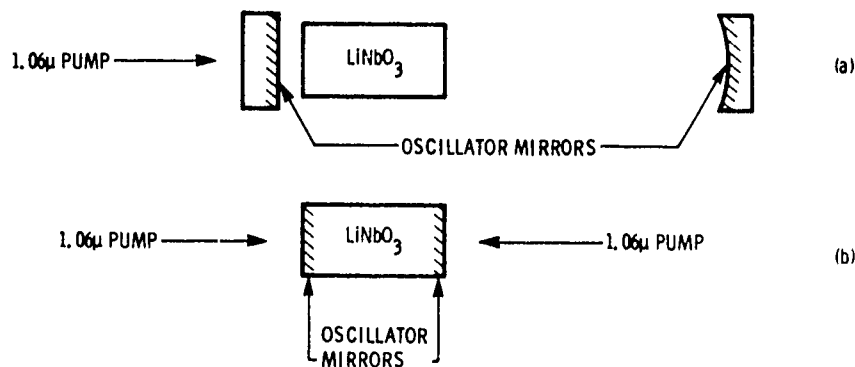


Figure 4 Parametric oscillator resonators for (a) external oscillator and (b) internal oscillator.

2.3.1 Mirror Coating Type #1

Coating type #1 is a relatively simple coating to design and fabricate, but one which is very important. This coating is a conventional high-reflectivity coating centered at the signal wavelength of the parametric oscillator. This coating would be used on both ends of the internal and external oscillators of Figs. 4a and 4b to produce singly-resonant operation. The coating is highly reflecting at the signal wavelength, but is transmitting at the idler wavelength. In addition, it is desirable to have low reflectivity at the pump wavelength of 1.08 microns. For the external oscillator of Fig. 4a, this allows most of the pump to enter the lithium niobate crystal. The 1.08 micron reflectivity is important for a different reason for the internal oscillator of Fig. 4b. The coated lithium niobate crystal with its flat end faces acts as an etalon inside the Nd:YAlO₃ laser. If the 1.08 micron reflectivity is too large, it will be very difficult to make the laser operate.

The type #1 coating will also be useful in a second situation. If the high-reflectivity region is centered at 2.16 microns, then this coating will be appropriate for use on one end of the crystal in a doubly-resonant oscillator operating near degeneracy. Because the high-reflectivity region would cover from about 1.95 to 2.35 microns, the oscillator output could be tuned over the same range. The early coatings fabricated on this program were centered at 2.1 microns and were intended for use in a doubly-resonant oscillator. Later HR coatings were centered at 1.6 microns and were used in a singly-resonant 3 micron oscillator.

The design used for HR coatings is shown in Fig. 5 for ZnS - ThF₄ mirrors. The initial coating layer is ThF₄ and is $\lambda/12$ wavelength thick (at the signal wavelength). This is followed by 21 alternating quarter-wave layers of ZnS and ThF₄. ThF₄ is used as the initial layer because of its superior adhesion to the substrate; ZnS is used as the final layer because of its apparent better durability as an outer layer. The initial ThF₄ layer could have been $\lambda/4$ thick instead of $\lambda/12$ thick. If fused quartz is the substrate, the $\lambda/12$ layer is used since the indices of ThF₄ and fused quartz are nearly equal. If lithium niobate is the substrate, a $\lambda/4$ thickness should be used for the initial layer.

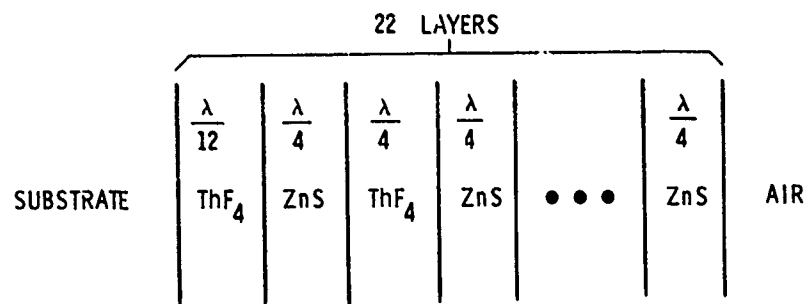


Figure 5 Design used for ZnS - ThF_4 highly reflecting mirrors

For HR mirrors composed of ZnS and cryolite, a total of 21 alternating layers was used with the initial layer being a $\lambda/4$ layer of ZnS. In this case, both the first and last layers were ZnS.

2.3.2 Mirror Coating Type #2

Coating type #2 is similar to #1 but contains fewer layers. This coating is designed to transmit a few percent at the signal (or idler) wavelength, and to be highly transmitting (85% or more) at the pump wavelength. This coating was used primarily as the transmitting coating for the doubly-resonant 2.16 micron oscillator. The composition of this coating is shown in Fig. 6. An initial $\lambda/12$ layer of ThF_4 is followed by 9 alternating $\lambda/4$ layers of ZnS and ThF_4 . For the ZnS - cryolite mirrors, a 9 layer coating starting with a $\lambda/4$ layer of ZnS was used.

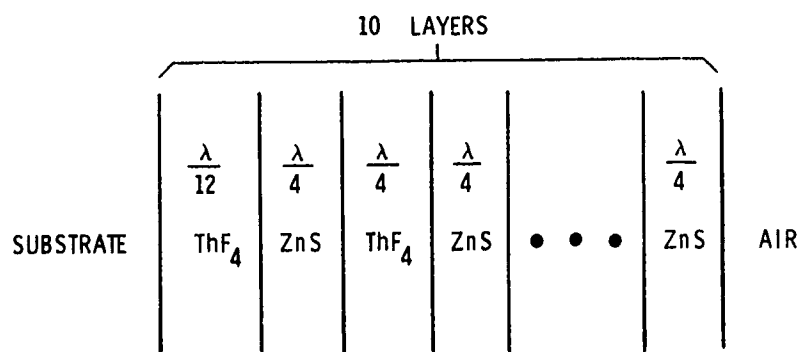


Figure 6 Design used for ZnS - ThF_4 partially transmitting mirrors

The coatings of Figs. 5 and 6 are standard multilayer designs and reflect the fact that mirror reflectivity increases as the number of layers used increases. We have performed calculations of midband reflectance as a function of the number of layers used; this calculation was carried out for ZnS and ThF₄ alternating layers on both lithium niobate and fused quartz. In this calculation, we assume that the first layer is a $\lambda/4$ layer (rather than a $\lambda/12$ layer) of ThF₄. The indices of refraction which we used are fused quartz (1.437), lithium niobate (2.195), ZnS (2.20), and ThF₄ (1.50). The results of this calculation are shown in Table 1.

There are two important things to be noted from the data of Table 1. First for a given value of n , the reflectivity can be substantially different for fused quartz and lithium niobate substrates. As an example, for $n = 7$ reflectivities are 53% and 66% for quartz and niobate substrates, respectively. Thus one should not design lithium niobate coatings using fused quartz mirror design data. Secondly, from the viewpoint of minimizing the number of coatings required to achieve a particular reflectance, it is advantageous to have the top layer be ZnS. This is demonstrated by the fact that the reflectance is 99.7% for both $n = 18$ and $n = 21$.

2.3.3 Mirror Coating Type #3

Coating type #3 is designed to be highly reflecting at the oscillator signal wavelength, while having slight transmission at the idler wavelength. The mirror is designed to be used on one or both ends of the crystal in either an internal or external doubly-resonant, nondegenerate parametric oscillator. This mirror is designed by beginning with an HR (or slightly transmitting) stack at the idler wavelength, and placing on top of it an HR stack at the signal wavelength. The design which was used for $\lambda_{\text{idler}} = 3.6$ microns and $\lambda_{\text{signal}} = 1.56$ microns is shown in Fig. 7. This mirror was HR at 1.56 microns and transmitted about 5% at 3.6 microns. The difficulties involved with fabricating mirrors for a doubly-resonant oscillator are illustrated by the design of Fig. 7. These difficulties are primarily involved with the large amount of material which must be deposited on the substrate. The design of Fig. 7 consists of 32 layers, a large number by coating standards. Furthermore, the last 21 of these layers are almost 1 micron thick apiece. With

Table I

Mirror reflectivity as a function of the number of coating layers used. Odd-numbered layers are ThF_4 and even-numbered layers are ZnS .

Number of Layers n	MIRROR REFLECTIVITY (ρ^2)	
	Quartz Substrate	Lithium Niobate Substrate
1	.0486222	.0001531
2	.2612636	.4230889
3	.0248013	.1256932
4	.5454437	.6736115
5	.2443799	.4061487
6	.7557030	.8325963
7	.5302108	.6614031
8	.8780530	.9184006
9	.7460007	.8256031
10	.9413506	.9612062
11	.8728153	.9148127
12	.9722957	.9817752
13	.9387382	.9594594
14	.9870243	.9914861
15	.9710407	.9809454
16	.9939468	.9960330
17	.9864318	.9910964
18	.9971815	.9981539
19	.9936694	.9958510
20	.9986887	.9991414
21	.9970521	.9980691
22	.9993902	.9996007
23	.9986285	.9991019
24	.9997165	.9998144
25	.9993622	.9995824
26	.9998682	.9999137
27	.9997034	.9998058
28	.9999387	.9999599
29	.9998621	.9999097
30	.9999715	.9999813

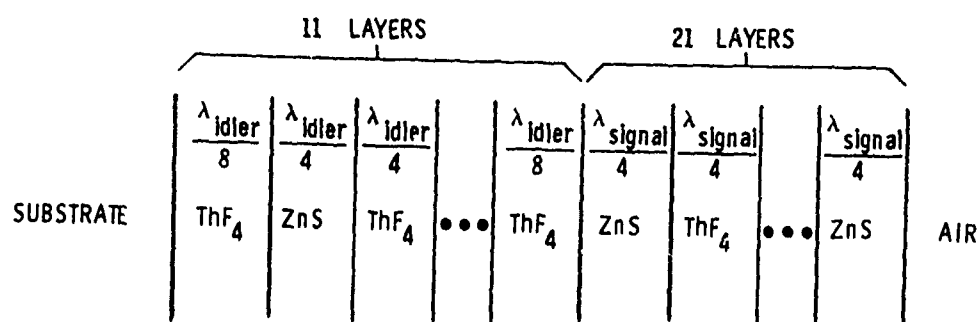


Figure 7 Design used for doubly-resonant ZnS-ThF₄ mirrors

this large amount of coating material, coating scatter and stress are the problems which must be overcome (and have been on this program) in order to obtain useful optical parametric oscillator coatings.

Section III

COATING AND TESTING PROCEDURES

3.1 COATING TECHNIQUES AND APPARATUS

The majority of the coating work on this program was performed by Lambda Optics and Coating, Inc., of Berkeley Heights, New Jersey. Lambda is a commercial supplier of various types of optical coatings and was a sub-contractor on this program.

Lambda has four Consolidated Vacuum Corp. LCV-18 vacuum evaporators. Each of these has a 6" diameter oil diffusion pump, chevron-type cooling baffles, and an 18 inch diameter bell jar plus all associated electrical, vacuum, and optical controls. Three of the four evaporators are used for depositing relatively volatile materials by means of resistive heating. One such evaporator is pictured in Fig. 8. The resistive heating technique was used to deposit the ZnS , ThF_4 , and cryolite films used on this program.

The fourth evaporator used on this program is shown in Fig. 9. This evaporator uses a four-pocket, 270 degree Airco Temescal electron gun driven by a 10 kW power supply to volatilize and deposit high-temperature materials. The Al_2O_3 films were deposited using this evaporation technique. Both resistive-heating evaporation and electron-beam evaporation are discussed by Macleod¹⁸.

Each Lambda evaporator has a thin-film thickness monitor which utilizes a He-Ne laser operating at 6328\AA . A complete description of this monitoring system has been given by Perry⁵.

3.2 SCATTER EVALUATION

Two tests were used on this program in order to evaluate scatter in the mirror coatings. The first of these is by visual observation using a microscope with camera attachment. A Leitz Ortholux large research polarizing microscope was used and is pictured in Fig. 10. This microscope is fitted with an FS binocular tube, which is a combination of a binocular viewing tube and photographic tube. The Leitz is fitted for dark-field microscopy and



Figure 8 Evaporator used for low-temperature materials such as ZnS , ThF_4 , and cryolite.



Figure 9 Evaporator with electron-gun source for evaporating high-temperature materials

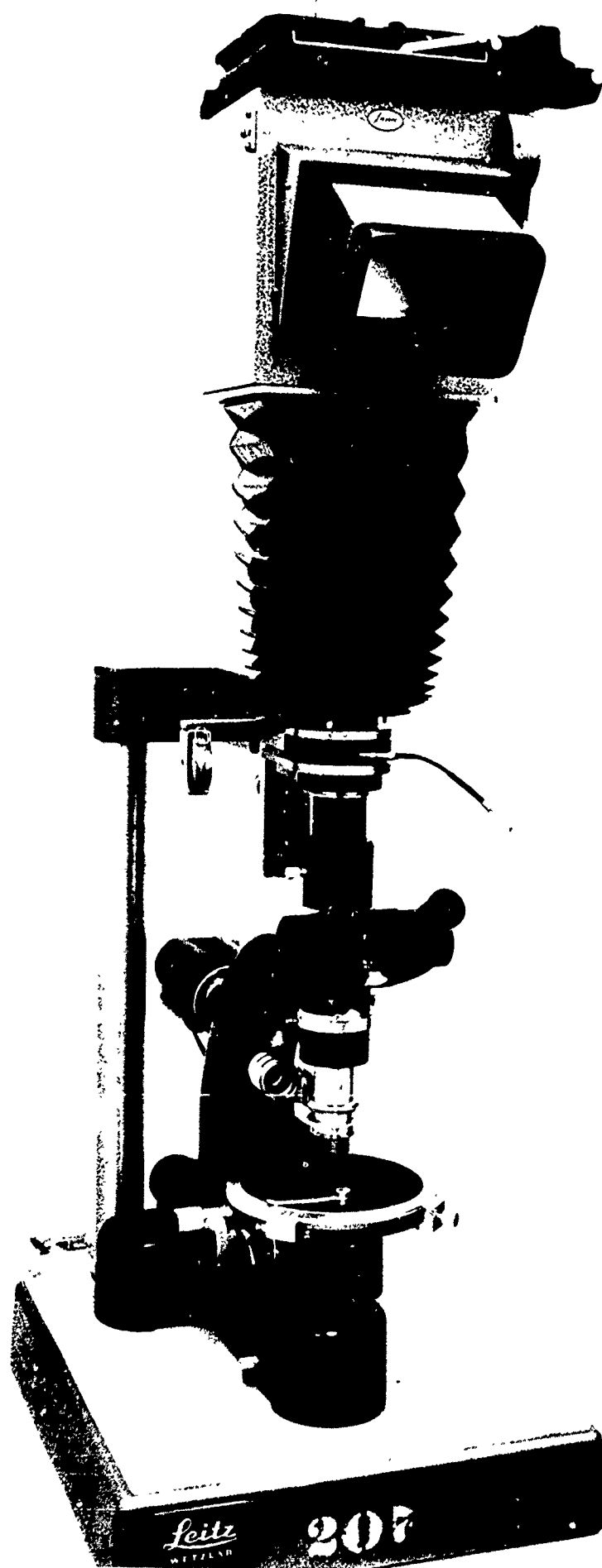


Figure 10 Leitz Ortholux polarizing microscope

accommodates a 4 x 5 inch bellows with a Polaroid-Land camera attachment. Three objective lenses were available which produced magnifications of 17, 28, and 78. The middle value was used for the majority of our work. Approximately two hundred photographs of coatings were taken during this program.

A second test was also employed to measure mirror scatter losses in addition to the photographic technique described above. We have used this test successfully the past 2 years on our oscillator programs as well as on this program. The setup for the test is shown in Fig. 11 and the procedure is as follows. The output power from a CW Nd:YAlO₃ laser is measured with nothing in the cavity. One of the coated substrates (shown dotted in Fig. 11) is then inserted in the laser cavity and adjusted so the laser's output is maximized. This coated substrate will act as an etalon inside the laser because its faces are flat and very parallel. This second output power will be less than the first because of the insertion loss of the substrate and because of scatter and absorption losses of the coating(s). The insertion loss of the substrate alone will have been previously determined by measuring the laser output power with the uncoated substrate in the laser, and thus it will be possible to determine losses due to scatter from the coatings alone. The advantages of this technique include (1) laser output powers typically vary rather widely for fairly small changes in insertion loss, and (2) the configuration of this test is identical with the actual operating conditions of an internal optical parametric oscillator, and thus this test gives directly useful results. Any of the three coated substrates mentioned earlier in Section 2.2 could have been used in these tests. However, we felt it would be most useful to perform this test using the coated oscillator crystals as the substrate. The crystals have two coatings and give the two-coating losses from this test. We note that uncoated fused quartz substrates consistently introduce virtually no loss at all inside the laser, while the loss from uncoated lithium niobate crystals varies from crystal to crystal and is considerably higher.

3.3 SPECTRAL TRANSMITTANCE EVALUATION

Tests were performed on each type of coating to measure its spectral transmittance and to determine whether it matches the desired transmittance. These tests were performed using a Perkin-Elmer model NIR 137G Infracord

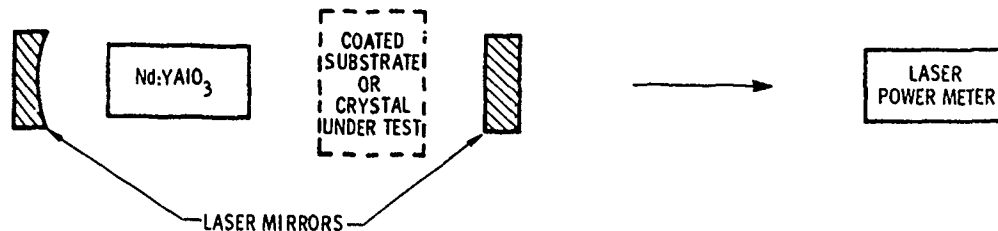


Figure 11 Technique for determining scatter losses from coated crystals and substrates.

spectrophotometer (shown in Fig. 12). This instrument is a double-beam grating spectrophotometer that covers the wavelength range from 0.9 micron to 7.65 microns. The 137G has an accuracy of ± 0.004 microns in range #1 (0.9 to 2.55 microns) and an accuracy of ± 0.012 microns in range #2 (2.45 to 7.65 microns). Reproducibility is 0.003 microns or better in range #1 and 0.008 microns or better in range #2. The transmission accuracy of the instrument is 1% or better.

3.4 DAMAGE THRESHOLD EVALUATION

Investigation of coating damage and substrate damage levels were carried out in two different ways. In the first, the coated substrate is mounted in front of the Nd:YAlO₃ laser. The laser output is focused onto the coating and damage measurements carried out. Coated lithium niobate disks and coated fused quartz substrates were used in these tests. In the second type of test, a coated oscillator crystal is placed inside the pump laser and an internal oscillator operated. Following operation of the oscillator, the crystal is removed and inspected for coating and substrate damage. There are at least two important differences between the two test procedures: (1) The first test uses a TEM₀₀ laser beam whereas the second test employs a high-order-mode laser; (2) In the first test, only the 1.08 micron pump is present; in the second test, signal, idler, and pump wavelengths are all present.

We now consider the first test procedure in more detail. The setup used in this first procedure is shown in Fig. 13. The laser used in these experiments is a Nd:YAlO₃ laser which is pumped by two tungsten-iodide lamps. The laser is continuously pumped and repetitively Q-switched by means of a CRL model 460 acousto-optic Q-switch. Tests were performed both with a TEM₀₀

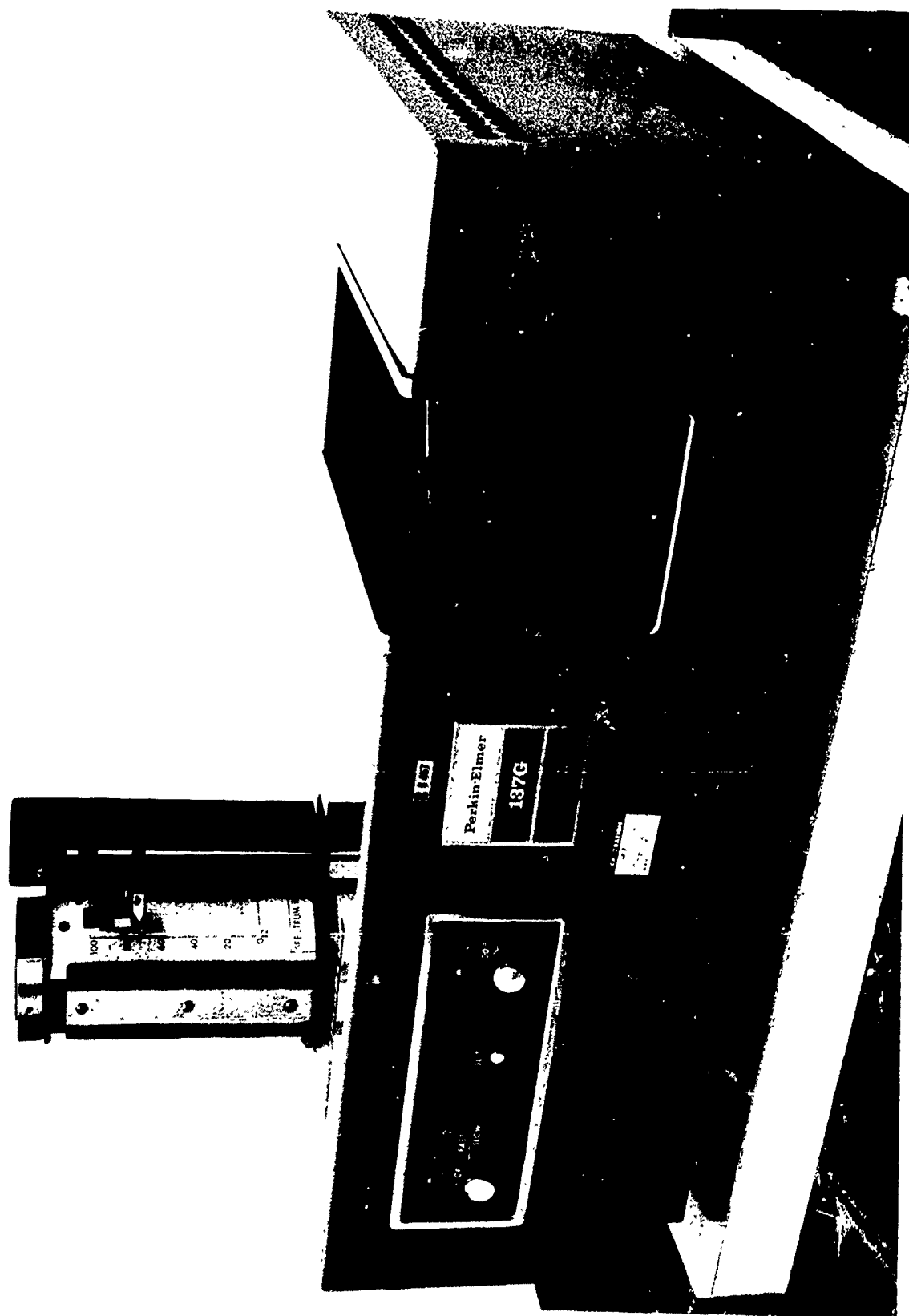


Figure 12 Perkin-Elmer Model 137G Spectrophotometer

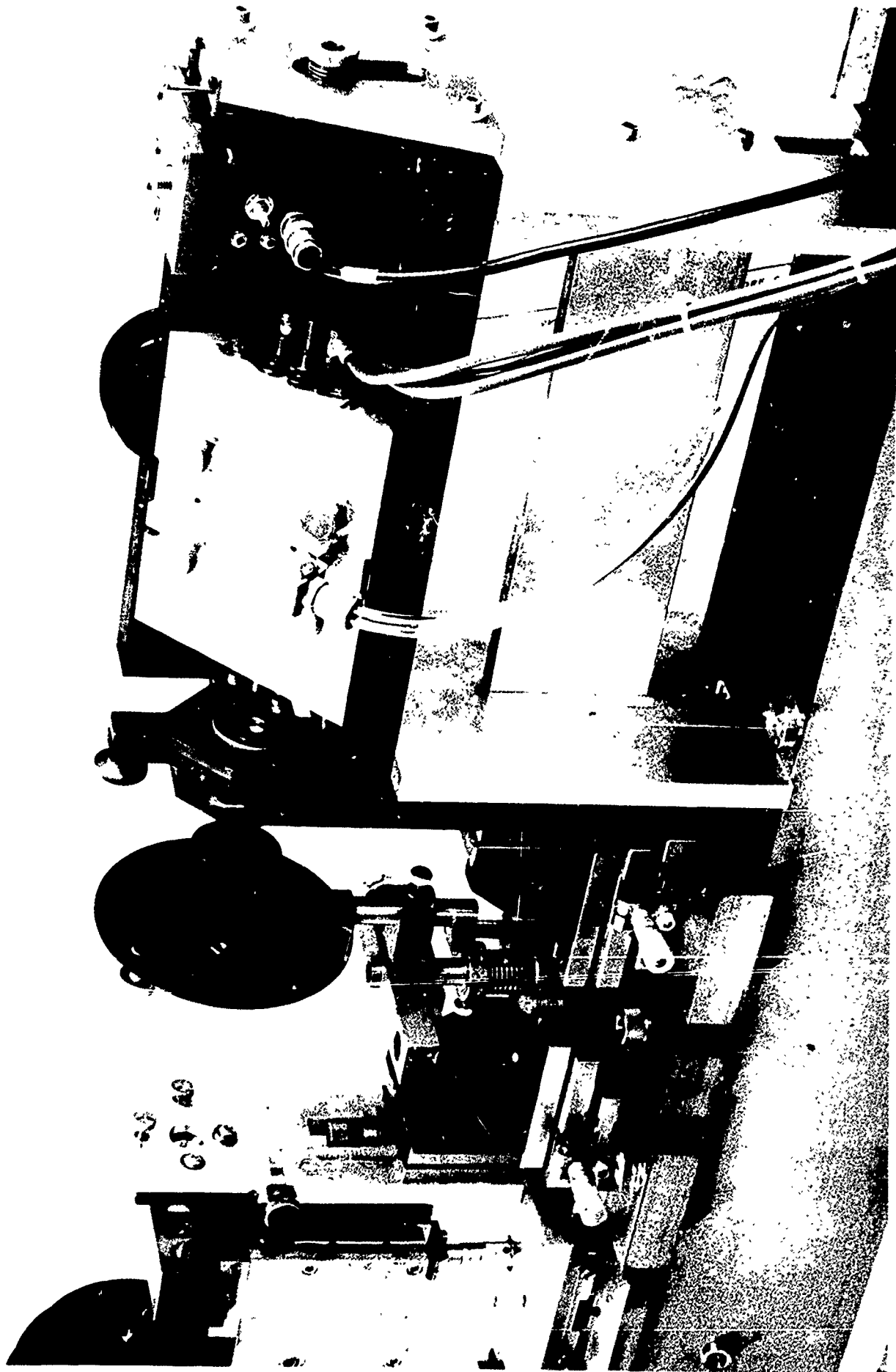


Figure 13 Test setup used for coating-damage threshold measurements

mode output and with a high-order mode output. The available 1.08 micron Q-switched average output power for these tests was 0.5 watts and 3.5 watts for fundamental mode and high-order mode operation, respectively. A repetition rate of 4 kHz was used in all tests; pulse lengths were 140 ns and 350 ns for fundamental and high-order mode operation.

The laser output was focused onto the specimen under test by a 1.3 cm lens. The coating under test was on the front surface of the substrate in all cases. A polarizer preceding the lens was employed as a continuously variable attenuator. A specimen holder in which four samples could be mounted side by side was located at the focus of the lens. This specimen holder is shown in more detail in Fig. 14. The specimen holder could be translated vertically and horizontally by means of micrometer adjustments. During a damage test, the specimen holder was translated back and forth horizontally three times with the laser power fixed at a particular level. The horizontal translation distance was 0.100 inches for each test. In this way, the laser beam impinges upon numerous areas of the test coating, rather than on a single location. As a coating first begins to damage, there will be only one or two damage spots across this line. As the power levels increase above the damage threshold for the coating, the number of damage spots occurring on the 0.100 inch line also increases. This type of test is compatible with the probabilistic nature of laser-induced damage¹⁹. At high power densities, the number of damage spots across the 0.100 inch line increases, reflecting the increased probability of damage occurring. After each test, the specimen holder was removed and the coatings examined under a microscope for damage. The coatings were photographed (under magnification) before and after each test in order to facilitate the search for damage.

The incident 1.08 micron power density at the test coating was calculated from the known incident average power, pulse length, repetition rate, and beam size at the lens focus. The beam size at the focus was determined by two different methods: (1) The beam diameter entering the lens was measured and the focused spot size then calculated using standard formulas; and (2) the spot size at the focus was measured directly using a very small aperture. These two methods gave results which agreed to within approximately

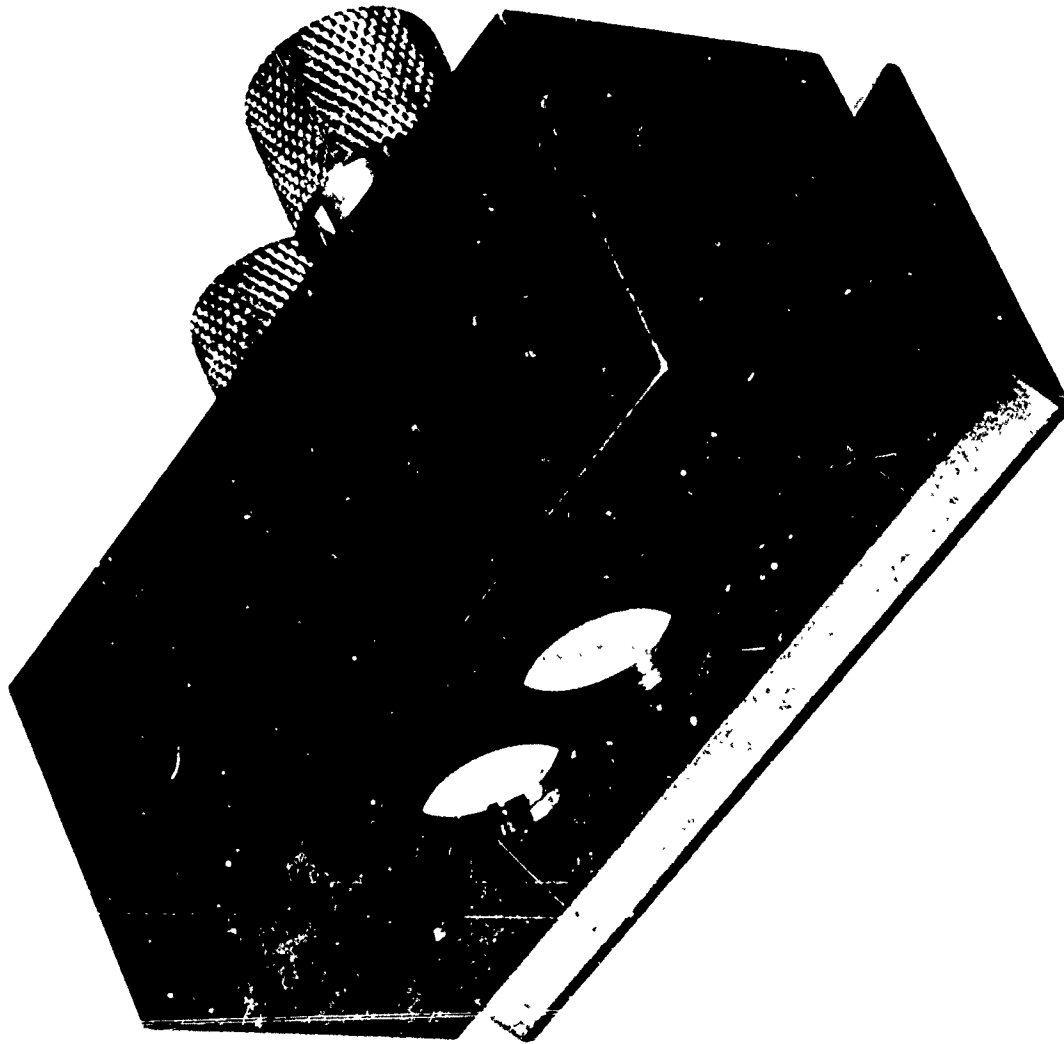


Figure 14 Specimen holder for coating damage tests.

10%. The definition of beam diameter used here is the familiar $1/e^2$ power points of the TEM_{00} mode. The power densities which we quote in Section VI are the power densities at the center of the Gaussian mode. These are obtained by first using the $1/e^2$ area to calculate an average power density, and then multiplying this by two to allow for the fact that the center power density of a Gaussian beam is twice the average power density.

The maximum 1.08 micron TEM_{00} power densities which were attainable with our setup were about 200 MW/cm^2 . The Rayleigh range for the beam in our setup was only 0.034 inches. Thus it was necessary to take special precautions to ensure that the coating under test was actually located at the beam focus. A small test aperture was inserted into one of the holes of the mirror fixture of Fig. 14. This test aperture butted against the same retaining lip that the substrates did when they were in the holder. The test aperture (in the holder) was used to locate the beam focus. The test aperture was then removed and a coated substrate inserted in the same hole. A series of damage tests were run on the coated substrate, with longitudinal translations of 0.005 inches being made between tests. By noting the longitudinal position at which the severest damage occurred, the correct holder position was determined to within 0.005 inches. Once this longitudinal position had been established, the test fixture could be removed and replaced (as when photographing coating damage) without altering this position. We estimate that the power densities quoted in this report are accurate to within $\pm 20\%$.

Section IV

SCATTER CHARACTERISTICS OF FABRICATED MIRRORS

As noted in Section 1, it is crucial that parametric oscillator mirrors contain very little scatter. One of the reasons that Lambda Optics and Coating, Inc. was selected to be the subcontractor on this program is that we had previously determined that Lambda coatings have very little scatter. Perry⁵ has elaborated on the techniques which he has developed and used, first at Bell Laboratories and now at Lambda, to obtain low-scatter coatings. These and subsequent techniques employed by Lambda for this program are discussed below in Section 4.1.

4.1 TECHNIQUES USED TO OBTAIN LOW-SCATTER COATINGS

The scatter properties of multi-layer coatings are greatly dependent upon (1) proper cleaning and preparation of the substrates involved, (2) careful selection of the material to be deposited, and (3) the use of proper deposition techniques. We will consider substrate preparation first. The polished surface should, of course, be free of pits and scratches. Lambda Optics uses a final cleaning procedure (just prior to coating) which consists of washing the blank with a solution of Alconox and water applied with a soft camel's hair brush. This solution is rinsed off with tap water, and the blank then is rinsed thoroughly with distilled deionized water. The surface to be coated then is blown dry with nitrogen. If the surface is clean, the water will disappear rapidly with no droplets remaining. Such cleaning eliminates evaporation of the water from the surface which, if allowed to occur, will usually produce water marks that are difficult to detect until after coating. The rest of the mirror blank then is dried with nitrogen, making sure that no water reappears on the surface to be coated. The surface to be coated then is inspected by shining a bright light (microscope lamp) through the blank and observing the amount of scattered light from the surface. Poor polish and grinding defects may be detected in this manner.

The above cleaning procedure is performed in close proximity to a dust-free portable hood. In order to minimize further the possibility of dust particles accumulating on the clean surfaces, the hood containing the clean

substrates is located next to the coating station. The mirror blanks are placed into the coating adapters within 5 or 10 min after the cleaning procedure. The back surfaces are kept free of unwanted vapor deposition by being covered during the evaporation. Initial roughing of the bell jar is done slowly to avoid raising a dust of small particles remaining from previous evaporations.

One step in the coating procedure which is rather widely recommended in the literature is that a glow discharge be used to clean the substrate just prior to deposition. Lambda has found that the use of glow-discharge cleaning results in greater coating scatter than if glow-discharge cleaning is not used. This scatter is possibly due to the glow discharge sputtering particles which have previously accumulated on the coater walls onto the clean substrate. A glow discharge was not used in any of the work done on this program.

As discussed later in Section 4.2, ThF_4 presents more of a problem in achieving low-scatter coatings than do other materials. The number of suppliers of this type of coating material is limited and their materials differ greatly. Using the radiant-heat type of evaporation, it is advisable to make test runs with each lot of material received, and to select that which shows the least scattering effect. The absence of scattering (and absorption) losses in a mirror coating can be determined very nicely by using these mirrors with a helium neon laser and obtain lasing action at 5433\AA , the shortest wavelength to lase in helium neon, as well as by visual observation by microscope.

The form of the ThF_4 prior to evaporation is also very important in determining coating scatter. Lambda Optics found⁵ that minimum scatter centers resulted when the ThF_4 was evaporated just below its wetting temperature. Further improvement in mirror quality was obtained when the ThF_4 powder was sifted through a U.S. standard series 200 sieve. The most pronounced decrease in scatter centers occurred when the ThF_4 was evaporated from chunks as received from the supplier. A possible reason for this may be that in the powder state trapped gases can form pockets which are liberated suddenly when the material is heated, releasing small showers of the surface material. The temperature required to evaporate the ThF_4 in the chunk state appeared to be more nearly constant for a given number of layers than when the powdered state was used.

4.2 RESULTS OF SCATTER TESTS

As indicated in Section 2.1, several different types of coating materials were tried on this program. Lambda Optics fabricated mirrors which were composed of (a) ZnS-ThF₄; (b) ZnS-ThF₄ overcoated with Al₂O₃; (c) ZnS-cryolite; (d) ZnS-cryolite overcoated with Al₂O₃; and (e) ZnS-ThF₄ undercoated and overcoated with Al₂O₃. In addition, Spectrum Systems fabricated mirrors composed of layers which were mixtures of materials. Photographs were taken of each type of mirror using the Leitz microscope of Fig. 10. The results are given in Fig. 15. All coatings shown in Fig. 15 were HR at 2.16 microns and were deposited on fused quartz substrates.

The following conclusions can be drawn from the data of Fig. 15.

(1) The ZnS-ThF₄ coatings of Fig. 15a have very little scatter. These coatings are excellent from a scatter viewpoint. For comparison we show photos of similar mirrors from Laser Optics and Valpey Corp. in Figs. 15g and 15h, respectively. The Lambda mirrors are clearly superior from a scatter viewpoint.

(2) The ZnS-cryolite coating of Fig. 15c has even less scatter than the ZnS-ThF₄ coating of Fig. 15a.

(3) An Al₂O₃ overcoating contributes virtually no additional scatter to the mirror. This can be seen by comparing Fig. 15b to 15a and Fig. 15d to 15c.

(4) The scatter present in the coating of Fig. 15e is about double that of Fig. 15a. We believe that this is not due to the Al₂O₃ undercoating and overcoating, but rather to the ZnS-ThF₄ layers. The ZnS-ThF₄ layers of Fig. 15e were not deposited at the same time as those of Figs. 15a and 15b.

(5) The hard coatings from Spectrum Systems shown in Fig. 15f have somewhat more scatter than the Lambda coatings, but this scatter level is still acceptable. Unfortunately however, Spectrum Systems coatings on lithium niobate have much more scatter than Lambda coatings on niobate. This phenomenon is discussed further in Section 4.3.

Coating scatter was also evaluated using the insertion-loss test of Fig. 11. These tests were run using oscillator crystals with 2.16 micron coatings on both ends. The results are shown in Table 2. It can be seen that the presence of two Lambda coatings inside the pump laser caused only



(a)



(b)



(c)



(d)

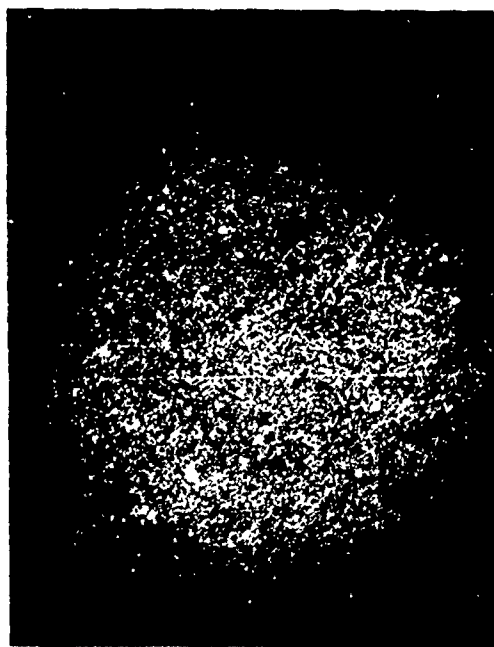
Figure 15 Scatter Characteristics (magnification 20) of 2 micron HR mirrors fabricated by (a) Lambda (ZnS-ThF_4), (b) Lambda (ZnS-ThF_4 overcoated), (c) Lambda (ZnS-cryolite), (d) Lambda (ZnS-cryolite overcoated), (e) ZnS-ThF_4 undercoated and overcoated, (f) Spectrum Systems, (g) Laser Optics, and (h) Valpey. All coatings are on fused quartz substrates.



(e)



(f)



(g)



(h)

Figure 15 Scatter Characteristics (magnification 20) of 2 micron
(Continued) HR mirrors fabricated by (a) Lambda (ZnS-ThF_4), (b) Lambda
(ZnS-ThF_4 overcoated), (c) Lambda (ZnS-cryolite), (d) Lambda
(ZnS-cryolite overcoated), (e) ZnS-ThF_4 undercoated and
overcoated, (f) Spectrum Systems, (g) Laser Optics, and (h)
Valpey. All coatings are on fused quartz substrates.

relatively small power decreases; typically the power dropped from about 5.5 watts to 4.4 watts due to the coatings. This decrease is quite acceptable for internal oscillator operation. The Spectrum Systems coatings fared very poorly on this test, but this cannot be blamed entirely on scatter. As we will see in Section 5, the 1.08 micron transmission of the Spectrum System coatings was quite low and this, rather than scatter, was probably primarily responsible for these results.

As already noted, the 2 micron HR ZnS-ThF₄ coatings by Lambda had excellent scatter properties. These coatings used the design given in Fig. 5. The more complicated mirror design of Fig. 7 has more coating layers, and hence might be expected to show greater scatter. Figure 16 shows a photograph (28 times magnification) of a Lambda mirror employing the design of Fig. 7. It can be seen by comparing Figs. 16 and 15a that the additional layers have caused only a slight increase in scatter. Thus acceptable scatter levels are obtained for all mirror designs needed when Lambda ZnS-ThF₄ coatings are used.

There is occasionally some variation in scatter from lot to lot of Lambda coatings. The photos of Figs. 15a-15d and 16 are typical of the best results obtained; in other instances such as Fig. 15e, similar coatings have



Figure 16 Scatter characteristics (magnification 28) of Lambda 3.5 micron doubly-resonant ZnS-ThF₄ mirror.

Table II
Insertion loss tests on coated lithium niobate crystals

Supplier of Coating	Coating Materials	Laser Power without Crystal	Laser Power w Uncoated Crystal	Laser Power w Coated Crystal
Lambda	ZnS-ThF ₄	8.0 watts	5.2 watts	4.1 watts
Lambda	ZnS-ThF ₄ Al ₂ O ₃ overcoat	8.0	5.8	4.3
Lambda	ZnS-cryolite	8.0	5.4	4.3
Lambda	ZnS-cryolite Al ₂ O ₃ overcoat	8.0	5.4	--
Lambda	ZnS-ThF ₄ Al ₂ O ₃ undercoat and overcoat	8.0	5.4	4.4
Spectrum Systems		8.0	4.7	0.1

had up to twice the number of scatter centers. These higher scatter levels have not resulted in significantly greater values of insertion loss, however, and hence they are still acceptable. They do point up the fact that the sources of coating scatter are not completely understood. It appears that scatter centers are due almost entirely to the inclusion of foreign particles of dust or other contaminants in the coating. The dust can arise from a number of sources such as improperly cleaned substrates, material on the inside of the coater from previous runs, and the coating materials themselves.

A test was performed in an attempt to shed some light on the source(s) of scatter in ZnS-ThF_4 coatings. A thick layer of ZnS was deposited on one quartz substrate and a thick layer of ThF_4 on a second substrate. (Both of these layers were approximately 20 quarterwaves thick at 2.16 microns.) These coatings were then examined for scatter using the Leitz microscope. The results are shown in Fig. 17. Both coatings had relatively little scatter, but the ThF_4 coating contained about twice as many scatter centers as the ZnS coating. If accumulated material from the inside of the coating chamber was the sole source of scatter, we would expect the scatter to be the same for both coatings. It thus appears that particles from ZnS and ThF_4 account for at least part of the scatter present, with ThF_4 providing more scatter particles than ZnS. When Perry performed thick film scatter comparisons on ZnS and ThF_4 in 1965⁵, he found that ThF_4 was the source of almost all the scatter centers. Since that time, however, he has found ways of greatly reducing the ThF_4 contribution until it now only slightly exceeds the ZnS contribution.

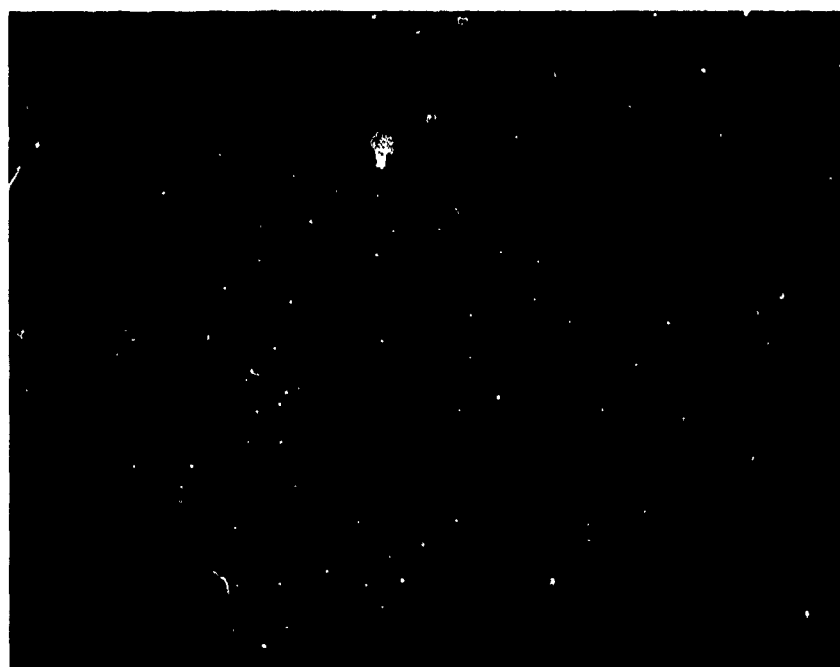
It appears that cryolite contributes even fewer scatter centers than ThF_4 . Evidence for this is provided by Figs. 15c and 15a which show that a ZnS-cryolite coating has less scatter than a ZnS- ThF_4 coating.

4.3 COATING SCATTER CAUSED BY THE PYROELECTRIC EFFECT

The coating scatter data of Section 4.2 was for coatings deposited on fused quartz substrates. One would expect that the scatter properties of coatings on lithium niobate substrates would be similar. This has not been the case, however. During the past several years, we have consistently found that when lithium niobate and fused quartz substrates were coated at the same time, the coating scatter was much greater in the lithium niobate coating.



(a)



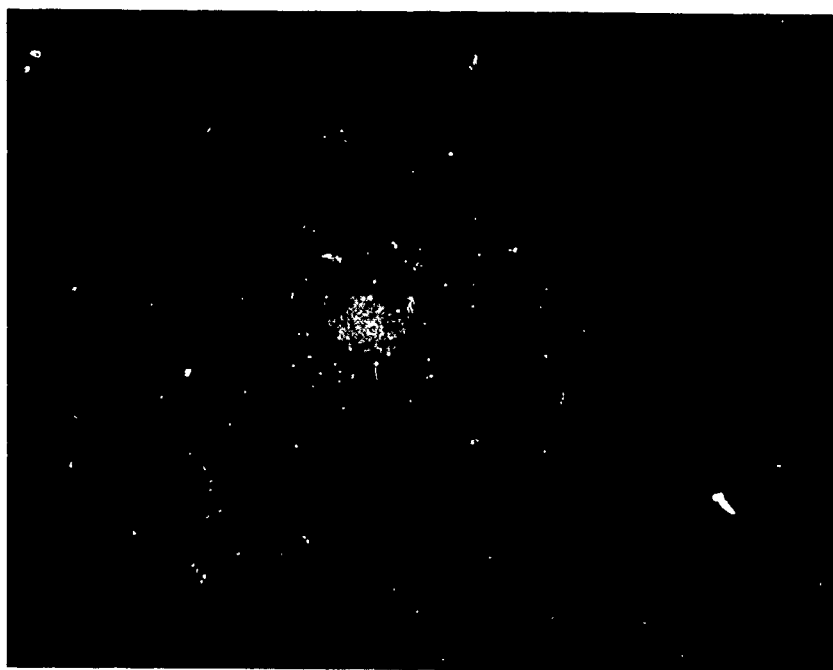
(b)

Figure 17 Thick layer of (a) ZnS and (b) ThF_4 on fused quartz substrates. Both layers are about 10 microns thick.

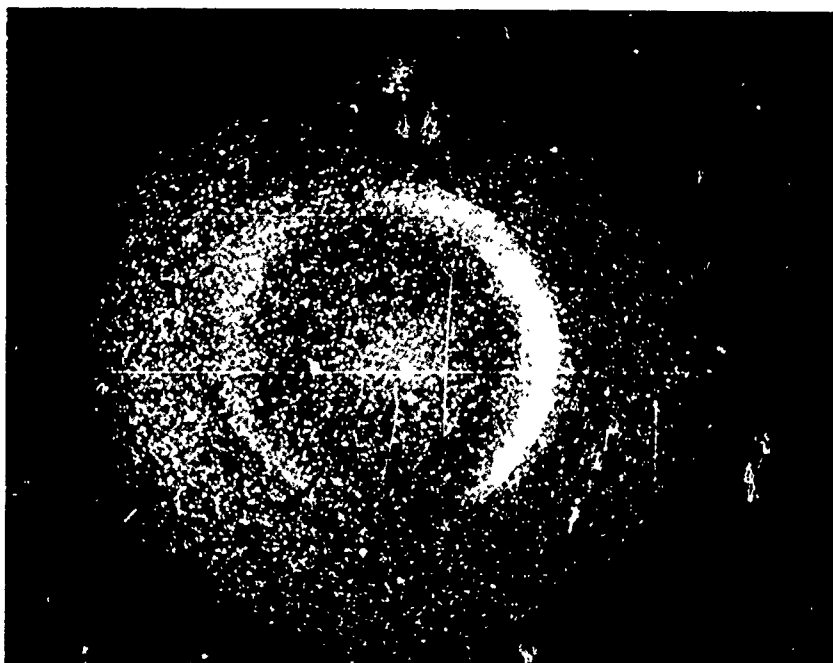
Examples of this are given in Figs. 18 and 19. Figure 18 shows doubly-resonant ZnS-ThF_4 coatings of the design of Fig. 7 deposited on (a) fused quartz and (b) lithium niobate. These two substrates were coated at the same time mounted in the same holder. Figure 19 shows doubly-resonant 2.16 micron hard coatings of the design of Fig. 5 deposited on (a) fused quartz and (b) lithium niobate. These two coatings were also deposited at the same time with the two substrates adjacent to each other. The coatings of Fig. 18 are by Lambda; the coatings of Fig. 19 are by Spectrum Systems. The Fig. 18 coatings are composed of ZnS-ThF_4 ; the Fig. 19 coatings are composed of hard, refractory materials. Yet this effect is seen in both these cases and we have observed it in numerous other cases. We have a theory concerning the cause of this effect which will now be given.

We propose that the pyroelectric effect in LiNbO_3 is responsible for the increased scatter evident in coatings deposited on its surfaces. Pyroelectric crystals have the property of developing an electric polarization when their temperature is changed. For lithium niobate, the induced polarization is along the crystalline z axis. With this induced polarization, the crystal is effectively electrically charged and will attract other charged particles (such as dust particles in a coating chamber) to its surface. In a coating chamber, the lithium niobate crystal (and all other substrates also) is heated either intentionally or by accident (such as by heat radiated from the resistive-heating coil located at the source). As we will show, even a temperature rise of 10°C or so is sufficient to induce a substantial polarization in the crystal.

We have performed tests to measure the induced polarization as a function of temperature on two different lithium niobate crystals. The first crystal was oriented with its z axis at an angle of 46° to its end faces as in Fig. 1. This crystal was a typical oscillator crystal and was uncoated. Since the z axis has a component perpendicular to the crystal end faces, we expect to see induced charge on the crystal ends. The second crystal was oriented with its z axis parallel to its end faces. This crystal orientation is not useful for our oscillator work, but is widely used in second-harmonic generation work. For the second crystal, the z axis has no component perpendicular to its end faces, and thus we expect no induced charge. During our tests, the crystals were mounted in (a) a copper (parametric oscillator) oven and (b) an insulating oven. These ovens made good contact with the sides of the

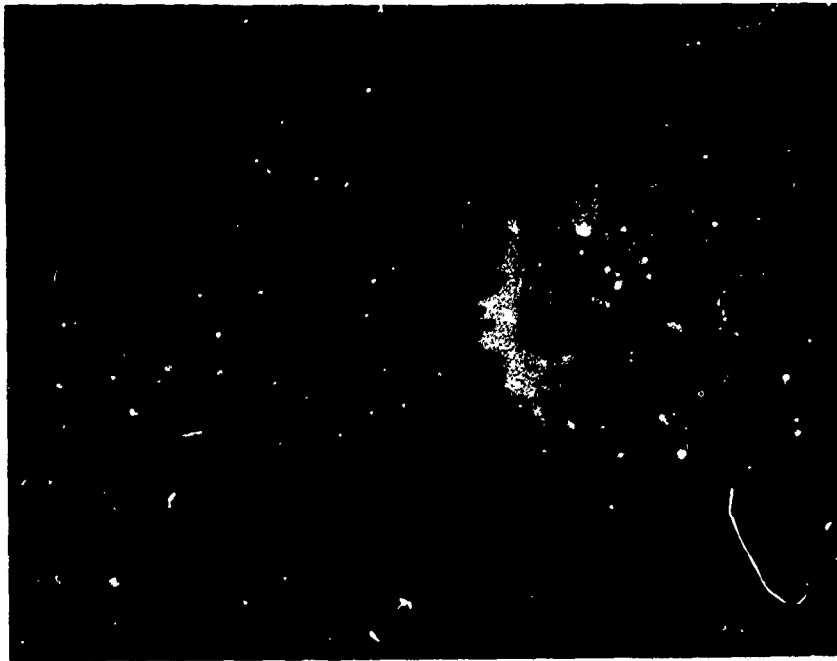


(a)

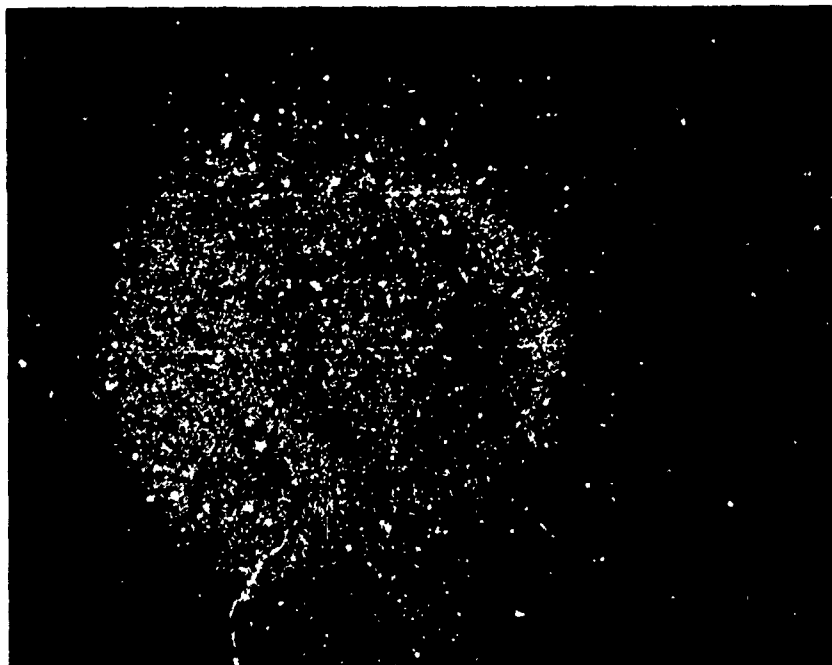


(b)

Figure 18 Scatter present in ZnS-ThF₄ coatings deposited on (a) fused quartz substrate, and (b) lithium niobate substrate.



(a)



(b)

Figure 19 Scatter present in Spectrum Systems coatings deposited on
(a) fused quartz substrate, and (b) lithium niobate substrate.

crystals but did not touch the crystal ends. An electro-static probe was placed about 0.035" from one face of the crystal under test and was connected to an electrometer. The electrometer reading drove the y axis of an x-y recorder and the x axis plotted the oven temperature. The following results were obtained from our experiments:

1) As expected, the crystal with $\theta = 44^\circ$ has a substantial induced polarization whereas the crystal with $\theta = 90^\circ$ has virtually none. The data from this experiment is shown in Fig. 20. Both of these tests were performed with the crystals held in snug-fitting copper ovens.

2) The data of Fig. 21 shows that lithium niobate with $\theta = 44^\circ$ has a large induced polarization whereas a fused quartz substrate has none. Fused quartz is an amorphous material and hence is not expected to have a pyroelectric effect. Thus in a coating chamber, fused quartz substrates would not attract charged dust particles but lithium niobate substrates would.

3) Figure 22 shows the induced polarizations for a lithium niobate crystal with $\theta = 44^\circ$ which was mounted in three different ways. The crystal was mounted in (a) an (electrically) insulating oven, (b) a copper oven, but with the crystal protruding 1/8" out the end, and (c) a copper oven with the crystal flush to the end. With the $\theta = 44^\circ$ orientation, polarization is induced on the sides of the crystal as well as the ends. This experiment points up the importance of having good electrical contact to the sides of the crystal in order to neutralize that polarization.

4) The results of Fig. 23 are for a similar experiment as in 3), but this time the crystal is lithium niobate with $\theta = 90^\circ$. These results show that even for $\theta = 90^\circ$, some net induced polarization will appear unless good electrical contact is made between the holder and the crystal sides.

5) Tests were run in order to determine whether the induced polarization would gradually disappear with time (say, through leakage conduction inside the crystal). We found that any such decay which is present has a very long time constant. Over a 15 minute period during which the oven temperature was held constant, the induced polarization decayed less than 2%. Thus if polarization is induced in a crystal which is to be coated, that polarization will not "leak off" of its own accord.

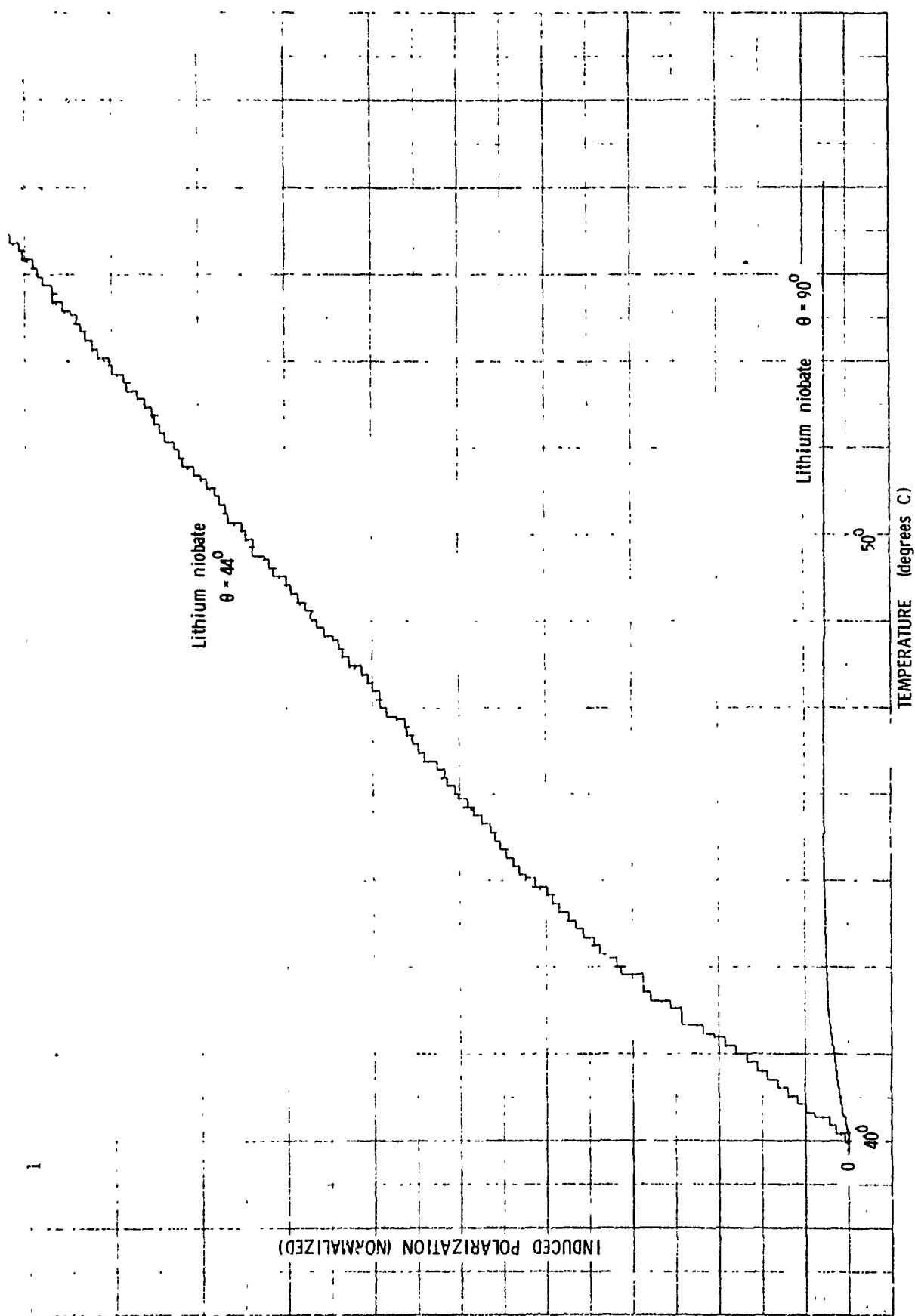


Figure 20 Pyroelectric induced polarizations for lithium niobate crystals having (a) $\theta = 44^\circ$, and (b) $\theta = 90^\circ$

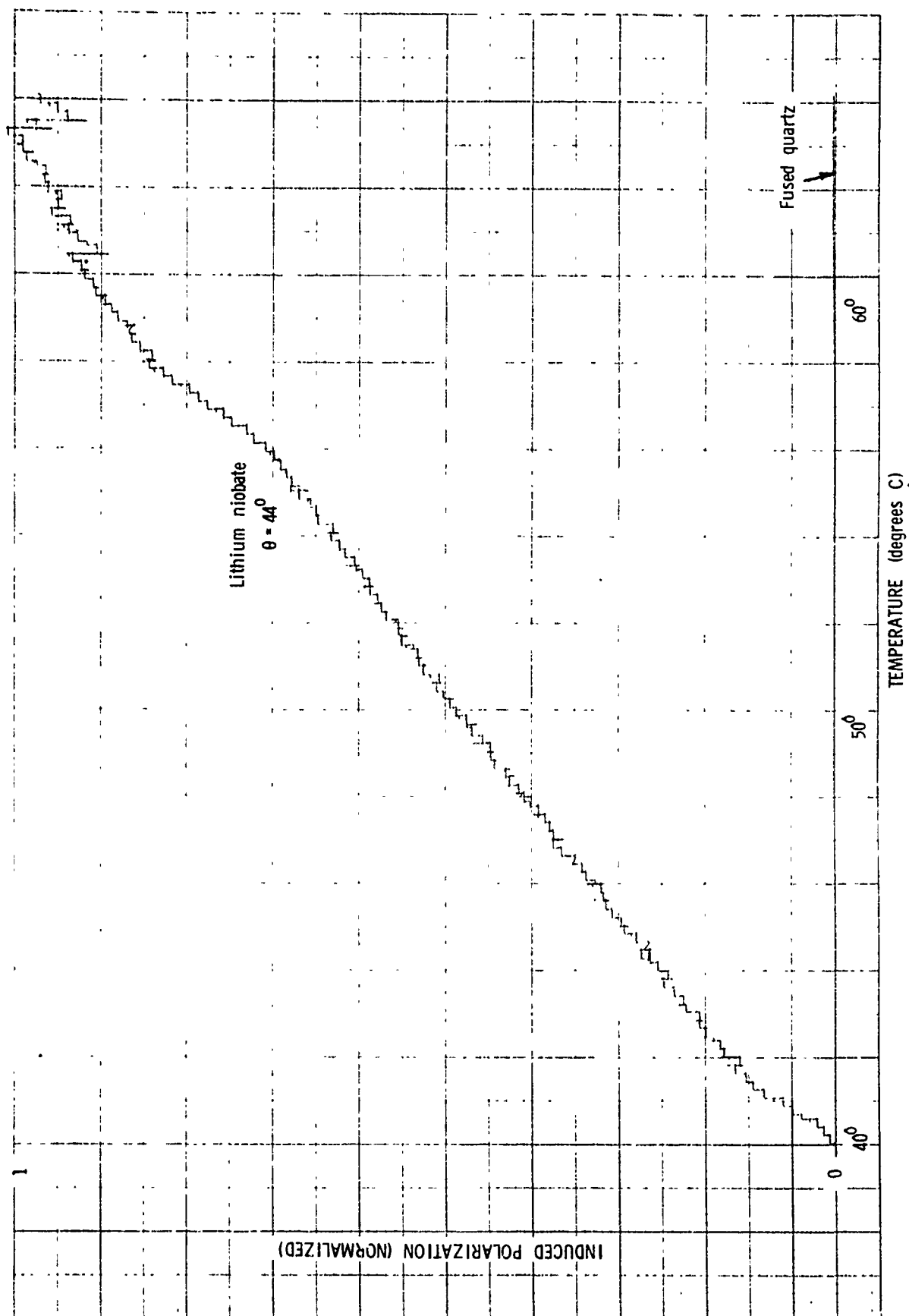


Figure 21 Pyroelectric induced polarizations for (a) lithium niobate with $\theta = 44^\circ$, and (b) fused quartz substrate.

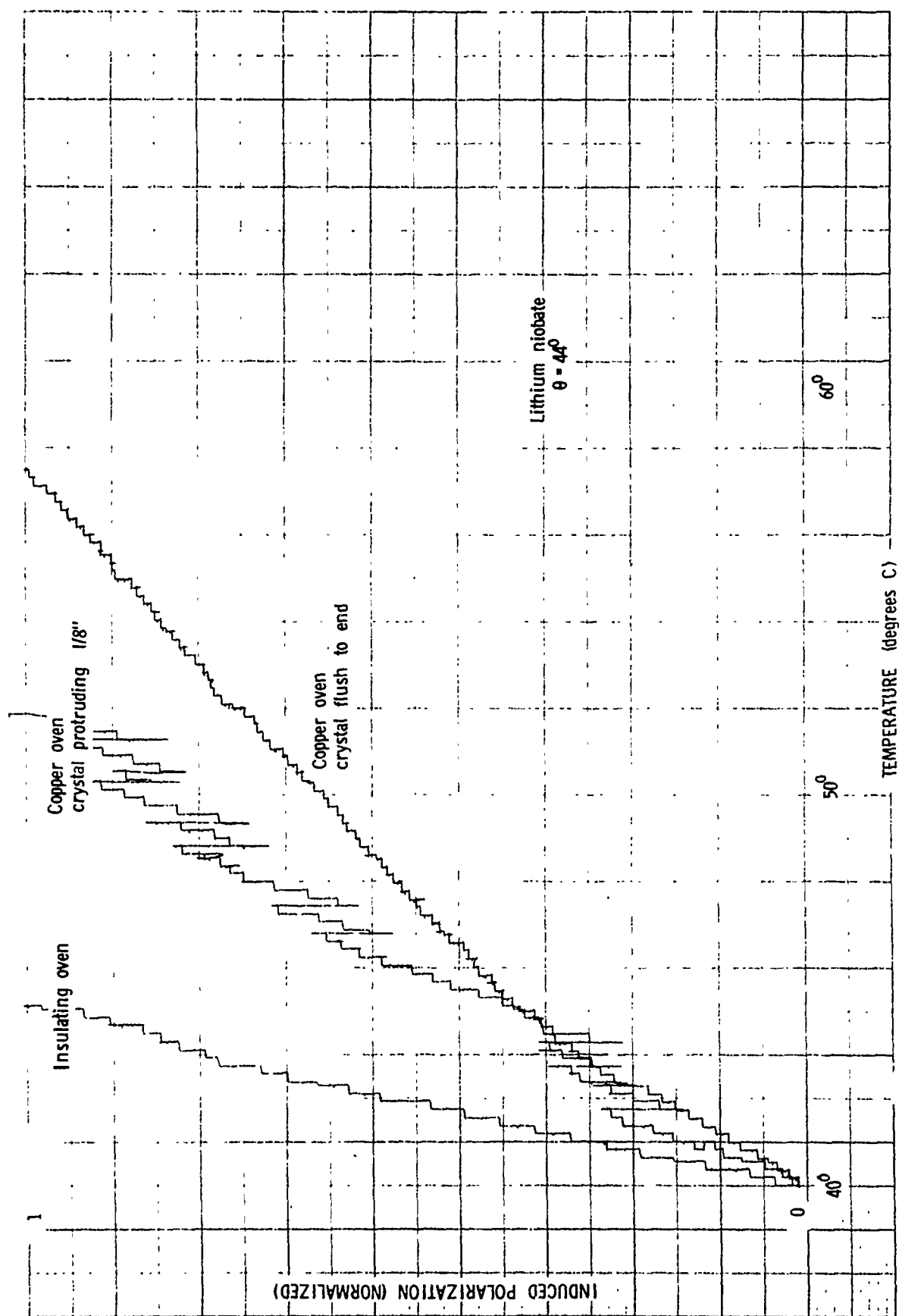


Figure 22 Pyroelectric induced polarizations for lithium niobate having $\theta = 44^\circ$ for three different mountings: (a) electrically insulating oven, (b) copper oven, but with the crystal protruding 1/8" beyond the end, and (c) copper oven with crystal flush to end.

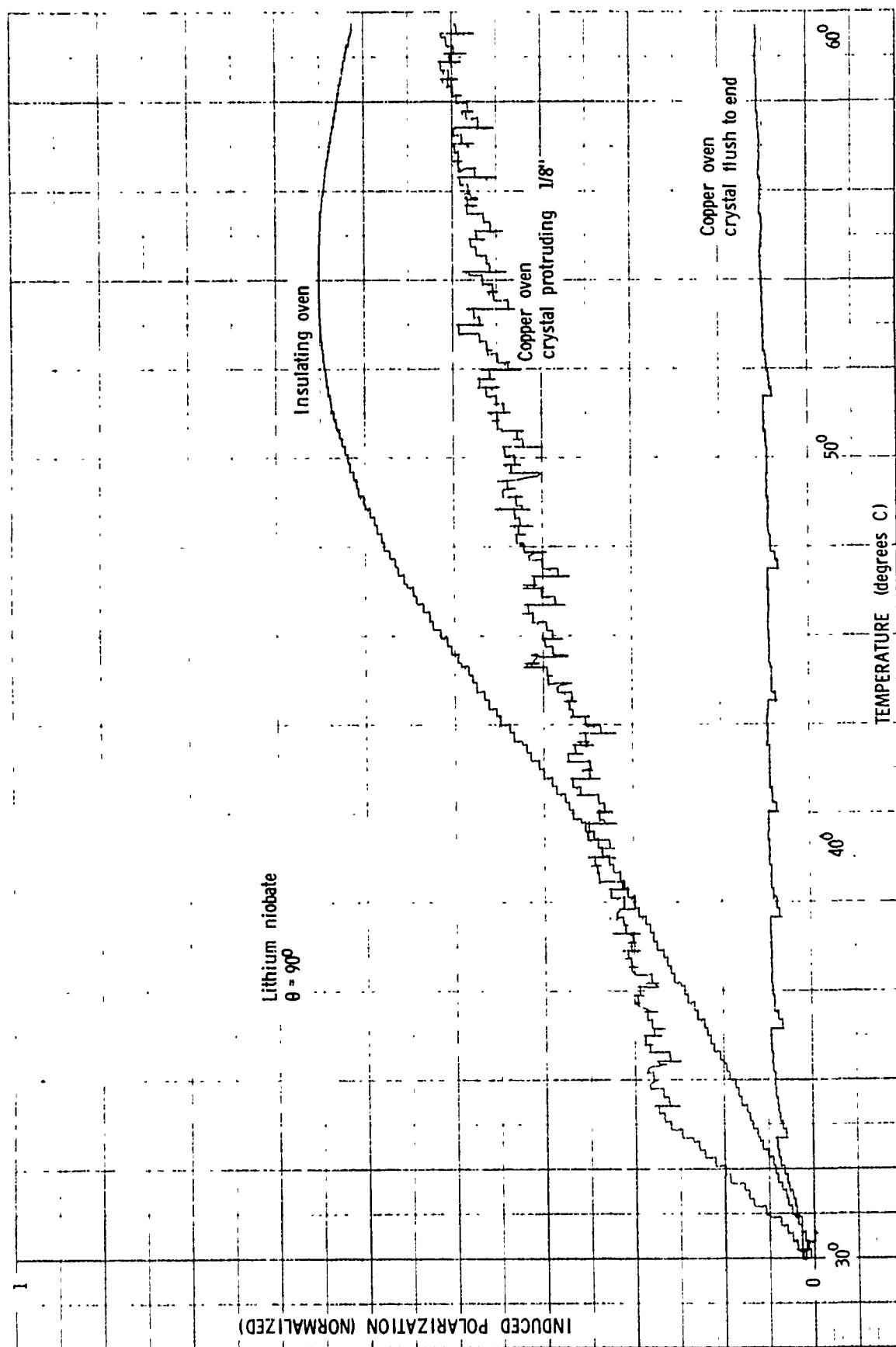


Figure 23 Pyroelectric induced polarizations for lithium niobate having $\theta = 90^\circ$ for three different mountings: (a) electrically insulating oven, (b) copper oven, but with the crystal protruding 1/8" beyond the end, and (c) copper oven with crystal flush to end.

In light of these results, several conclusions can be stated with respect to the pyroelectric effect in lithium niobate crystals which are to be coated. In order to minimize the induced pyroelectric polarization, one could try the following approaches:

(1) The lithium niobate crystal should be kept as near to room temperature as possible. For coatings which don't require heated substrates, one might consider circulating cooling water through the substrate holder to minimize heating. If the coating requires a heated substrate, then this problem is much more difficult to cope with.

(2) The lithium niobate should be placed in an electrically conducting holder which makes good electrical contact with the sides of the crystal. The holder should be electrically grounded.

(3) Care should be taken when cleaning the crystal and preparing it for insertion into the coating chamber. If, for example, the crystal is cooled during cleaning and then grounded while cool, it will have an induced polarization when it again reaches room temperature.

(4) If the initial coating deposited were conducting, then this coating would serve to ground the crystal face. One must take care however, to use a conducting coating that has satisfactory scatter and damage properties, and this may not be easy to find.

It should be emphasized that the pyroelectric effect theory which we have discussed here has not yet been conclusively proven. This idea occurred very late in this program when insufficient time or money remained to conclusively test its validity. We feel there is a high probability that it is correct, however, and suggest that it is worthy of further investigation.

Section V

SPECTRAL TRANSMITTANCES OF FABRICATED MIRRORS

5.1 MIRROR COATING TYPES #1 AND #2

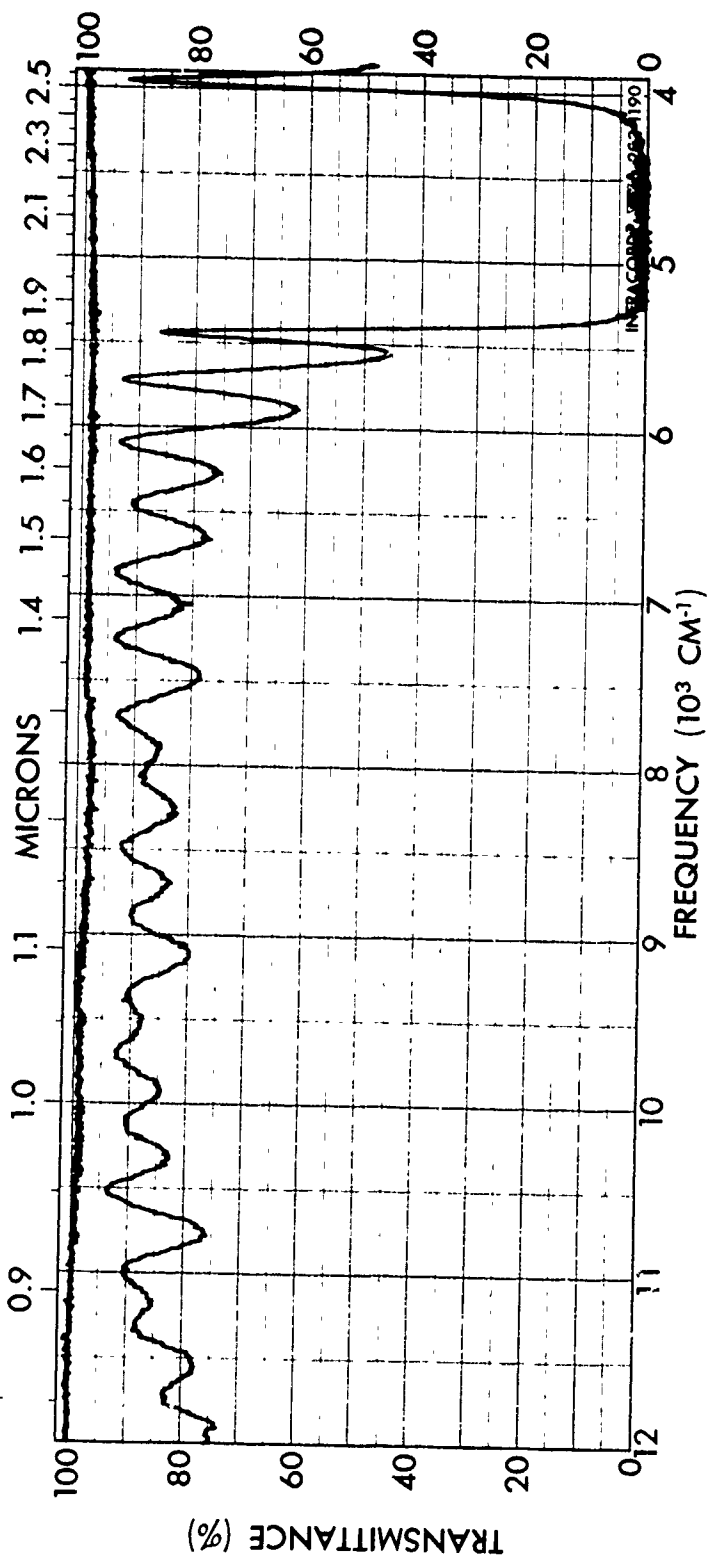
In this section, we give data on the measured spectral transmittances of oscillator coatings which are (1) HR, and (2) slightly transmitting at 2.16 microns. These types of coatings have the general designs shown in Figs. 5 and 6 and were discussed in Sections 2.3.1 and 2.3.2. The transmittances shown were measured on the PE 137G spectrophotometer shown in Fig. 12.

5.1.1 ZnS-ThF₄ Mirrors

As mentioned in Section 2.1.1, ZnS and ThF₄ are materials which have excellent behavior during deposition. Their indices of refraction are well known, and do not vary appreciably during a coating run. This means that the spectral transmittance of mirrors which employ these materials can be controlled quite well.

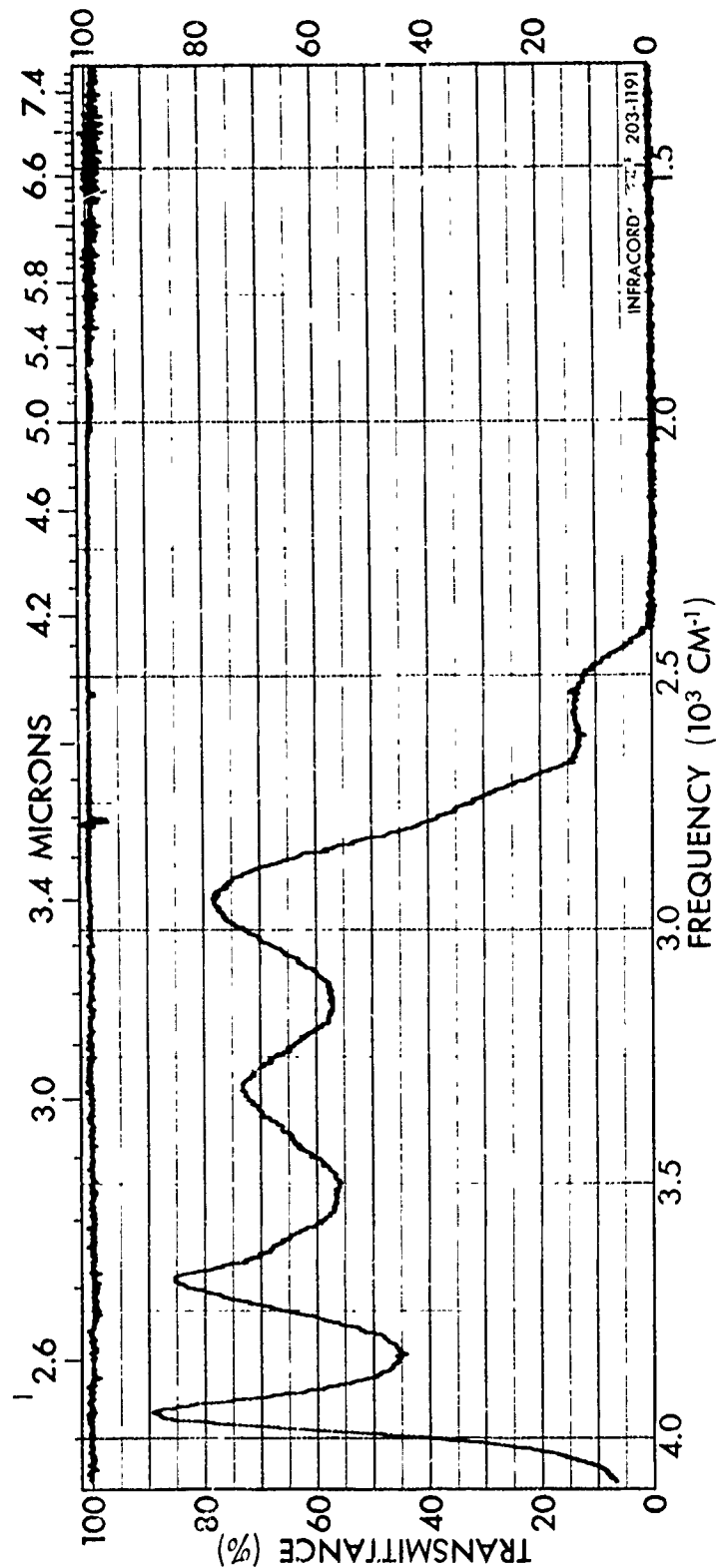
In Figs. 24a and 24b we show the measured spectral transmittance of a ZnS-ThF₄ mirror which is HR at 2.16 microns. This mirror is on a fused quartz substrate. As seen in Figs. 24, the HR region extends from about 1.90 to 2.32 microns, a bandwidth of about 0.42 microns. At the pump wavelength of 1.08 microns the transmittance is 85%. Since the back surface of the fused quartz substrate is uncoated, the true 1.08 micron transmittance of the coating is actually more like 89% instead of 85%. All of the spectral characteristics of this coating are quite satisfactory.

Figures 25a and 25b show the measured spectral transmittance of a ZnS-ThF₄ mirror which is slightly transmitting at 2.16 microns. This mirror is also on a fused quartz substrate. The transmission is approximately 7% at 2.15 microns. The 1.08 micron pump transmission is 90%. It should be noted that the bandwidth of the transmitting mirror is smaller than that of the HR mirror. This characteristic is inherent in the mirror designs of Figs. 5 and 6. The bandwidth of a doubly-resonant 2 micron parametric oscillator is essentially limited by the bandwidth of the transmitting coating. A recommendation for future work in this area is that studies be carried out to develop partially transmitting mirror designs with greater bandwidths than presently attainable.



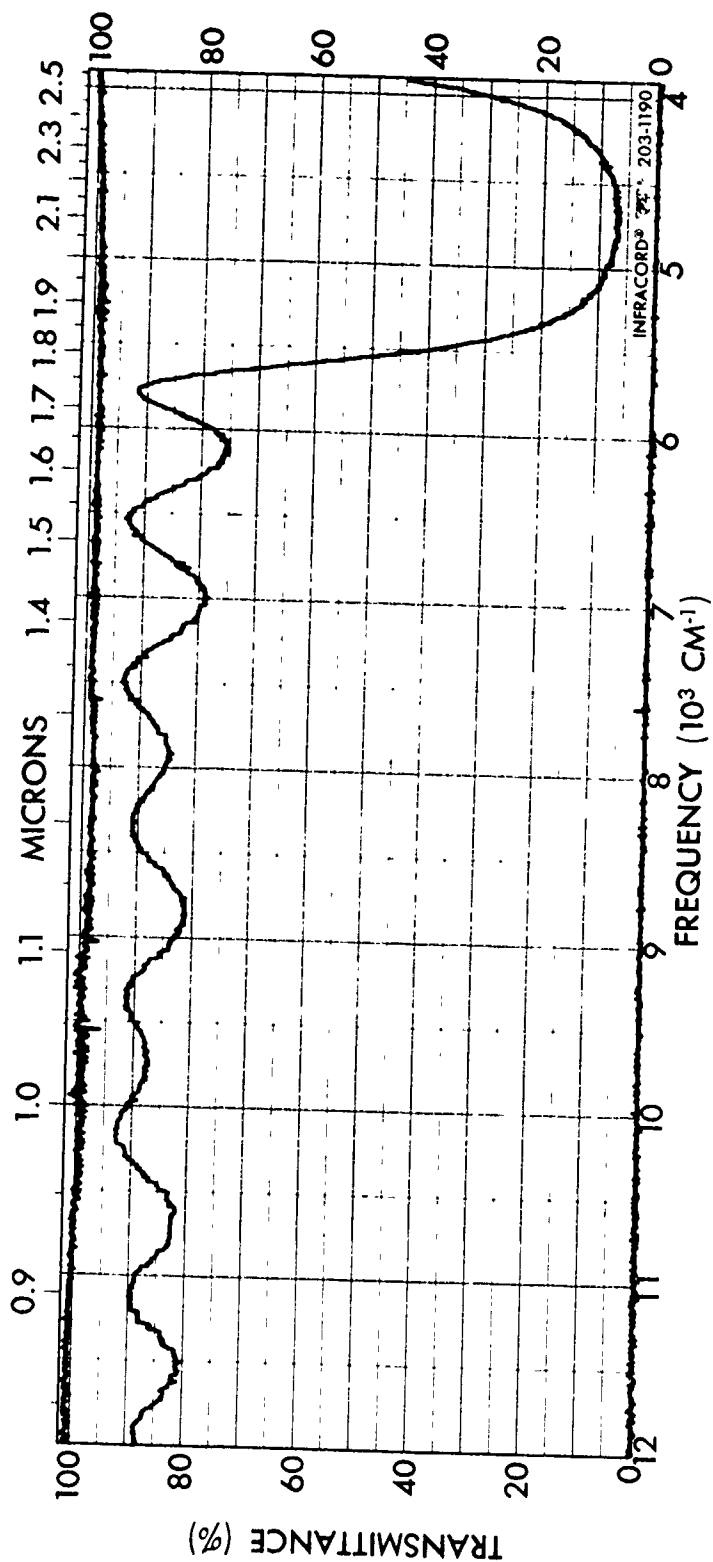
SPECTRUM NO. _____		LEGEND		REMARKS	
SAMPLE Substrate #2		1. _____		infrasil fused quartz sub- strate	
ZnS-ThF ₄ coating		2. _____			
HR at 2.16 microns		DATE			
		THICKNESS		OPERATOR Wintemute	

Figure 24 Measured spectral transmittance of ZnS-ThF₄ mirror which is
(a) HR at 2.16 microns.



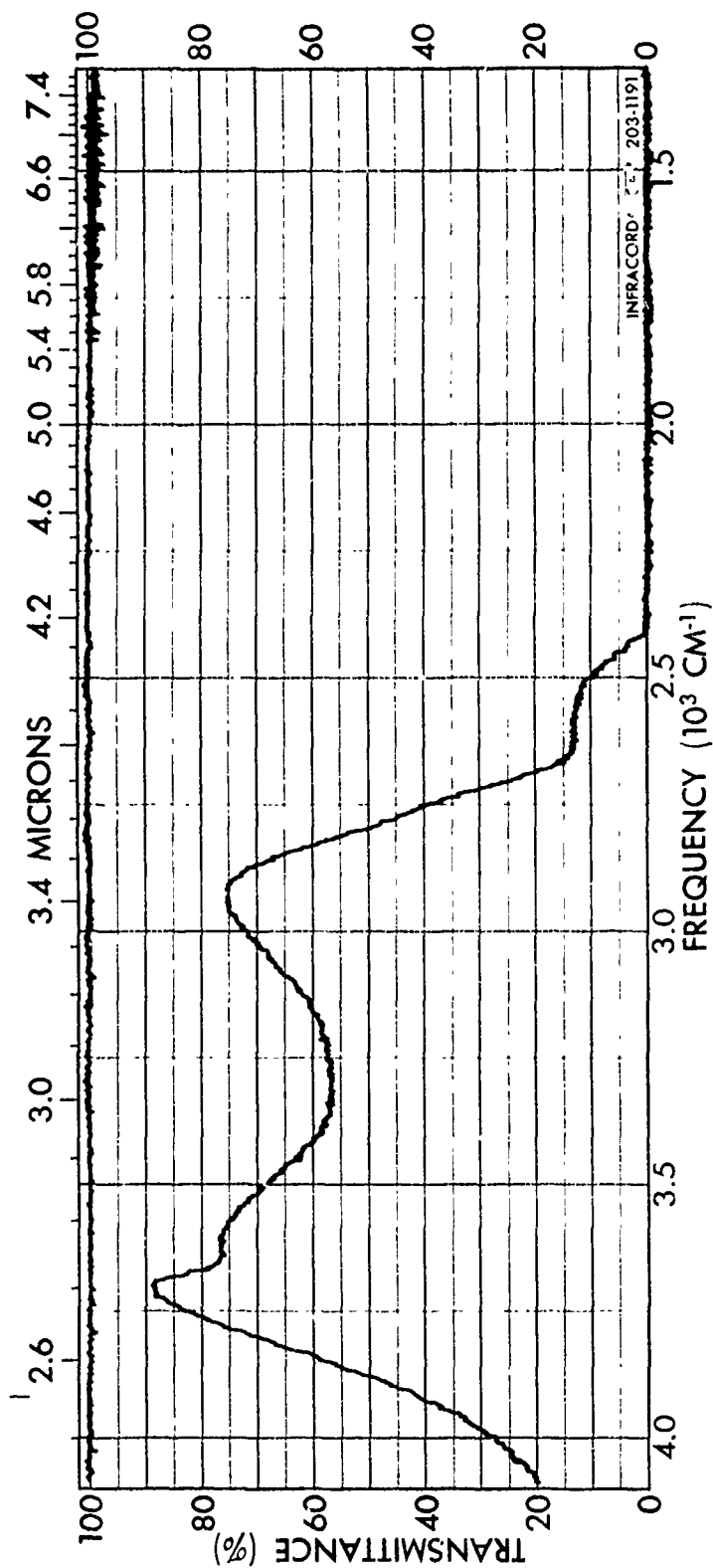
SPECTRUM NO. _____		REMARKS _____	
SAMPLE Substrate #2		Infrasil fused quartz sub- strate	
ZnS-ThF ₄ coating		1. _____	
IR at 2.16 microns		2. _____	
THICKNESS _____		DATE _____	
ORIGIN Lambda Optics		OPERATOR Wintemute	
PURITY _____			
PHASE _____			

Figure 24 Measured spectral transmittance of ZnS-ThF₄ mirror which is HR (b) at 2.16 microns.



SPECTRUM NO. _____		SPECTRUM NO. _____	
SAMPLE Substrate #5		SAMPLE _____	
ZnS-ThF ₄ coating		infrasil fused quartz sub- strate	
Transmitting at 2.16 microns		1. _____	
PHASE _____		2. _____	
THICKNESS _____		DATE _____	
_____		OPERATOR Wintemite	

Figure 25 Measured spectral transmittance of ZnS-ThF₄ mirror which is slightly transmitting at 2.16 microns.
(a)



SPECTRUM NO. _____
SAMPLE _____

SPECTRUM NO. _____	ORIGIN <u>Lambda Optics</u>	LEGEND _____	REMARKS _____
SAMPLE <u>Substrate #5</u>	1. _____	2. _____	<u>Infrasil fused quartz sub-</u> <u>strate</u>
<u>ZnS-ThF₄ coating</u>	PURITY _____	DATE _____	
<u>Transmitting at 2.16 microns</u>	PHASE _____	OPERATOR <u>Wintemute</u>	
	THICKNESS _____		

Figure 25 Measured spectral transmittance of ZnS-ThF₄ mirror which is slightly transmitting at 2.16 microns.

5.1.2 ZnS-ThF₄ Overcoated with Al₂O₃

An important question is whether the half-wave overcoating of Al₂O₃ affects the spectral transmittance of ZnS-ThF₄ mirrors. In Figs. 26a and 26b we show measured spectral transmittances for HR ZnS-ThF₄ coatings with and without an Al₂O₃ overcoating. The ZnS-ThF₄ portions of these two coatings were deposited at the same time. It can be seen from Figs. 26 that the transmittance of the ZnS-ThF₄ coating is virtually unaffected by the presence of an Al₂O₃ overcoating. The slight differences in transmittance which do occur in Figs. 26 are due to other causes as will be explained in Section 5.3.

Figures 27a and 27b show transmittances for transmitting 2 micron coatings of ZnS-ThF₄ with and without Al₂O₃ overcoatings. Again we see that the overcoating has a negligible effect on the coating transmittance.

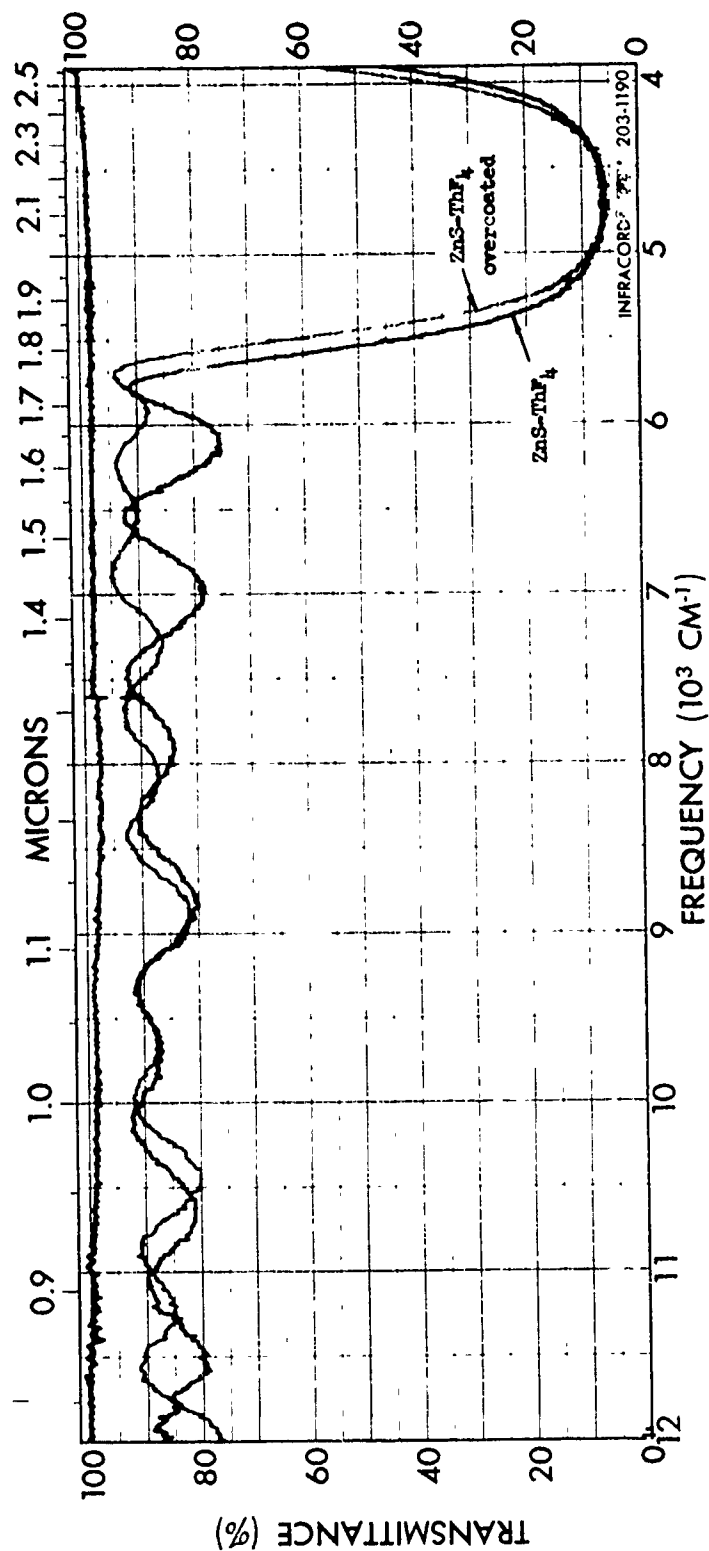
5.1.3 ZnS-Cryolite Mirrors

Cryolite is another material having reproducible, well behaved coating properties. Thus we would not expect to encounter difficulties in obtaining desired transmittances with ZnS-cryolite mirrors. The spectral transmittance of an HR ZnS-cryolite mirror is shown in Figs. 27a and 27b. The HR region of this mirror extends from 1.86 to 2.42 microns, covering a region of 0.56 microns. This bandwidth is greater than that obtainable from ZnS-ThF₄ mirrors because of the greater difference in indices of ZnS and cryolite. The 1.08 micron transmission is 87%, which is quite acceptable.

The spectral transmittance of a transmitting 2 micron ZnS-cryolite coating is given in Figs. 28a and 28b. The coating has transmission of 4% at a wavelength of 2.15 microns, and a transmission of 91% at 1.08 microns. Again the bandwidth of this coating is greater than that of the corresponding ZnS-ThF₄ coating because of the indices of the materials involved.

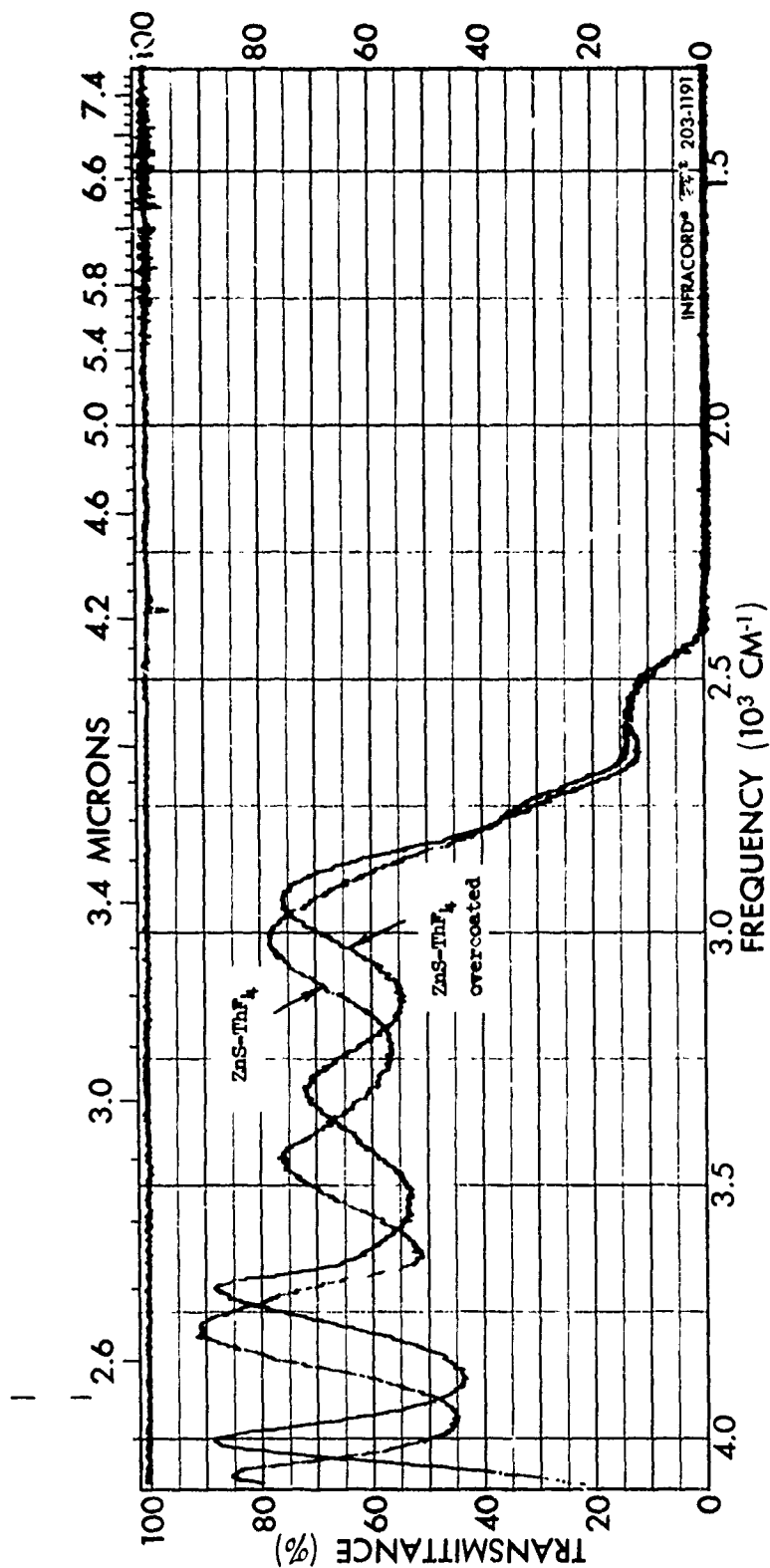
5.1.4 ZnS-Cryolite Overcoated with Al₂O₃

The transmittances of HR and transmitting overcoated ZnS-cryolite mirrors are shown in Figs. 30 and 31, respectively. The Al₂O₃ overcoating again causes no problems with mirror transmittance and, if anything, slightly increases the transmittance away from the 2 micron region. The wavelength effect of Fig. 30 is not due to the overcoating as mentioned earlier, but will be explained later.



SPECTRUM NO. 14a		REMARKS Comparison of regular and overcoated ZnS-ThF ₄ transmitting coatings.	
SAMPLE Lot #1 (red) Lot #2 (blue)			
Substrate #5 (red) Substrate #10 (blue)		LEGEND	
Trans 2u coating (red) Trans 2u coating (blue)		ORIGIN Lambda coatings (red) ZnS-ThF ₄ (blue) ZnS-ThF ₄ overcoated	
PURITY		DATE December 6, 1971	
PHASE		OPERATOR J. Wintermute	
THICKNESS			

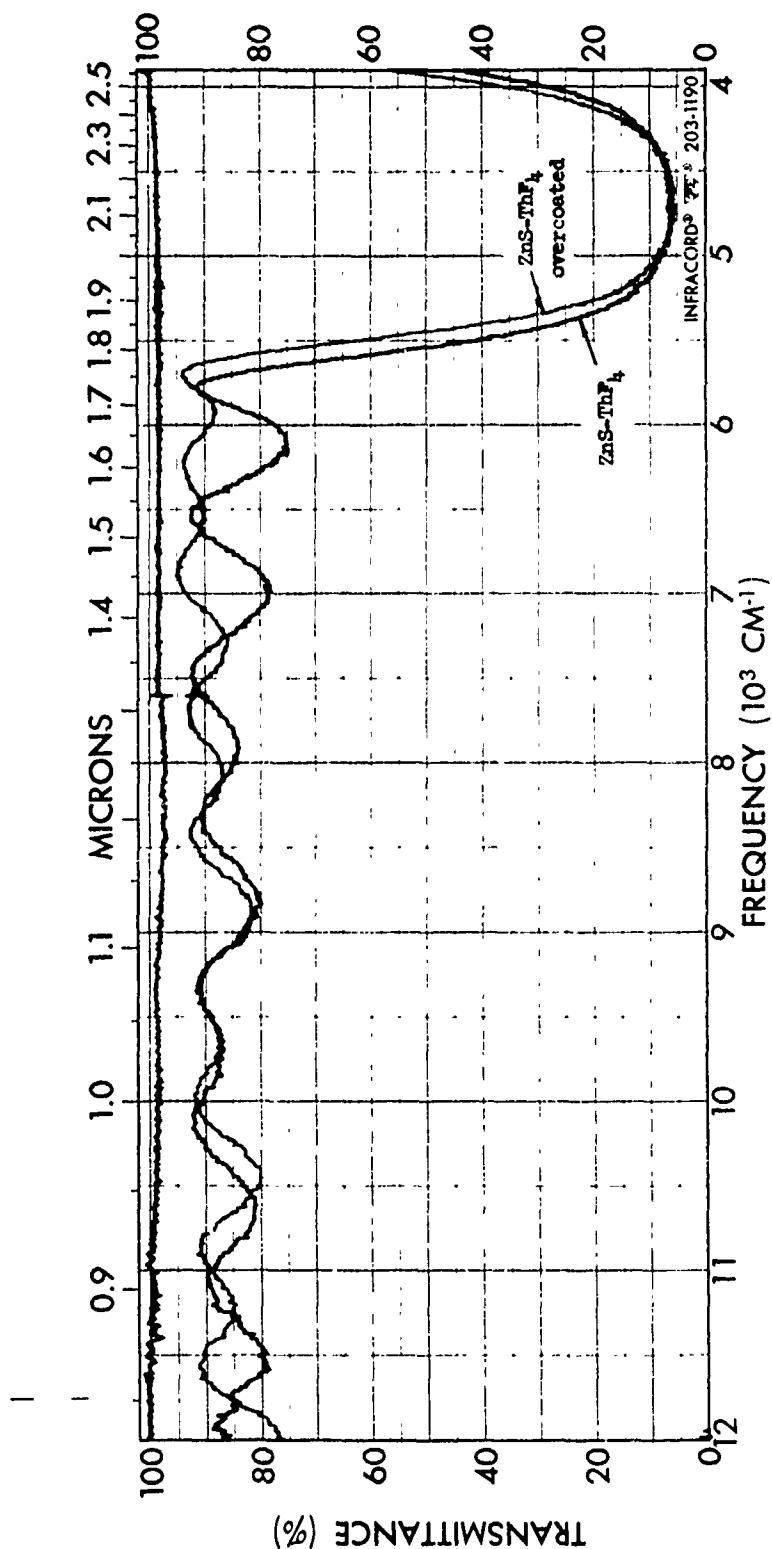
Figure 26 Comparison of spectral transmittances of ZnS-ThF₄ mirrors with and without Al₂O₃ overcoatings which are HR at 2.16 microns.



SPECTRUM NO. _____
SAMPLE _____

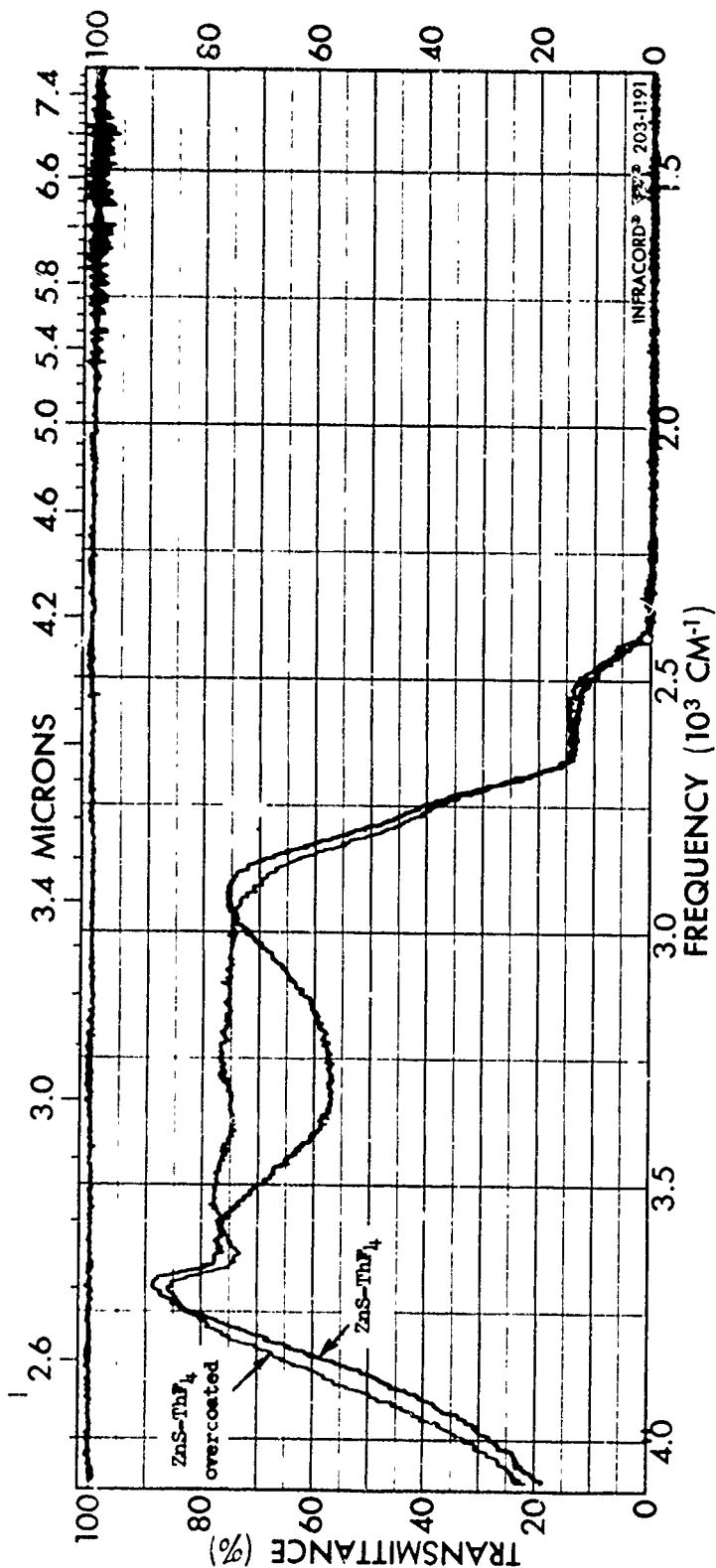
<p>SPECTRUM NO. 1b</p> <p>SAMPLE Lot #1 (red) Lot #2 (blue)</p> <p>Substrate #1 (red) Substrate #7 (blue)</p> <p>HR 2u coating (red) HR 2u coating (blue)</p>	<p>ORIGIN Lambda coatings</p> <p>(red) ZnS-ThF₄ (blue) ZnS-ThF₄ overcoated with Al₂O₃</p> <p>PURITY</p> <p>PHASE</p> <p>THICKNESS</p>	<p>LEGEND</p> <p>DATE November 12, 1971</p> <p>OPERATOR J. Wintermute</p>	<p>REMARKS Comparison of regular and overcoated HR ZnS-ThF₄ coatings</p>
---	---	--	--

Figure 26 Comparison of spectral transmittances of ZnS-ThF₄ mirrors with and without Al₂O₃ overcoatings which are HR at 2.16 microns.



SPECTRUM NO. 14a		SPECTRUM NO. _____	
Lot #1 (red)		REMARKS Comparison of regular and overcoated ZnS-ThF ₄ transmitting coatings.	
Lot #2 (blue)			
Substrate #5 (red)		LEGEND	
Substrate #10 (blue)			
Trans 2u coating (red)		ORIGIN Lambda coatings	
Trans 2u coating (blue)		(red) ZnS-ThF ₄	
		(blue) ZnS-ThF ₄ overcoated	
PURITY		DATE December 6, 1971	
PHASE		OPERATOR J. Wintemute	
THICKNESS			

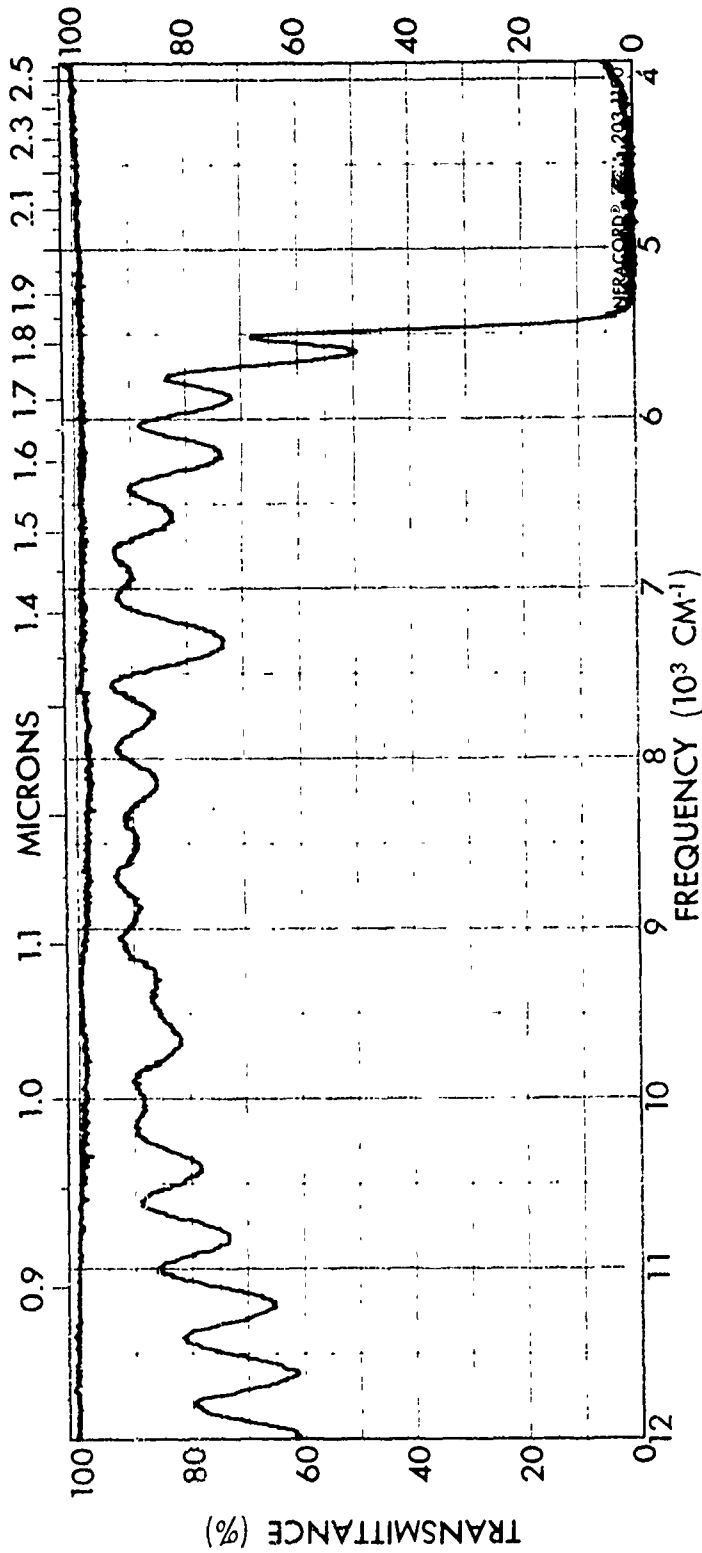
Figure 27 Comparison of spectral transmittances of ZnS-ThF₄ mirrors with and without Al₂O₃ overcoatings which are slightly transmitting at 2.16 microns.



SPECTRUM NO. _____
SAMPLE

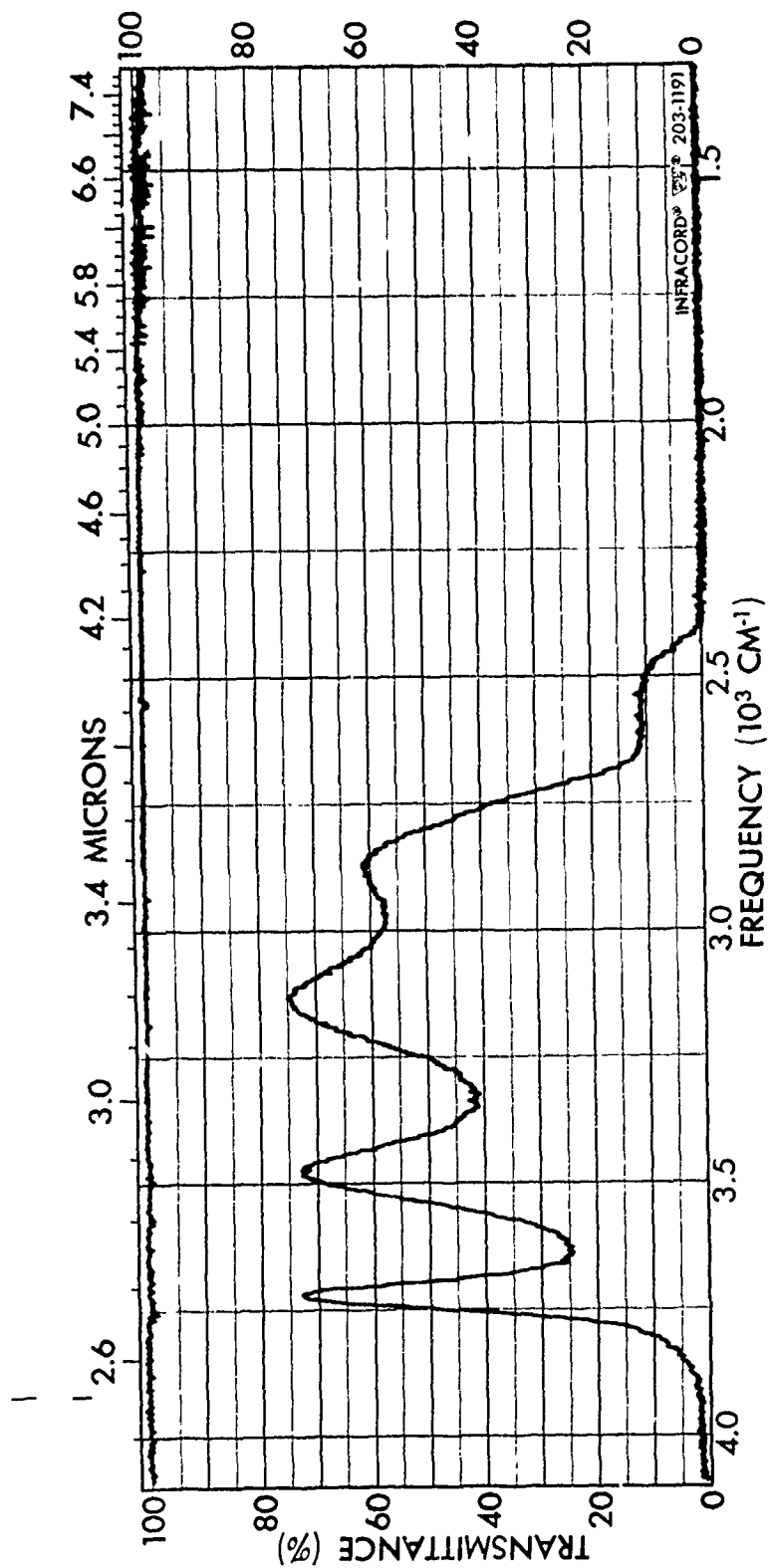
SPECTRUM NO. 14b Lot #1 (red) Lot #2 (blue)	ORIGIN Lambda coatings (red) ZnS-ThF ₄ (blue) ZnS-ThF ₄ overcoated	LEGEND	REMARKS Comparison of regular and overcoated ZnS-ThF ₄ transmitting coatings.
Substrate #5 (red) Substrate #10 (blue)	PURITY		
Trans Al coating (red) Trans Al coating (blue)	PHASE	DATE December 6, 1971	
	THICKNESS	OPERATOR J. Wintemute	

Figure 27 Comparison of spectral transmittances of ZnS-ThF₄ mirrors with and without Al₂O₃ overcoatings which are slightly transmitting at 2.16 microns.
(b)



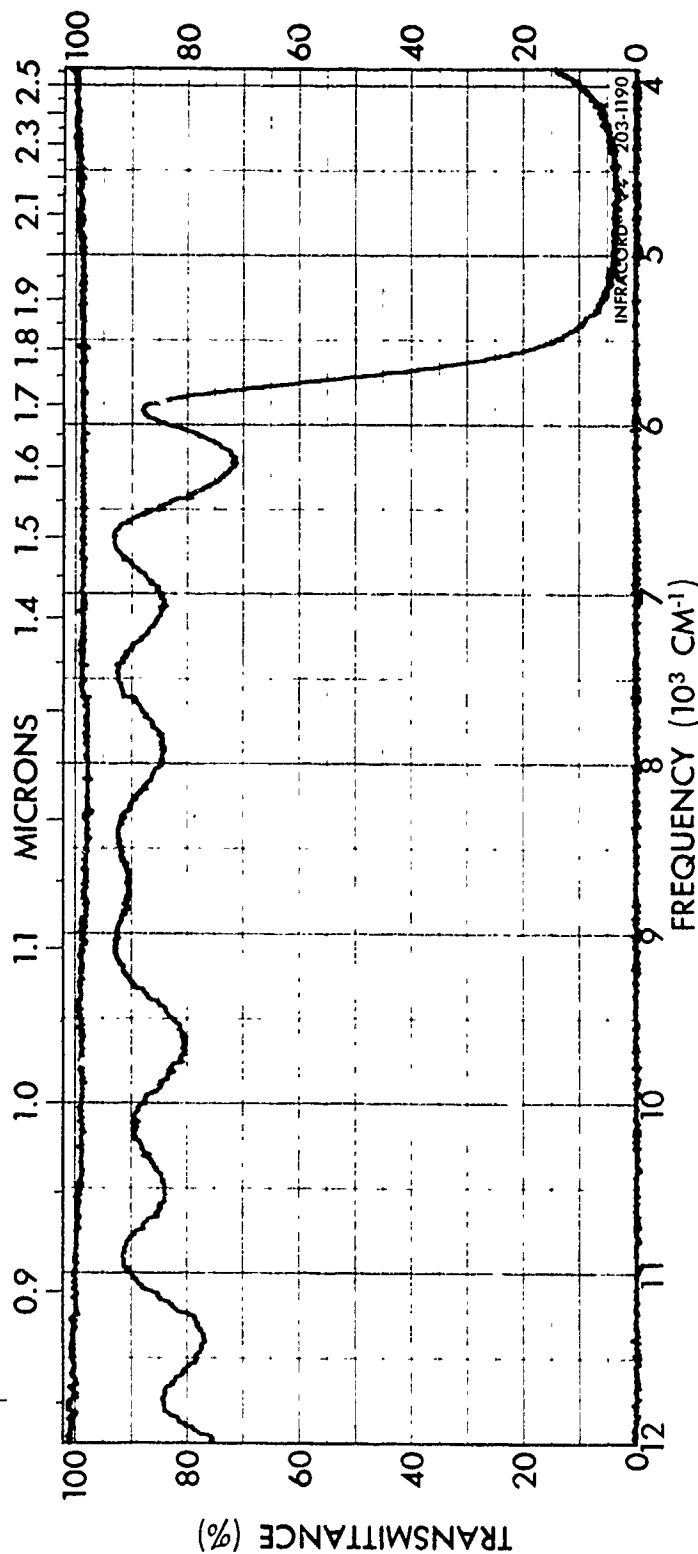
SPECTRUM NO. _____		SPECTRUM NO. _____	
SAMPLE Substrate #13		SAMPLE _____	
ZnS-cryolite coating		Infrasil fused quartz substrate	
HR at 2.16 microns		DATE _____	
THICKNESS _____		OPERATOR Wintemute	

Figure 23 Measured spectral transmittance of ZnS-cryolite mirror which is HR at 2.16 microns.



SPECTRUM NO. _____		LEGEND _____		REMARKS _____	
SAMPLE Substrate #13		1. _____		Infrasil fused quartz sub- strate	
ZnS-cryolite coating		2. _____		_____	
HR at 2.16 microns		DATE _____		_____	
THICKNESS _____		OPERATOR Wintemute		_____	

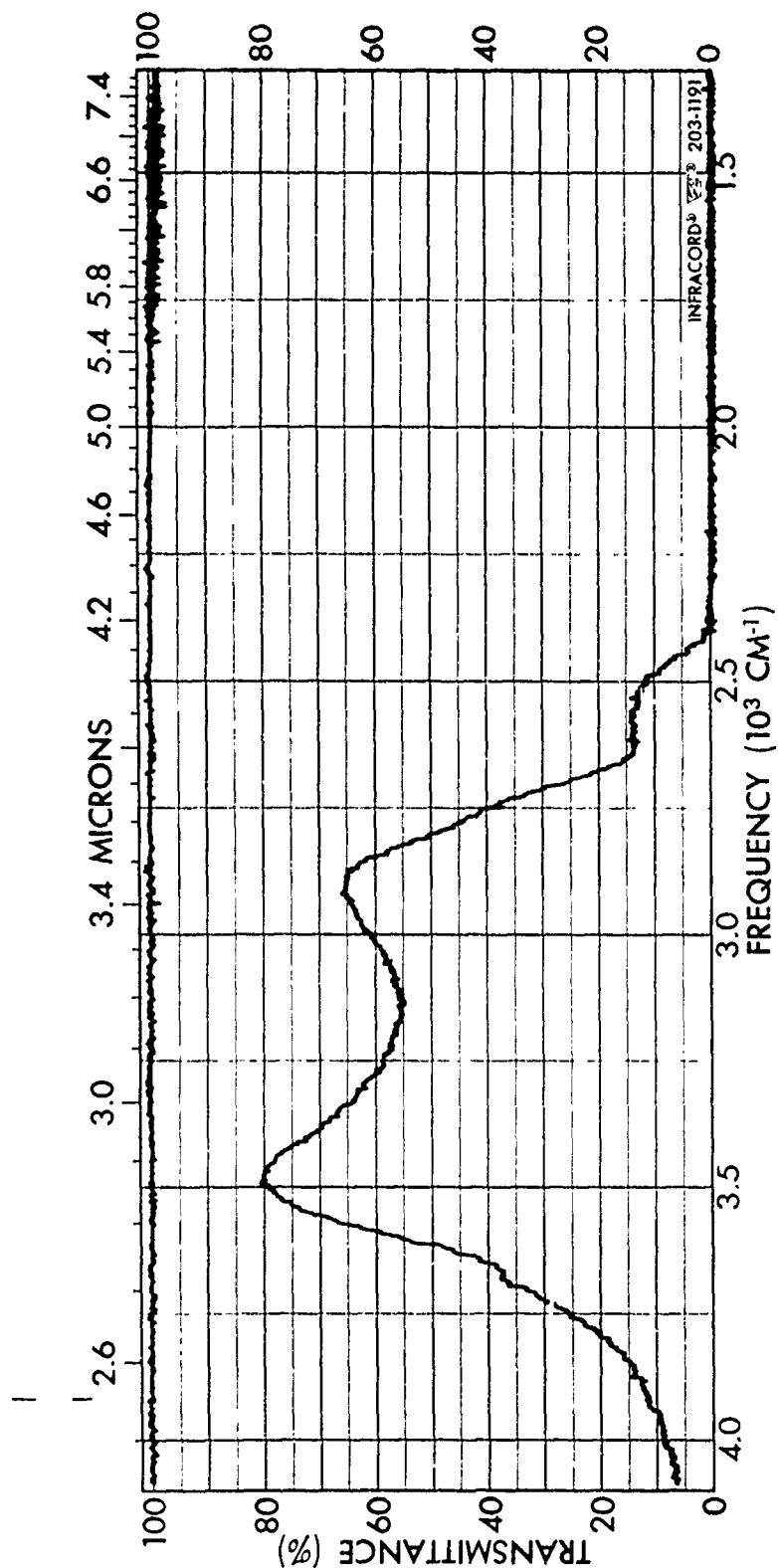
Figure 28 Measured spectral transmittance of ZnS-cryolite mirror which
(b) is HR at 2.16 microns.



SPECTRUM NO. _____
SAMPLE _____

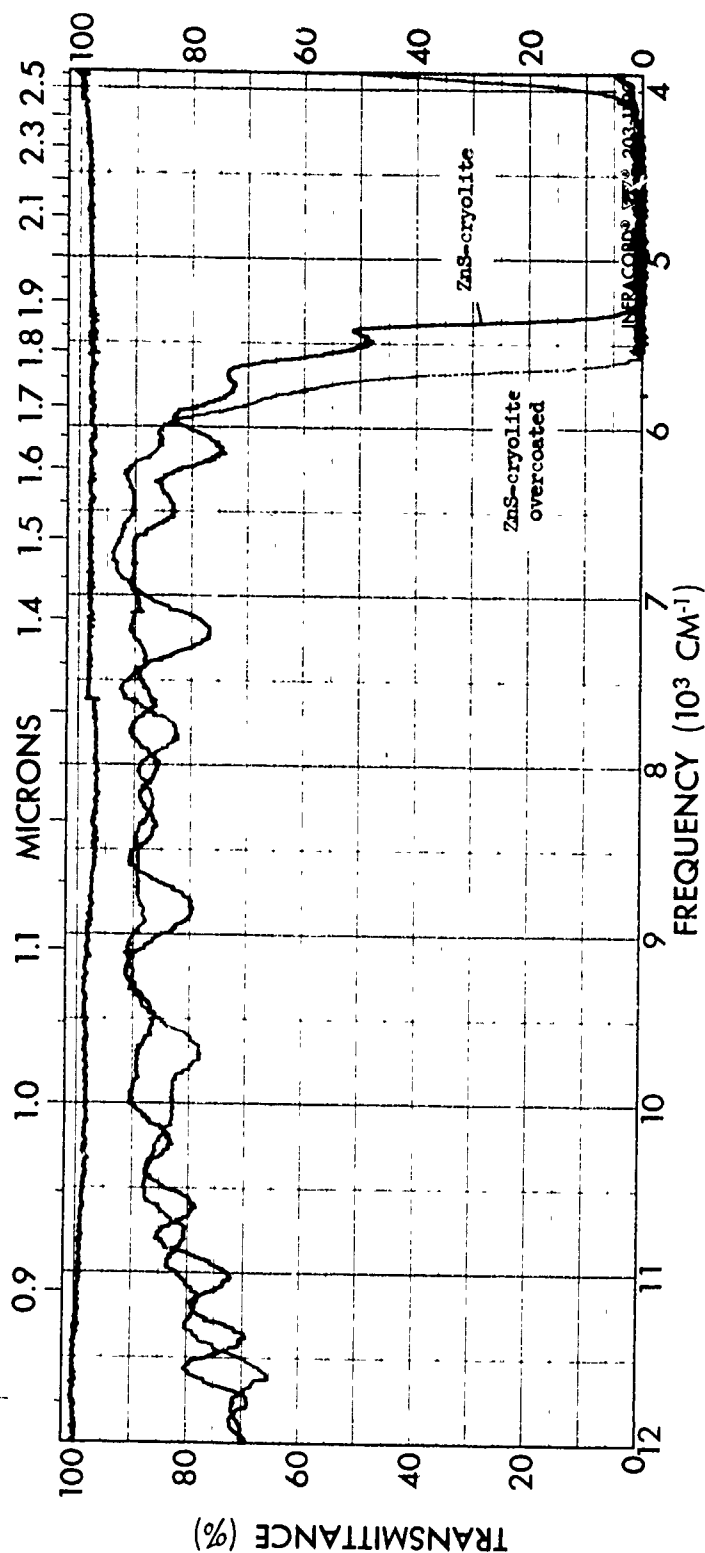
SPECTRUM NO. _____	ORIGIN <u>Lambda Optics</u>	LEGEND _____	REMARKS _____
SAMPLE <u>Substrate #14</u>	1. _____	1. _____	<u>Infrasil fused quartz sub-</u>
<u>ZnS-cryolite coating</u>	PURITY _____	2. _____	<u>strate</u>
<u>Transmitting at 2.16 microns</u>	PHASE _____	DATE _____	
	THICKNESS _____	OPERATOR <u>Wintemute</u>	

Figure 29 measured spectral transmittance of ZnS-cryolite mirror which
(a) is slightly transmitting at 2.16 microns.



SPECTRUM NO. _____		REMARKS _____	
SAMPLE Substrate #14		Infrasil fused quartz substrate	
ZnS-cryolite coating		1. _____	
PURITY _____		2. _____	
Transmitting at 2.16 microns		DATE _____	
THICKNESS _____		OPERATOR Wintemite	

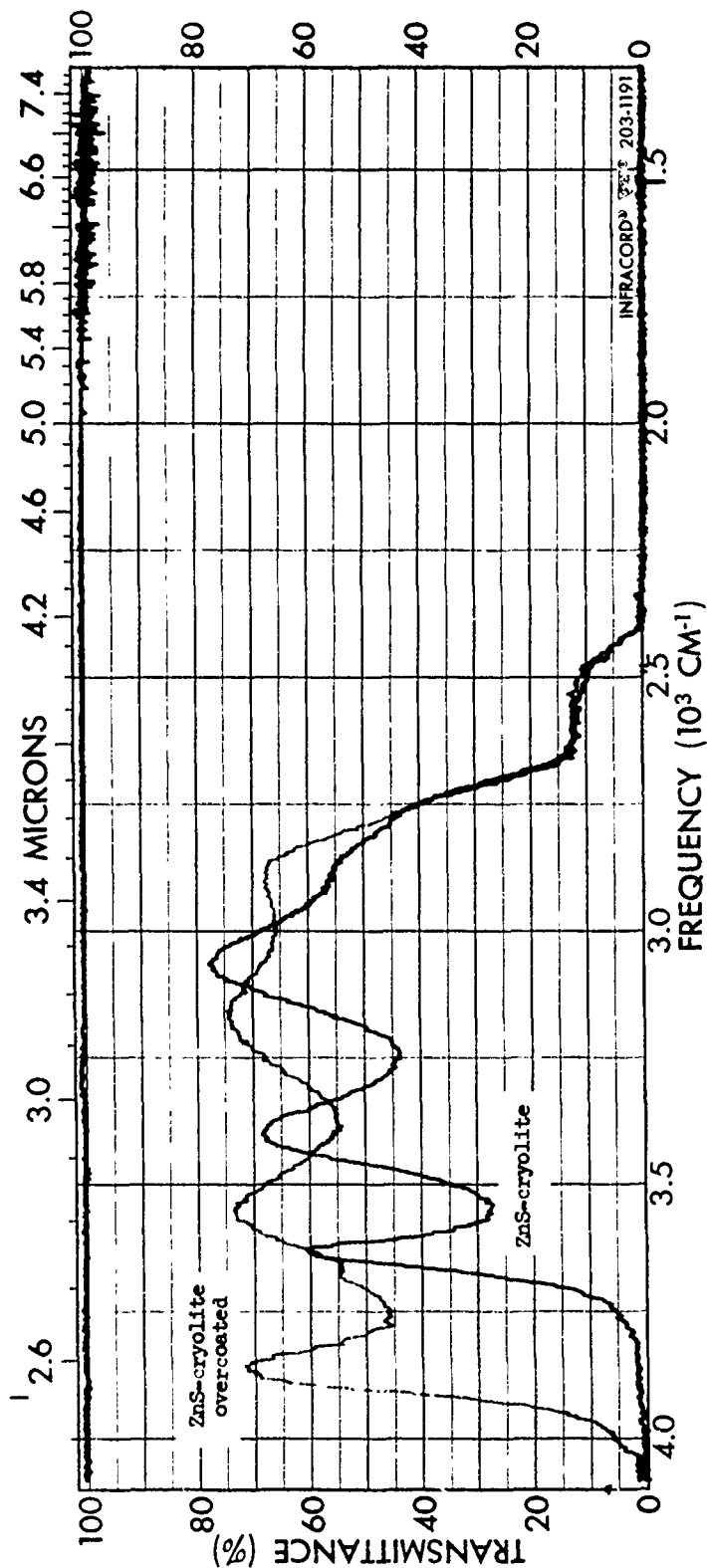
Figure 29 Measured spectral transmittance of ZnS-cryolite mirror which (b) is slightly transmitting at 2.16 microns.



SPECTRUM NO. _____
SAMPLE _____

SPECTRUM NO. 15a		ORIGIN	Lambda coatings	LEGEND	REMARKS Comparison of regular and overcoated ZnS-cryolite HR coatings.
SAMPLE Lot #3 (red) Lot #4 (blue)		(red) ZnS-cryolite (blue) ZnS-cryolite overcoated			
Substrate #12 (red) Substrate #16 (blue)		PURITY			
HR 2μ coating (red) HR 2μ coating (blue)		PHASE			
		THICKNESS		DATE December 6, 1971	
				OPERATOR J. Wintemute	

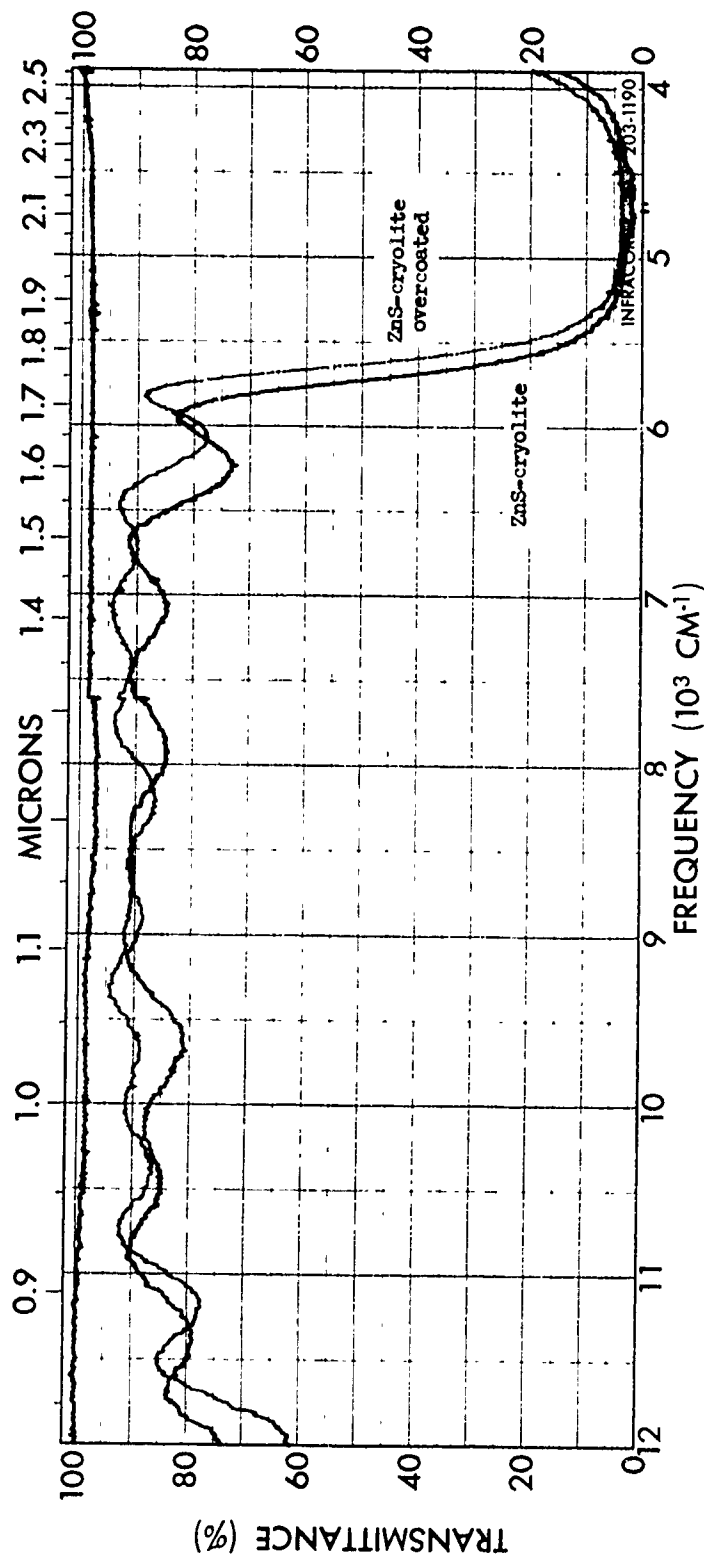
Figure 30 Comparison of spectral transmittances of ZnS-cryolite mirrors
(a) with and without Al_2O_3 overcoating which are HR at 2.16 microns.



SPECTRUM NO. _____
SAMPLE _____

<p>SPECTRUM NO. <u>15b</u> Lot #3 (red) Lot #4 (blue) Substrate #12 (red) Substrate #16 (blue)</p>	<p>ORIGIN <u>Lambda coatings</u> (red) ZnS-cryolite (blue) ZnS-cryolite overcoated</p>	<p>LEGEND _____</p>	<p>REMARKS <u>Comparison of regular and overcoated ZnS-cryolite HR coatings.</u></p>
<p>PURITY _____</p>	<p>DATE <u>December 6, 1971</u></p>	<p>OPERATOR <u>J. Wintemute</u></p>	
<p>THICKNESS _____</p>			

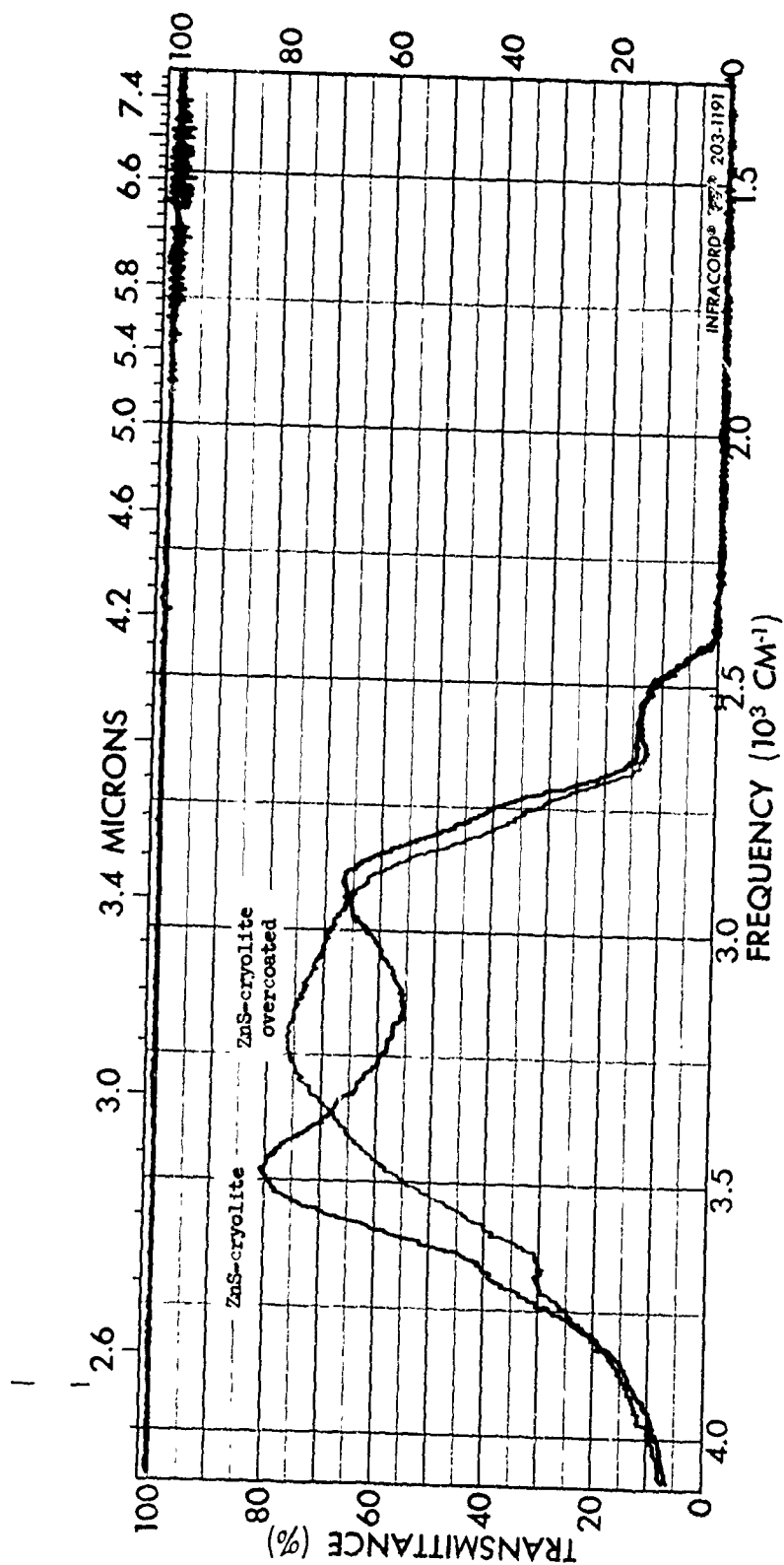
Figure 3C Comparison of spectral transmittances of ZnS-cryolite mirrors
(b) with and without Al_2O_3 overcoating which are HR at 2.16 microns.



SPECTRUM NO. _____
SAMPLE _____

SPECTRUM NO. 16a	ORIGIN Lambda coatings	LEGEND	REMARKS Comparison of regular and overcoated ZnS-cryolite transmitting coatings.
SAMPLE Lot #3 (red) Lot #4 (blue)	(red) ZnS-cryolite (blue) ZnS-cryolite overcoated		
Substrate #14 (red) Substrate #19 (blue)	PURITY		
Trans 2u coating (red) Trans 2u coating (blue)	PHASE	DATE December 6, 1971	
	THICKNESS	OPERATOR J. Wintemute	

Figure 31 Comparison of spectral transmittances of ZnS-cryolite mirrors
(a) with and without Al_2O_3 overcoating which are slightly transmitting at 2.16 microns.



SPECTRUM NO. 16b		SPECTRUM NO. _____	
SAMPLE Lot #3 (red) Lot #4 (blue)		REMARKS Comparison of regular and overcoated ZnS-cryolite transmitting coatings.	
Substrate #14 (red) Substrate #19 (blue)		LEGEND	
Trans Au coating (red) Trans Au coating (blue)		ORIGIN Lambda coatings (red) ZnS-cryolite (blue) ZnS-cryolite overcoated	
PURITY		DATE December 6, 1971	
PHASE		OPERATOR J. Wintemute	
THICKNESS			

Figure 31. Comparison of spectral transmittances of ZnS-cryolite mirrors with and without Al_2O_3 overcoating which are slightly transmitting at 2.16 microns.

5.1.5 ZnS-ThF₄ Undercoated and Overcoated with Al₂O₃

Figures 32 and 33 show measured transmittances for ZnS-ThF₄ coatings which are undercoated and overcoated with Al₂O₃. By comparing these with the results of Figs. 24 and 25, we see that the undercoating and overcoating have negligible effect on the mirror transmittance. Thus in none of the cases investigated did Al₂O₃ have an adverse effect upon the coating transmittance.

5.1.6 Spectrum Systems Coatings

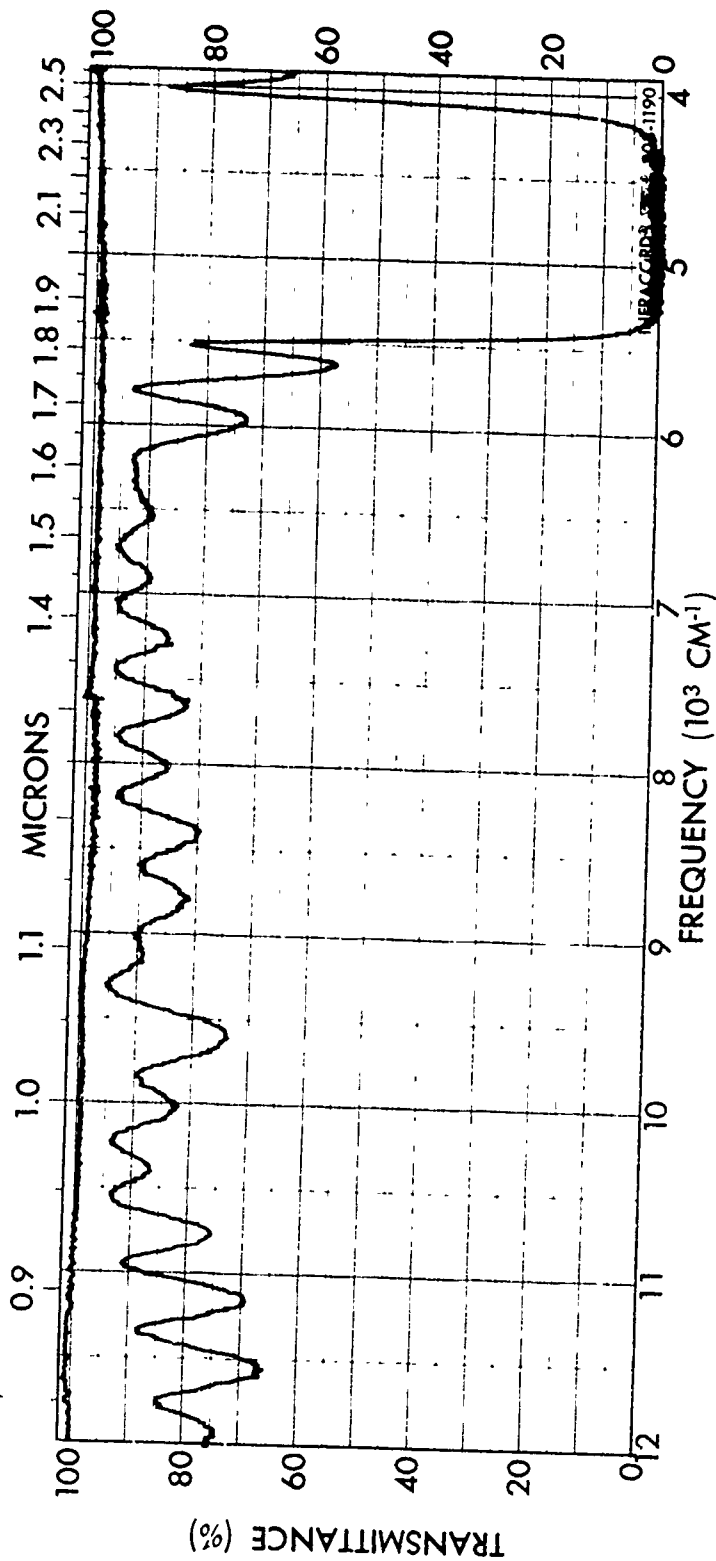
The spectral transmittance of HR and transmitting coatings from Spectrum Systems are shown in Figs. 32 and 33. As mentioned earlier, some of the very durable coating materials can offer difficulties during deposition. Often the index of refraction will vary during a coating run making it difficult to achieve a desired transmittance exactly. A second difficulty which is not uncommon is that the coating materials decompose during deposition because of the high temperatures required. The new materials thus formed have an incorrect index of refraction and may even be absorbing in the wavelength region of interest.

In Figs. 34 and 35 we show measured transmittance of the Spectrum Systems mirrors. For the HR coating of Fig. 34, the HR range is quite large, extending from 1.78 microns to 2.8 microns! Unfortunately in the middle of this region at 2.35 microns, the coating becomes somewhat transmitting. An even worse problem, however, is that the 1.08 micron transmission is only about 45%. This is an unacceptably low value.

The transmitting mirror of Fig. 35 also has this problem. Its 1.08 micron transmission is about 65%, a value which is still too low. The bandwidth of the transmission region is very large, a highly desirable feature. For both Figs. 34 and 35 an uncoated quartz substrate was placed in the reference beam of the spectrometer. The mirror transmission data of Figs. 34b and 35b is valid up to 4 microns, but not beyond because of substrate absorption.

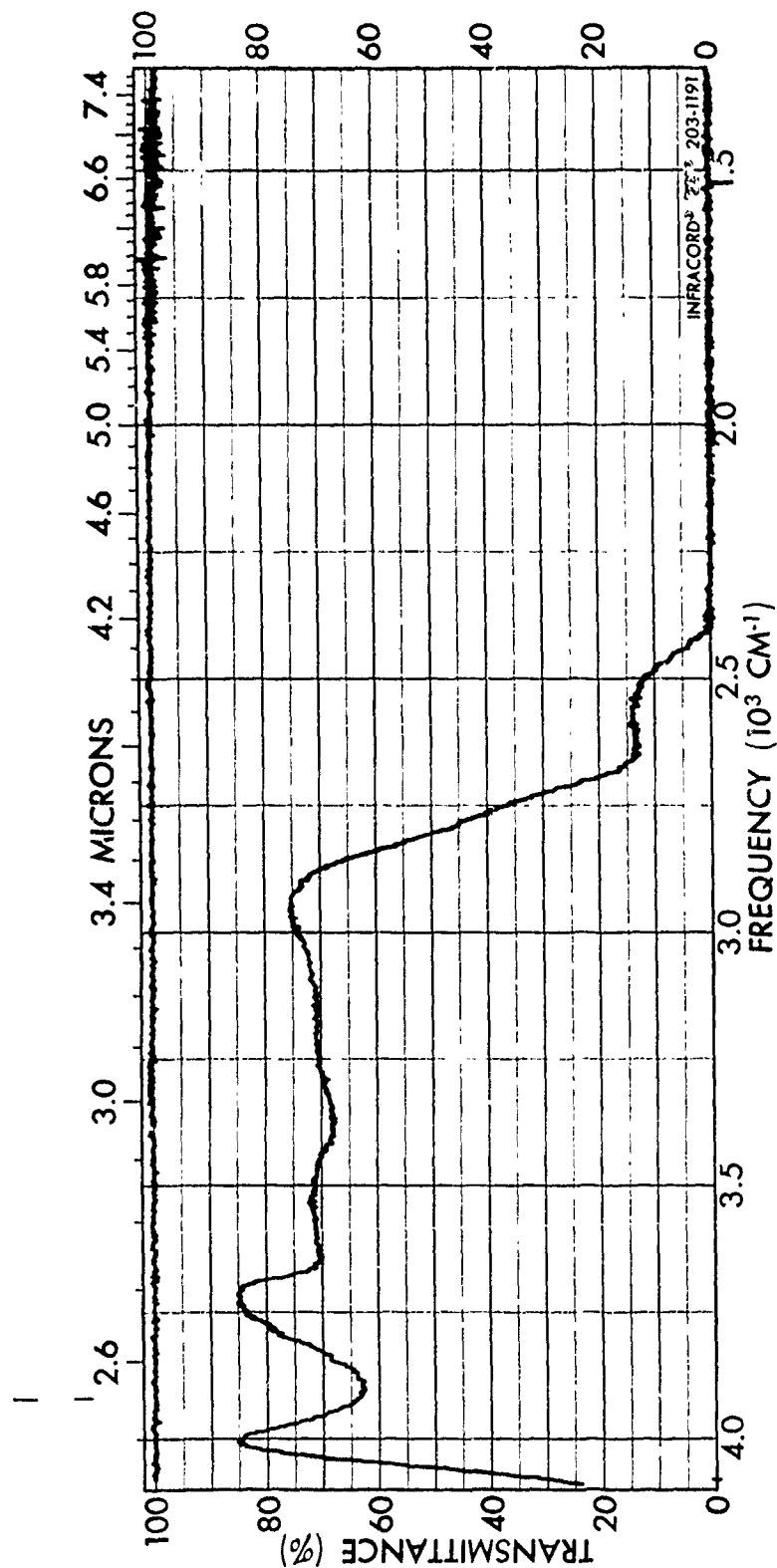
5.2 MIRROR COATING TYPE #3

As described in Section 2.3.3, this type of coating is designed to be highly reflecting at the oscillator signal wavelength, while having slight transmission at the idler wavelength. ZnS-ThF₄ coatings of this type were fabricated with the following design parameters: signal wavelength - 1.56 microns; idler wavelength - 3.5 microns; signal transmission - HR; idler



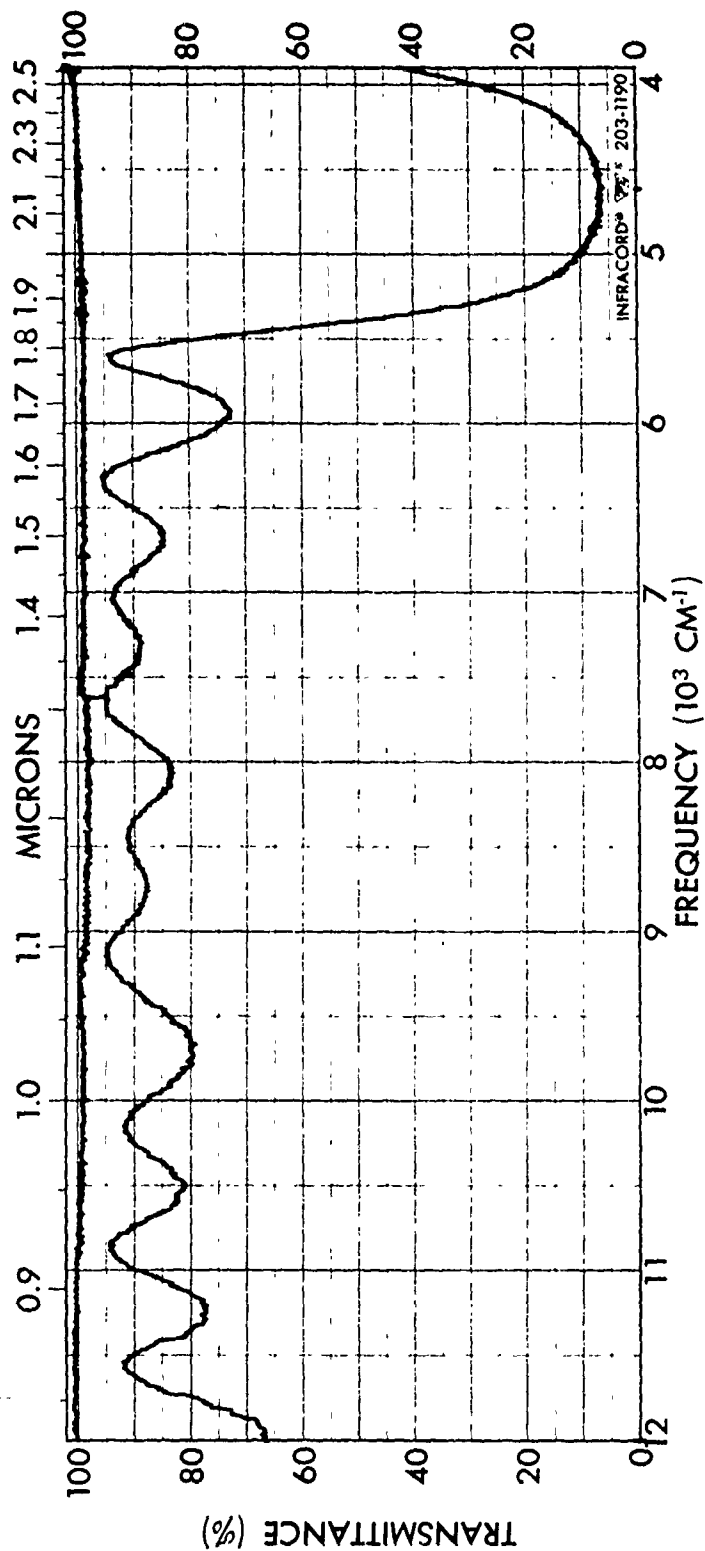
SPECTRUM NO. 25a		SPECTRUM NO. _____	
SAMPLE Lot #5		SAMPLE _____	
Substrate #21		LEGEND	
ORIGIN Lambda coating		1. _____	
ZnS-ThF ₄ with Al ₂ O ₃ under- and over-coatings		2. _____	
PURITY		DATE April 3, 1972	
PHASE		OPERATOR J. D. Wintemute	
THICKNESS			

Figure 32 Measured spectral transmittance of ZnS-ThF₄ mirror undercoated and overcoated with Al₂O₃ which is HR at 2.16 microns.



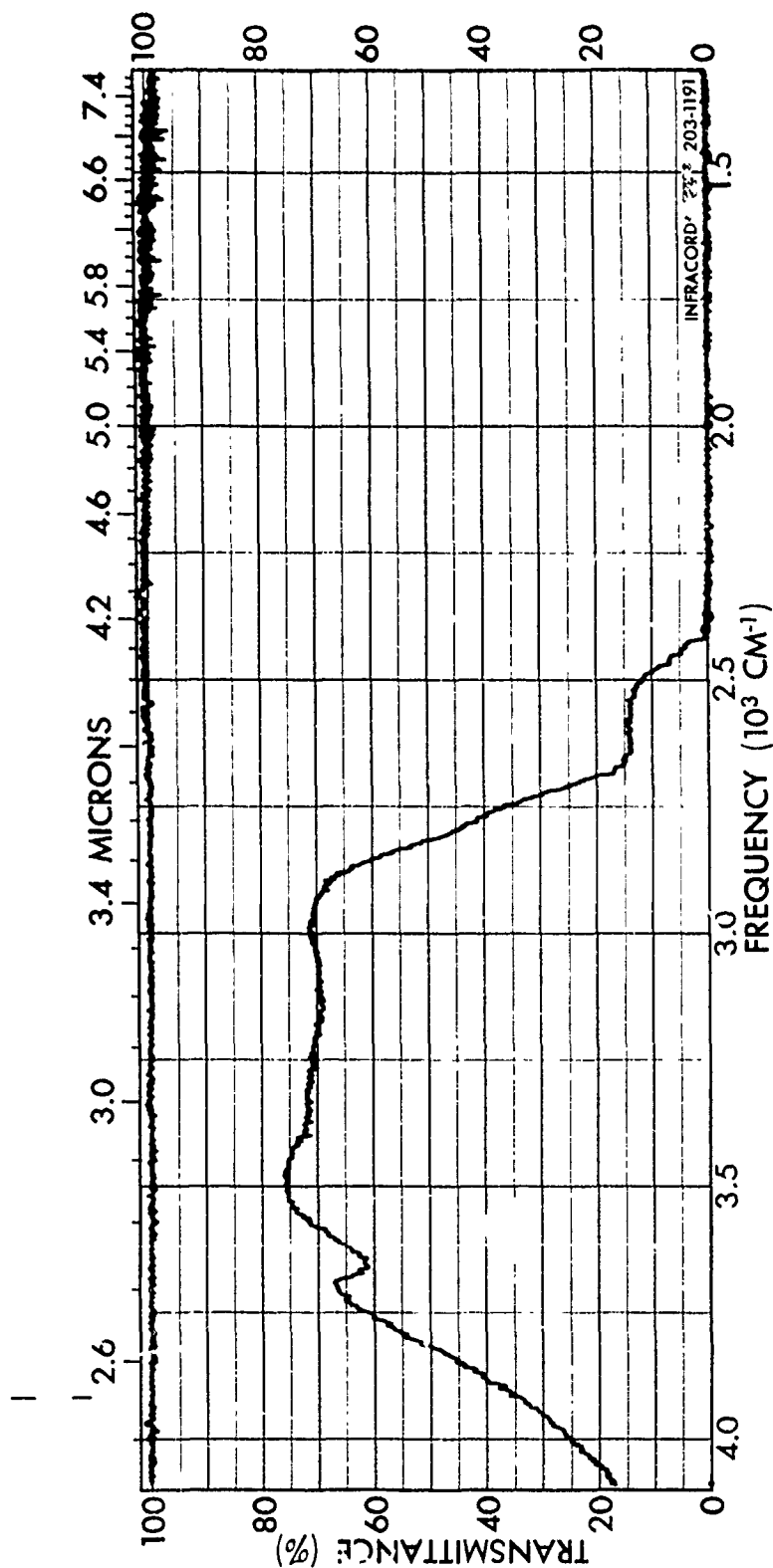
SPECTRUM NO. <u>25b</u>		SPECTRUM NO. _____	
SAMPLE Lot #5		SAMPLE _____	
Substrate #21		LEGEND	
HR 2u coating		1. _____	
PURITY _____		2. _____	
PHASE _____		DATE April 3, 1972	
THICKNESS _____		OPERATOR J. D. Wintemute	
ORIGIN Lambda coating		REMARKS	
ZnS-ThF ₄ with Al ₂ O ₃ under- and overcoatings			

Figure 32 Measured spectral transmittance of ZnS-ThF₄ mirror undercoated
(b) and overcoated with Al₂O₃ which is HR at 2.16 microns.



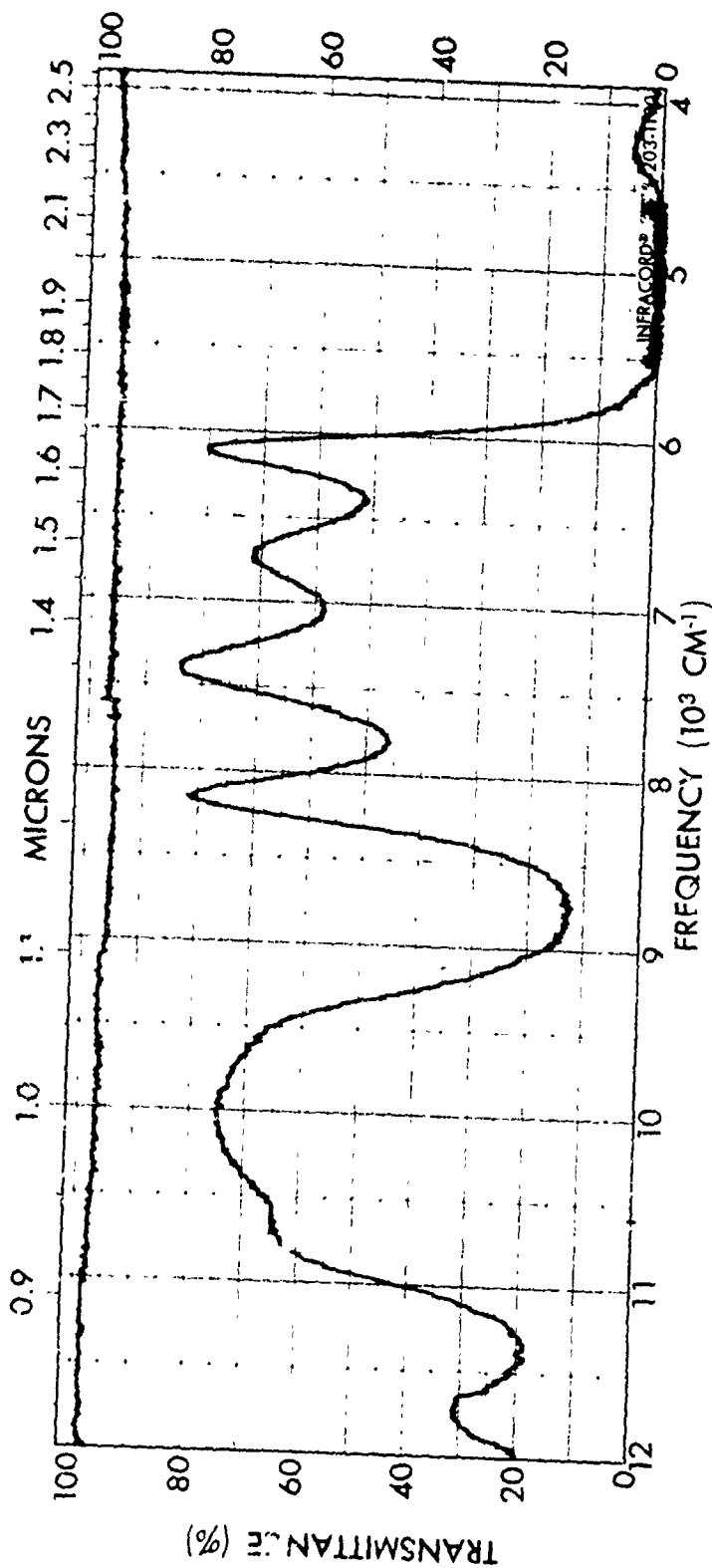
SPECTRUM NO. <u>26a</u>		SPECTRUM NO. _____	
SAMPLE <u>Lot #5</u>		SAMPLE _____	
Substrate # <u>23</u>		REMARKS _____	
Trans <u>2μ</u> coating		LEGEND _____	
ORIGIN <u>Lambda coating</u>		1. _____	
ZnS-ThF ₄ with Al ₂ O ₃ under- and overcoatings		2. _____	
PURITY _____		DATE <u>April 3, 1972</u>	
PHASE _____		OPERATOR <u>J. D. Wintemute</u>	
THICKNESS _____			

Figure 33 measured spectral transmittance of ZnS-ThF₄ mirror undercoated (a) and overcoated with Al₂O₃ which is slightly transmitting at 2.16 microns.



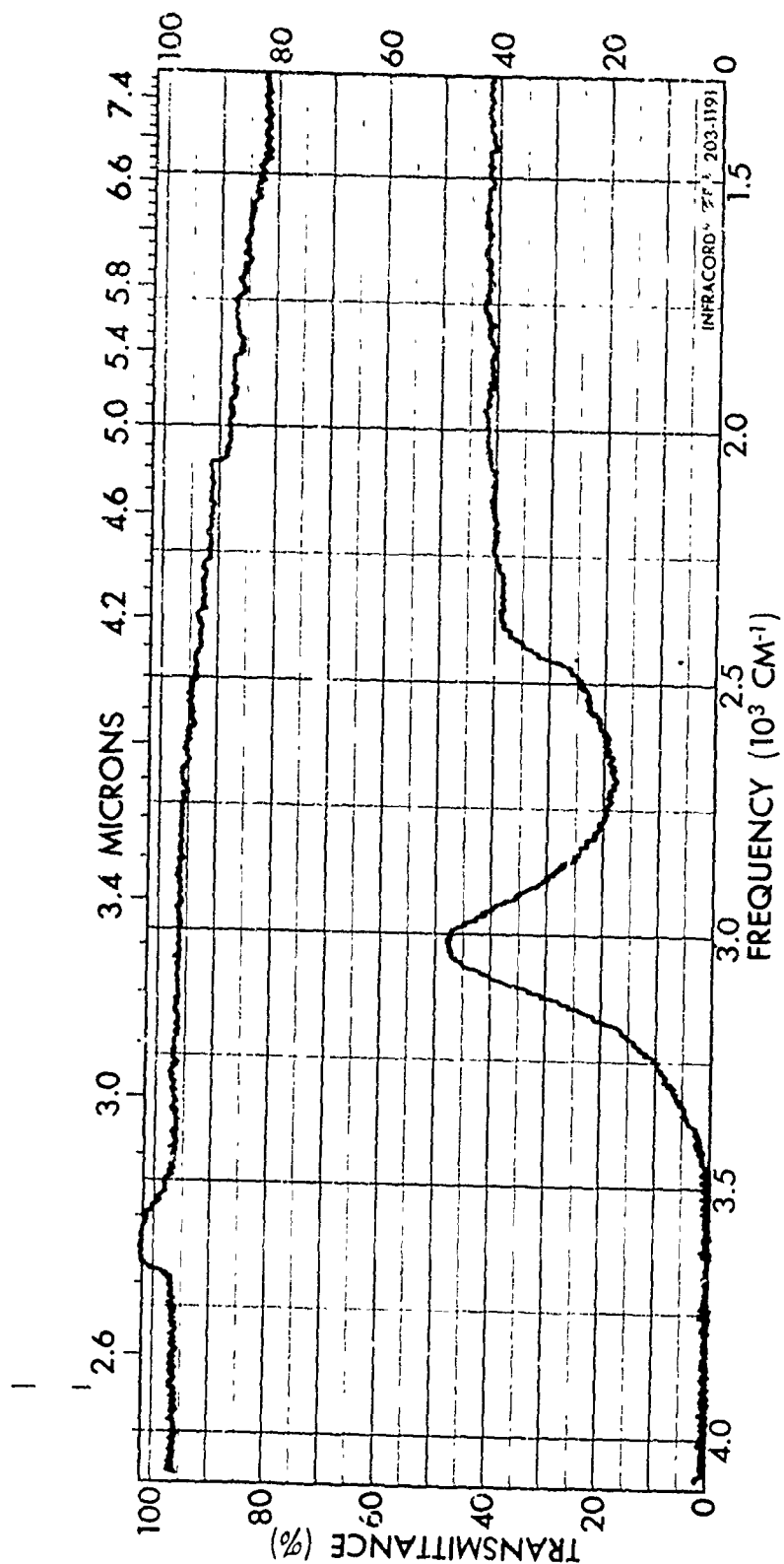
SPECTRUM NO. <u>26b</u>		SPECTRUM NO. _____	
SAMPLE Lot # <u>5</u>		SAMPLE _____	
Substrate # <u>23</u>		REMARKS _____	
Trans <u>2u</u> coating		1. _____	
ORIGIN <u>Lambda coating</u>		2. _____	
PURITY _____		DATE <u>April 3, 1972</u>	
PHASE _____		OPERATOR <u>J. D. Wintermute</u>	
THICKNESS _____			

Figure 33 Measured spectral transmittance of ZnS-ThF₄ mirror undercoated
(b) and overcoated with Al₂O₃ which is slightly transmitting at
2.16 microns.



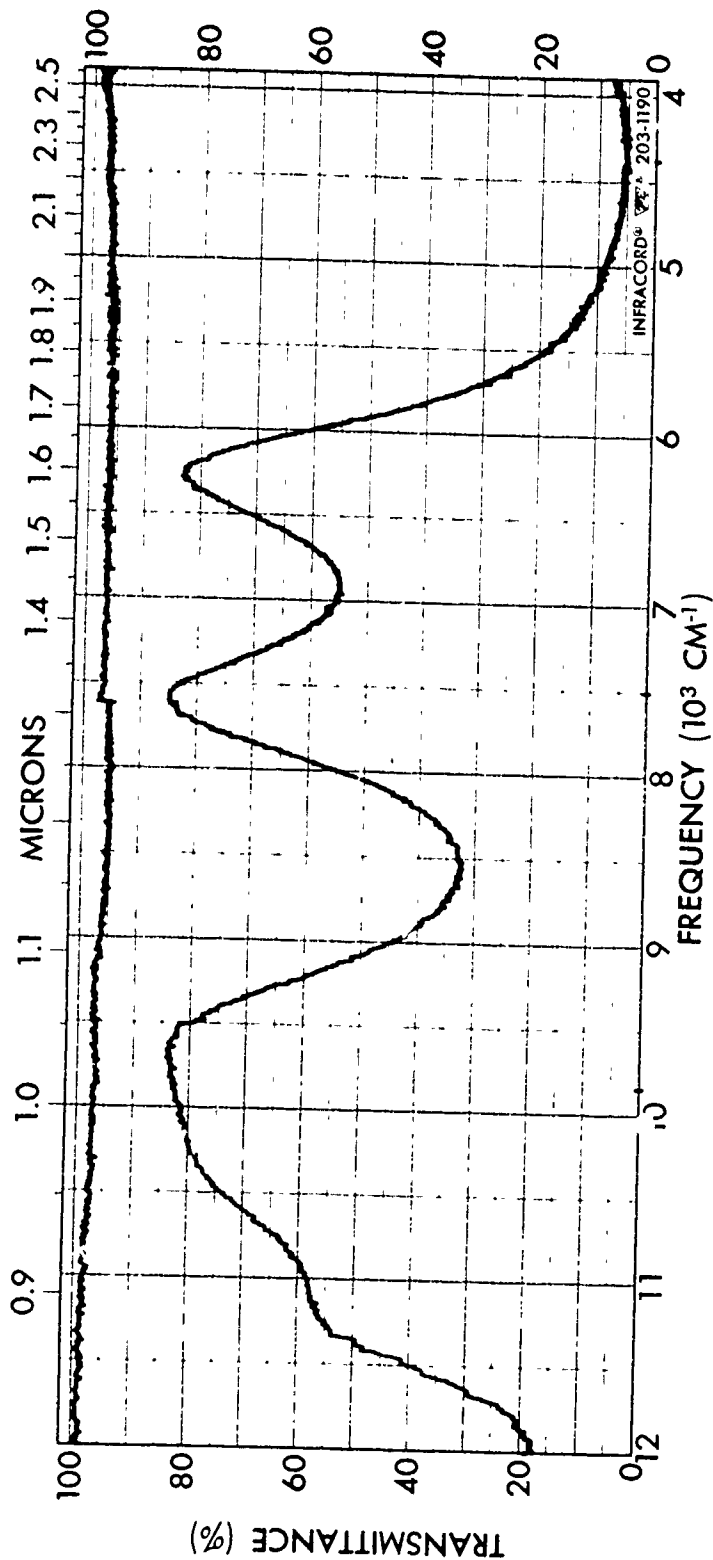
SPECTRUM NO. _____		SPECTRUM NO. _____	
SAMPLE _____		SAMPLE _____	
Substrate is _____		REMARKS This substrate is coated the same as the HR end of lithium niobate crystal [C-1]	
HR coating _____		An uncoated infrasil fused quartz substrate was used in the reference beam.	
ORIGIN Spectrum Systems		LEGEND	
PURITY _____		1. _____	
PHASE _____		2. _____	
THICKNESS _____		DATE March 14, 1972	
		OPERATOR J. Wintemute	

Figure 34 Measured spectral transmittance of Spectrum Systems mirror (a) which is HR at 2.16 microns.



SPECTRUM NO. _____		SPECTRUM NO. _____	
SAMPLE _____		SAMPLE _____	
Substrate <u>Ag</u>		REMARKS This substrate is coated the same as the HR end of lithium niobate crystal LC-1	
HR coating		An uncoated infrasil fused quartz substrate was used in the reference beam.	
ORIGIN <u>Spectrum Systems</u>		LEGEND	
PURITY _____		1. _____	
PHASE _____		2. _____	
THICKNESS _____		DATE <u>Mar 14, 1972</u>	
		OPERATOR <u>J. Winterte</u>	

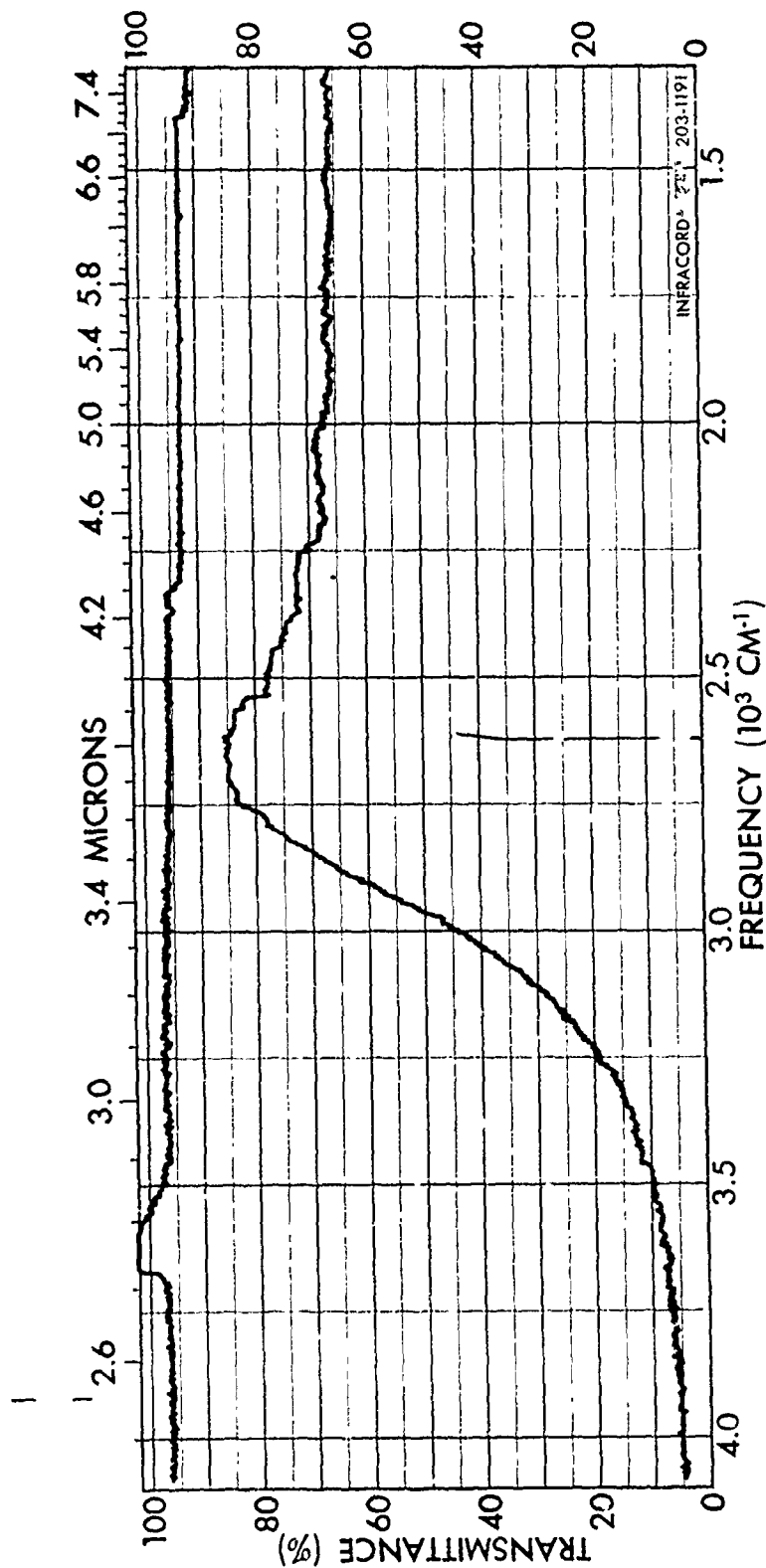
Figure 34 Measured spectral transmittance of Spectrum Systems mirror (b) which is HR at 2.16 microns.



SPECTRUM NO. _____
SAMPLE _____

SPECTRUM NO. _____	ORIGIN <u>Spectrum Systems</u>	LEGEND _____	REMARKS This substrate is coated the same as the transmitting end of lithium niobate crystal LC-1. An uncoated infrasil fused quartz substrate was used in the reference beam.
	SAMPLE _____	1. _____	
Substrate #100	PURITY _____	2. _____	DATE <u>March 14, 1972</u> OPERATOR <u>J. Wintemute</u>
5T@2.16u	PHASE _____		
	THICKNESS _____		

Figure 35 Measured spectral transmittance of Spectrum Systems mirror which is slightly transmitting at 2.16 microns.



SPECTRUM NO. _____
SAMPLE

SPECTRUM NO. _____	ORIGIN	Spectrum Systems	REMARKS This substrate is coated the same as the transmitting end of lithium niobate crystal LC-1
	PURITY		
SAMPLE	PHASE		An uncoated Infrasil fused quartz substrate was used in the reference beam.
Substrate #100	THICKNESS		
5%T @ 2.16μ	DATE	March 14, 1972	
	OPERATOR	J. Wintemute	

Figure 35 Measured spectral transmittance of Spectrum Systems mirror (b) which is slightly transmitting at 2.16 microns.

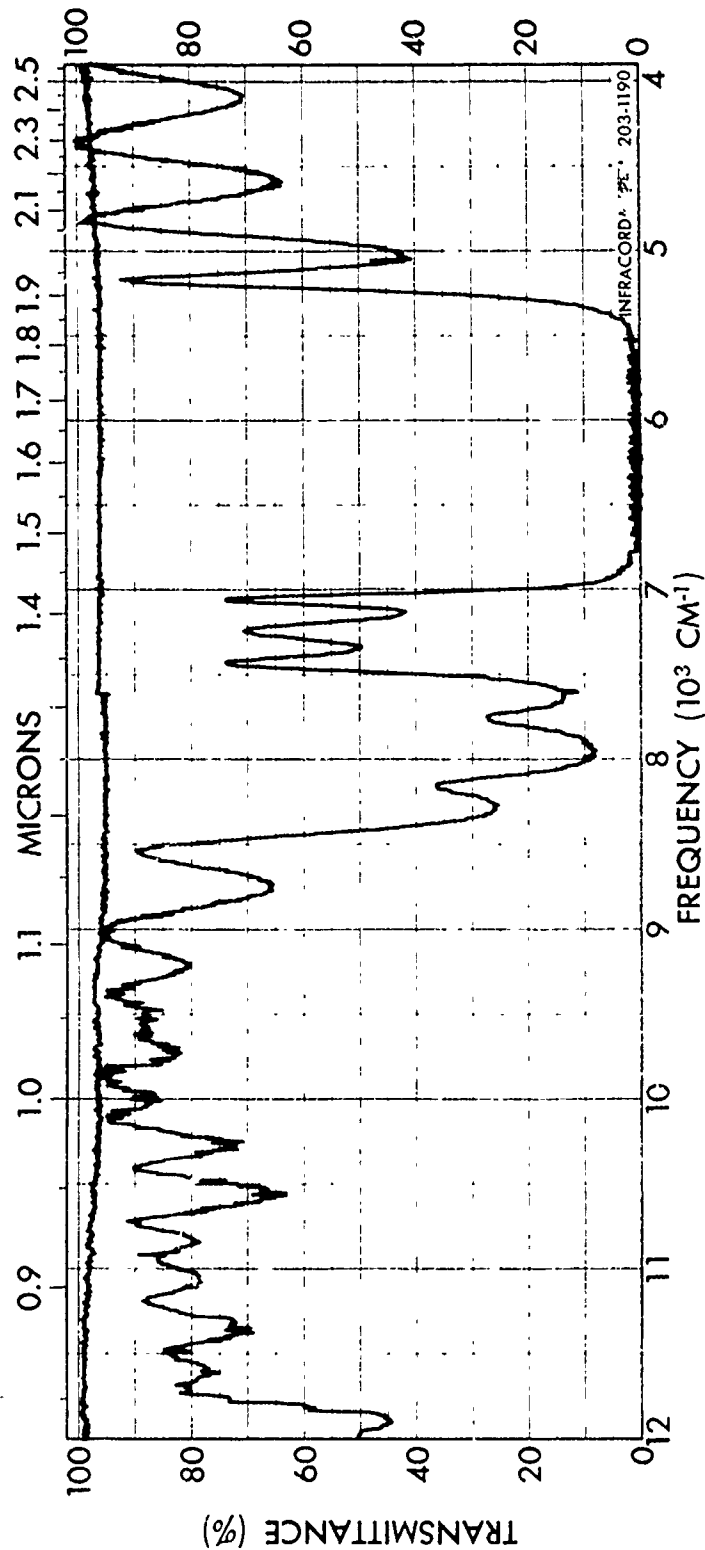
transmission - 10%; and 1.08 micron pump transmission - 80% or greater.

Measured transmission of the ZnS-ThF_4 type #3 mirror is given in Fig. 36. The HR region extends from 1.47 to 1.84 microns, and the 1.08 micron transmission is 86%. The idler transmission ranges from 8 to 18% over the wavelength range 3.3 to 3.7 microns. Thus all of the design parameters were met by this coating.

5.3 GENERAL OBSERVATIONS

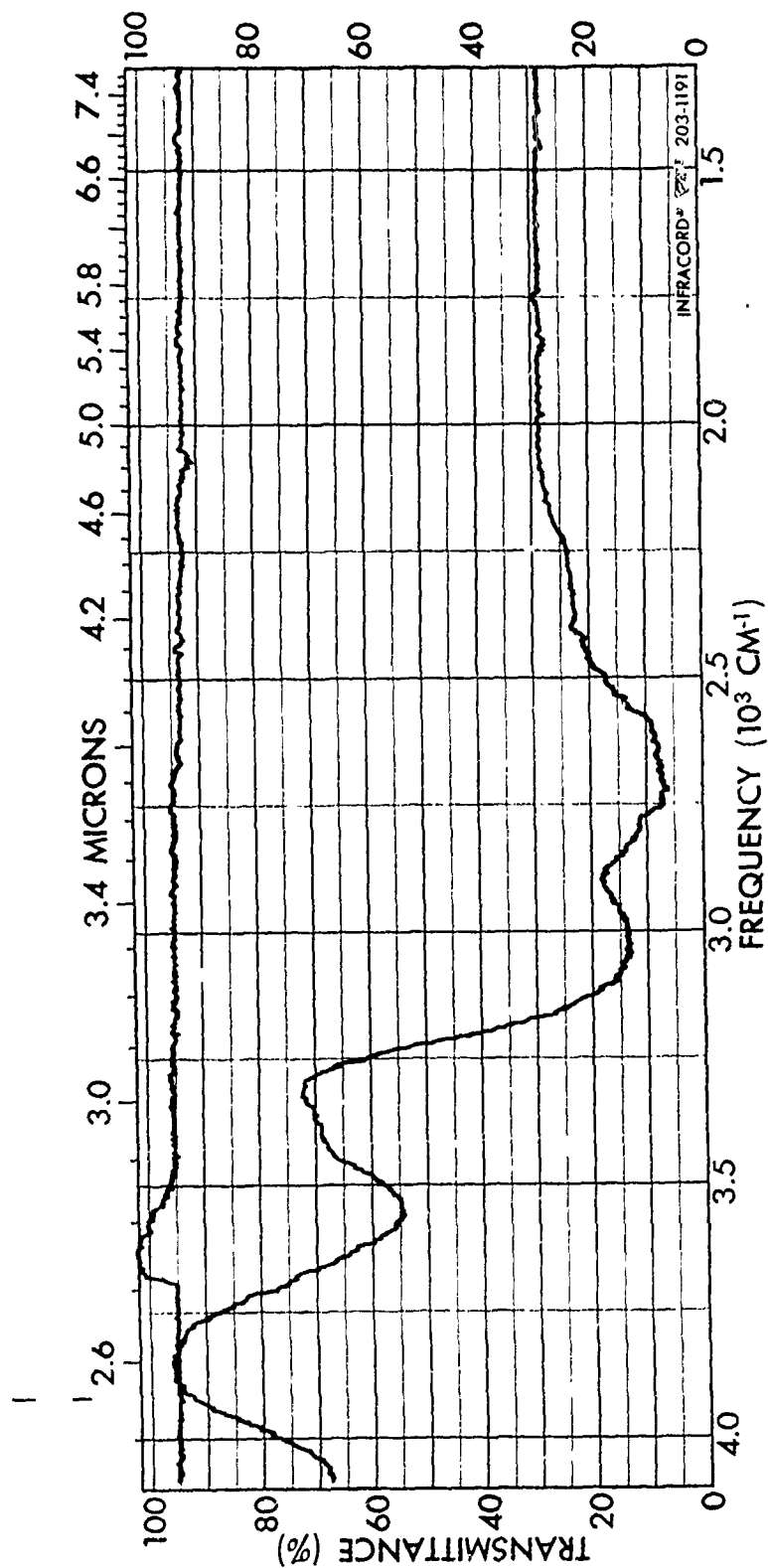
We have previously noted in Section 2.3.2 that mirror reflectivities varied somewhat when different substrates were employed. The data of Table 2 show that midband coating transmission is somewhat greater for a fused-quartz substrate than for lithium niobate. The transmission curve of Fig. 37 gives experimental proof of this phenomenon. The two curves of Fig. 37 show transmissions of the same ZnS-ThF_4 coating on fused quartz and on lithium niobate. The midband (2.1 micron) transmittances are 7% and 4%, respectively. This agrees quite well with the data of Table 2 for $n = 10$.

We also note that coating transmissions can vary somewhat from sample to sample even when the substrates are made of the same material. Figure 38 shows transmissions of two fused quartz substrates which were coated at the same time. It can be seen that the curves are similar in shape, but shifted in wavelength by about .06 microns. Thus there can be substantial variations from piece to piece in a given coating run. The transmission of the "monitor piece" will not necessarily be the same as the transmissions of the other pieces from that same lot. The safest procedure is to measure the transmittance of the piece in question directly.



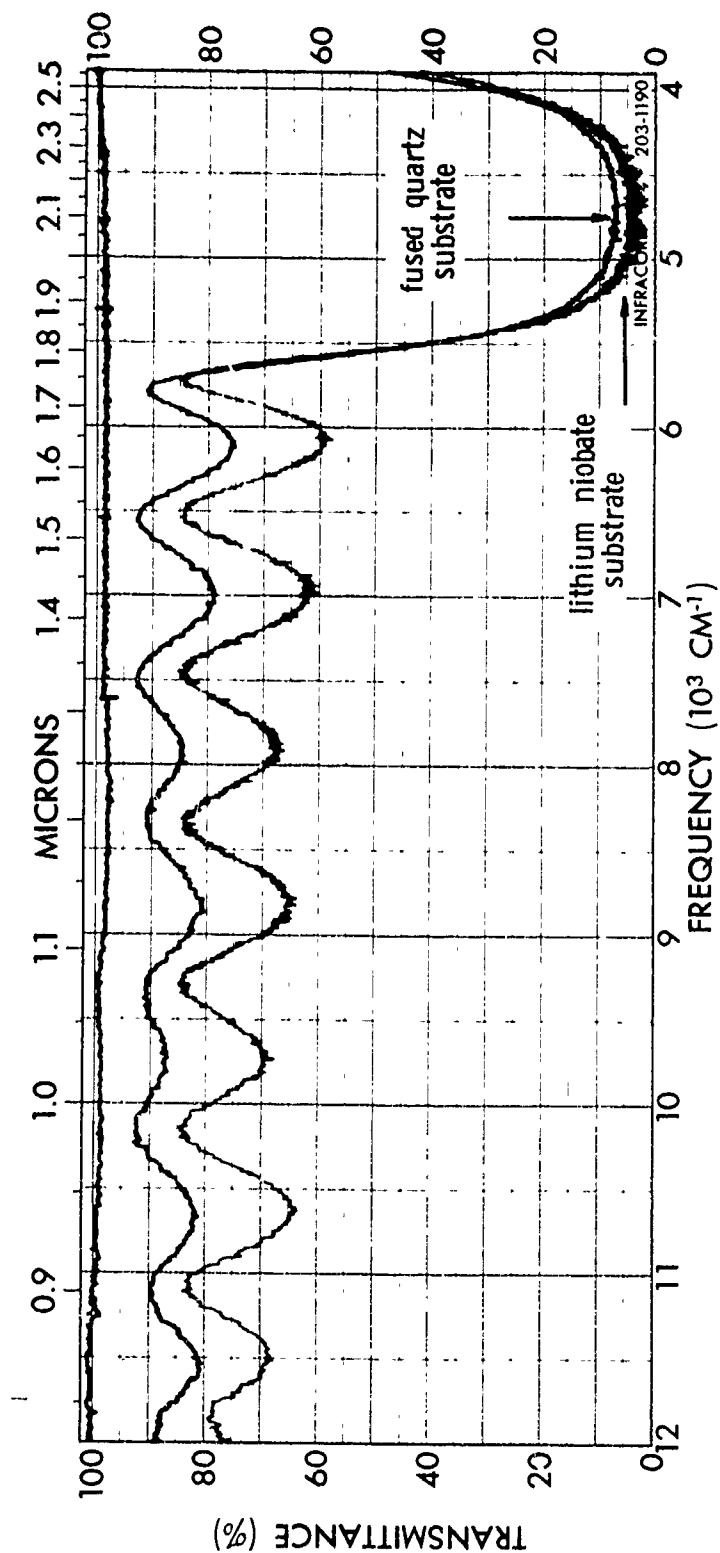
SPECTRUM NO. _____		SPECTRUM NO. _____	
SAMPLE Substrate #33		SAMPLE _____	
IR at 1.56 μ and 10% trans- mission at 3.5 μ		REMARKS An uncoated Infrasil fused quartz substrate was used in the reference beam.	
ORIGIN Lambda Optics	LEGEND		
ZnS-ThF ₄ coating	1.		
PURITY	2.		
PHASE	DATE		
THICKNESS	OPERATOR Wintemite		

Figure 36 Measured spectral transmittance of 3.5 micron doubly-resonant
(a) ZnS-ThF₄ mirror.



SPECTRUM NO. _____		LEGEND		REMARKS	
SAMPLE Substrate #33		ZnS-ThF ₄ coating		An uncoated infrasil fused quartz substrate was used in the reference beam.	
IR at 1.56μ and 10% trans- mission at 3.5μ		PURITY			
		PHASE		DATE	
		THICKNESS		OPERATOR Wintemute	

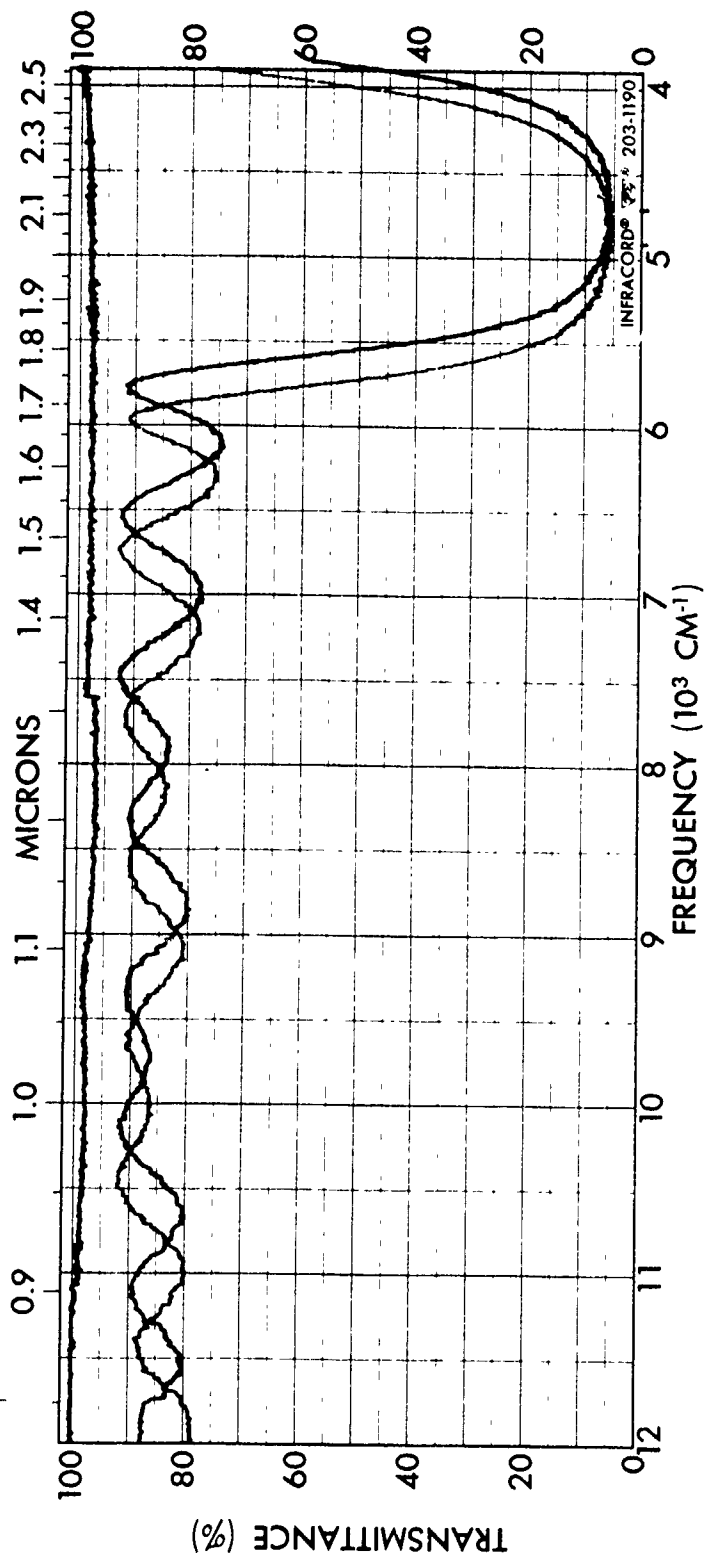
Figure 36 Measured spectral transmittance of 3.5 micron doubly-resonant
(b) ZnS-ThF₄ mirror.



SPECTRUM NO. _____
SAMPLE _____

SPECTRUM NO. <u>9a</u>		ORIGIN <u>Lambda coatings</u>		LEGEND	REMARKS <u>Same coating</u> <u>on fused quartz and lithium</u> <u>niobate substrates from</u> <u>Lot #1</u>
Lot #1 (red)		(red) <u>ZnS-ThF₄</u>			
Lot #1 (blue)		(blue) <u>ZnS-ThF₄</u>			
PURITY					
Substrate #5 (red)		PHASE		DATE <u>November 14, 1971</u>	OPERATOR <u>J. Wintemute</u>
Niobate disk C2 (blue)					
Trans 2μ coating (red)					
Trans 2μ coating (blue)		THICKNESS			

Figure 37 Dependence of spectral transmittance upon substrate.



SPECTRUM NO. 17a		SPECTRUM NO. _____	
SAMPLE Lot #1 (red) Lot #1 (blue)		SAMPLE _____	
Substrate #5 (red) Substrate #6 (blue)		REMARKS Identical coatings and substrates from Lot #1	
ORIGIN Lambda coatings (red) ZnS-ThF ₄ (blue) ZnS-ThF ₄			
PURITY			
PHASE		DATE December 6, 1971	
THICKNESS		OPERATOR J. Wintemute	

Figure 38 Variation from substrate to substrate of spectral transmittance.

Section VI

DAMAGE MEASUREMENTS ON FABRICATED MIRRORS

An important part of this program has been to measure the power densities at which optical damage occurs to the various oscillator coatings (and substrates). In addition, we have sought ways of improving these damage levels. The results of our investigations on damage are given in this section.

6.1 TYPES OF DAMAGE ENCOUNTERED

Several different types of damage have been encountered in our damage investigations. Damage can (and has) occurred to the coatings themselves, the substrates, and to dust particles on the coatings. As a first step in this work, we sought to identify and characterize the various types of damage. Each of the types of damage listed below has been observed both with the external test set-up of Fig. 13 and in actual parametric oscillator experiments.

In order to help clarify the causes of the different types of damage, tests were run on (1) uncoated lithium niobate and uncoated fused quartz substrates (2) coated lithium niobate, and (3) coated fused quartz. The results of these tests and the conclusions reached from them will now be given.

The first type of damage consists of a central damaged area surrounded by concentric cracked layers of coatings. No material is sprayed onto the surface of the coating. This type of damage is observed with coated quartz and lithium niobate substrates, but not with uncoated substrates. An example is shown in Fig. 39a where the two major damage spots illustrate this type of damage. The magnification for Fig. 39a is 77. We believe that this represents damage which occurs to one of the intermediate layers of the coating. The layers lying above the damaged area are cracked, perhaps from thermal stresses. One can tell approximately which layer of the coating has damaged by noting the number of rings surrounding the damage. In the remainder of this report, we will refer to this type of damage as "crater damage".

The second type of damage which we have encountered consists of a hole which extends completely through the coating layers into the lithium niobate substrate. A good deal of material is thrown out and scattered around



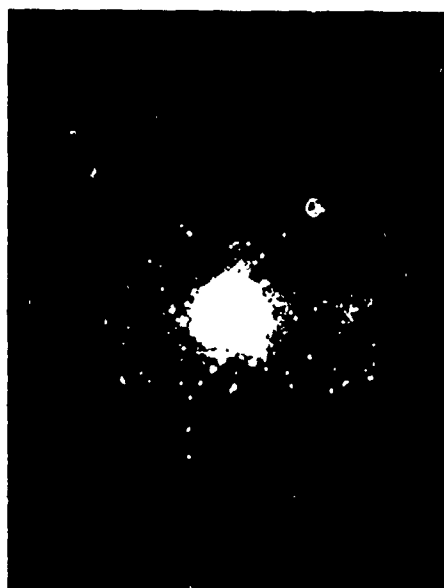
(a)



(b)



(c)



(d)

Figure 39 Types of coating and substrate damage encountered on this program:
 (a) crater (coating) damage; (b) lithium niobate (substrate)
 damage; (c) small-spot (coating) damage; and (d) dust damage.

the hole; most of this material cleans off when the coating (or uncoated crystal) is scrubbed with a Q-tip moistened with acetone. We have observed this type of damage with both coated and uncoated lithium niobate, but have not observed it with uncoated or coated fused quartz. We therefore deduce that this damage represents damage to the lithium niobate substrate. An example of this type of damage is shown in Fig. 39b near the center of the photo. We refer to this type of damage as lithium niobate damage.

A third type of damage consists of numerous small spots having diameters of perhaps 5 microns. These are probably shown most clearly in Fig. 39c where they occur in straight lines (the crystal was translated linearly during damage tests). The magnification for Fig. 39c is 27. These small spots can also be seen randomly arranged around the crater and niobate damages of Figs. 39a and 39b. We observe this type of damage with coatings on quartz and niobate; we do not observe it with uncoated quartz or niobate. We believe that this damage occurs in the top (ZnS) layer in the mirror coating. With this type of damage, there are no circular cracks surrounding the spot, and no material is thrown onto the surface. This type of damage is of special interest and importance, and is discussed again later in Section 6.3. We call this particular type of damage "small-spot damage".

The fourth and final type of damage which we have observed is caused by the laser beam striking dust particles lying on the mirror surfaces. This type of damage can cover a fairly large area, and often throws out material onto the coating. Some, but not all of this can be cleaned off by scrubbing with a Q-tip. An example of this type of damage is shown in Fig. 39d (77 times magnification). Because of the splattering, this type of damage is somewhat similar in appearance to lithium niobate damage, but does not extend down through the coating nor into the substrate. Careful cleaning of the mirrors prior to testing (or operation of an oscillator) is needed in order to minimize this type of damage.

6.2 LITHIUM NIOBATE DAMAGE LEVELS

One of the important and rather surprising results obtained on this program is that the presence of a coating can significantly affect the level at which lithium niobate surface damage (of the type shown in Fig. 39b) occurs.

Table III

1.08 Micron Damage Thresholds for Lithium Niobate with Various Coatings

Coating on LiNbO_3	Peak power density at which surface damage begin ^s MW/cm^2
uncoated	46 MW/cm^2
$\text{ZnS} - \text{ThF}_4$ multilayer	54 - 61 MW/cm^2
ZnS -cryolite multilayer	61 MW/cm^2
$\text{ZnS} - \text{ThF}_4$ multilayer overcoated with Al_2O_3	107 - 115 MW/cm^2
$\lambda/4$ layer of Al_2O_3	150 MW/cm^2
$\text{ZnS} - \text{ThF}_4$ multilayer under and overcoated with Al_2O_3	86, 150 MW/cm^2

Since lithium niobate surface damage occurs at approximately the same levels as does coating damage, and since we are able to separately identify the two types of damage, we are able to present lithium niobate damage data. The tests were performed on coated and uncoated lithium niobate disks using the test set-up of Fig. 13. Other conditions of the test are the same as described in Section 3.4. It should be emphasized that the variance in lithium niobate damage results is somewhat greater than in coating damage tests. Thus in some cases, a range of values is given rather than a single value. Nonetheless, certain trends are clearly discernable. Our results are listed in Table 3.

Tests were initially run on uncoated lithium niobate disks and damage was found to occur at about 46 MW/cm^2 . Tests were next run on a disk with a ZnS-ThF_4 multilayer coating; in this case damage occurred at about the 54 to 61 MW/cm^2 levels. Disks having ZnS-cryolite multilayer coatings were also found to damage at about 61 MW/cm^2 . The next tests were performed on disks having ZnS-ThF_4 multilayers overcoated with Al_2O_3 . For these overcoated mirrors, the LiNbO_3 damage level increased to $107\text{--}115 \text{ MW/cm}^2$. Tests were also carried out on disks with ZnS-cryolite overcoated coatings, but the Al_2O_3 was not adhering well and the tests were not considered to be valid.

Because of the success of overcoated mirrors in raising the damage level of LiNbO_3 , we coated a LiNbO_3 disk with a quarter-wave layer of Al_2O_3 and tested it. The damage threshold in this case was 150 MW/cm^2 . The success of this experiment prompted us to try a ZnS-ThF_4 multilayer with Al_2O_3 undercoating and overcoating. With this design it was hoped that the undercoating would protect the LiNbO_3 and the overcoating would protect the mirror. On the first test we obtained damage at 86 MW/cm^2 ; on subsequent tests, damage threshold was 150 MW/cm^2 or greater.

We can summarize these results as follows. Uncoated LiNbO_3 is the most susceptible to damage, with a damage threshold of about 46 MW/cm^2 . Any coatings which are used on the LiNbO_3 increase this threshold. ZnS-ThF_4 or ZnS-cryolite multilayers increase it moderately to approximately 60 MW/cm^2 . The use of Al_2O_3 overcoatings and/or undercoatings increases it even further, giving thresholds of 110 to 150 MW/cm^2 .

Before we give data on damage levels of the coatings which were fabricated and tested on this program, it is appropriate to consider the cause of the type of damage of Fig. 39d which we have termed small-spot damage. This type of damage is of particular interest since it occurs at lower power densities than the other types of damage; in the past it has been the major source of damage to ZnS-ThF_4 oscillator coatings. In connection with small-spot damage, we believe that (1) small-spot damage is damage to the top (ZnS) layer of a ZnS-ThF_4 or ZnS-cryolite coating, and (2) the damage is triggered by some change which takes place in this ZnS layer, such as oxidation to form a thin ZnO surface layer.

The experimental evidence which has led us to conclusion (1) is:

- (a) Small-spot damage is seen with both ZnS-ThF_4 and ZnS-cryolite coatings. For both coating types, the top layer is ZnS.
- (b) Small-spot damage is seen in a ZnS-ThF_4 multilayer which has ZnS as the top layer. Small-spot damage is not seen in a similar coating which has ThF_4 as the top layer.
- (c) Small-spot damage is observed in a coating which consists only of a quarter-wave layer of ZnS. Small-spot damage is not observed in a coating which is a quarter-wave layer of ThF_4 .

The experimental evidence which has led us to conclusion (2) is:

- (a) Susceptibility to small-spot damage can be greatly reduced by "scrubbing" the coating with a Q-tip moistened in acetone. Let us suppose that a damage test has just been performed in which substantial small-spot damage has occurred. The results of such a test are shown on line 1 of Fig. 40 where a row of small-spot damage can be seen. In this test, a power density of 76 MW/cm^2 was used on a ZnS-ThF_4 coating. The coating was then cleaned using a drop of acetone on a piece of lens tissue. The damage test was then repeated with the result shown in line 2 of Fig. 40; the damage is essentially the same as in line 1. Finally the coating was scrubbed using a Q-tip wetted with acetone, and the damage test repeated once more. As can be seen in line 3, small spot damage is completely gone (although lithium niobate damage and crater damage did occur). Thus

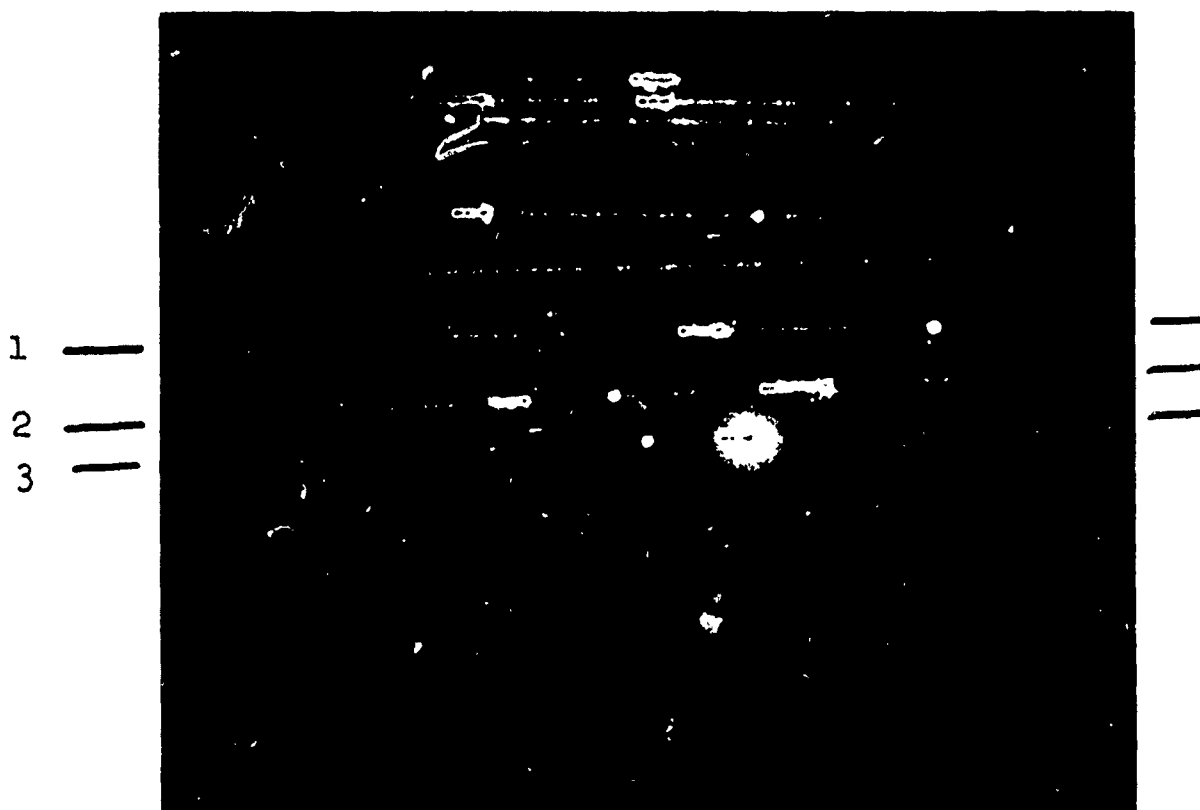


Figure 40 Damage tests performed in order to understand the behavior and cause of small-spot damage.

the Q-tip scrubbing increased the coating's resistance to small-spot damage, indicating that something has been removed from the surface of the top ZnS layer. The possibility that the presence of the acetone is somehow responsible for this effect can be ruled out by the results of lines (2) and (3) which show that light acetone scrubbing does not reduce small-spot damage, but firm acetone scrubbing does.

- (b) If this same coating is now left exposed to air for several days, its susceptibility to small-spot damage will gradually return and the entire cycle can once again be repeated.
- (c) Mirrors which are overcoated with Al_2O_3 do not exhibit small spot damage. With these mirrors, the top ZnS layer has never been exposed to air, being protected instead by Al_2O_3 .

We surmise that perhaps oxidation of the ZnS top layer is responsible for this effect, but there is not yet any conclusive experimental justification. Shalimova, et al¹⁹ have studied the oxidation of thin films of ZnS. They found that after 1 hour at a temperature of $550^\circ\text{--}600^\circ\text{C}$, an oxide film appeared on the surface of a ZnS film. They also found that after 4 hours, a 1 micron thick ZnS film was completely oxidized. We are operating at much lower temperatures, of course, but the possibility still exists that a thin film of ZnO forms on the ZnS surface.

Since ZnS is a widely used coating material, we feel that this effect is of considerable potential importance. Even though we cannot presently state with certainty the cause, we can prescribe several ways of avoiding small-spot damage if a ZnS- ThF_4 or ZnS-cryolite coating is to be used. These are:

- (1) Use an Al_2O_3 overcoating;
- (2) Make the top layer out of the other (non-ZnS) material.

If the top layer must be ZnS for some reason, then:

- (3) Scrub the coating and use it in an inert atmosphere, or simply rescrub the coating repeatedly.

6.4 COATING DAMAGE LEVELS

Damage tests were run on the various types of coatings using the apparatus of Fig. 13. The test conditions were the same as specified in Section 3.4, with the 1.08 micron laser operated in the TEM₀₀ mode. Damage levels for both small-spot damage (Fig. 39 c) and crater damage (Fig. 39 a) were recorded. The damage tests were performed by making a series of 0.100 inch long sweeps across the coating (using the micrometer translators) at successively higher power levels. At each new power level, the mirror holder was translated 0.005 inches vertically. The result appears as a series of lines on the coating showing increasing damage. A typical result is shown in Fig. 41 where damage to a ZnS-cryolite coating is pictured. The numbers along the right-hand edge of the photo denote the average power outputs in mW of the Nd:YA10₃ laser. In Fig. 41, two craters can be seen, one occurring at the 250 mW level and the other at the 400 mW level. The rest of the damage in this photo is small-spot damage.

Small-spot damage was judged to occur when two or three spots could be found in a single line. The density of small-spot damage points increases at higher power levels, and thus one can determine fairly accurately the level at which this type of damage first occurred. Crater damage, on the other hand, is much more random in its occurrence. Sometimes one or two craters will occur at a certain power level, and then no more craters will appear until a considerably higher power level is reached. We have listed the first power level at which crater damage was observed in Table 4. Tests were performed with both fused quartz and lithium niobate substrates, with there being little difference in the results obtained for these two cases.

The data of Table 4 show that with ZnS-ThF₄ and ZnS-cryolite coatings, small spot damage occurred at approximately 38 to 46 MW/cm². When overcoatings of Al₂O₃ were used, no small-spot damage was observed. These results are consistent with our hypothesis that small-spot damage occurs in the top ZnS layer of the coating.

Crater damage occurred in all the Lambda coatings at about 95 to 115 MW/cm². We believe that crater damage represents damage to an intermediate layer of the coating. We conjecture that it is an intermediate layer of ZnS



Figure 41 Typical result obtained from coating damage tests. The coating shown here was ZnS-cryolite on a fused quartz substrate. The magnification of this photograph is 28.

Table IV

Damage Levels of Multilayer Dielectric Coatings

Type of Coating	Power density at which small-spot damage occurred	Power density at which crater damage occurred
ZnS - ThF ₄	38 - 54 MW/cm ²	115 MW/cm ²
ZnS - ThF ₄ overcoated with Al ₂ O ₃	no damage	107 MW/cm ²
ZnS-cryolite	46 - 54 MW/cm ²	96 MW/cm ²
ZnS-cryolite overcoated with Al ₂ O ₃	no damage	115 MW/cm ²
ZnS - ThF ₄ undercoated and overcoated with Al ₂ O ₃	no damage	105 MW/cm ²
Spectrum Systems coatings	< 10 MW/cm ²	< 10 MW/cm ²

which causes this damage. In order to investigate this idea further, damage tests were performed on single quarter-wave layers of ZnS and ThF_4 . No damage of any type was observed with ThF_4 up to 155 MW/cm^2 (our achievable upper limit). Small-spot damage occurred with the ZnS coating beginning at about 62 MW/cm^2 . Thus as also found by Turner⁹, ThF_4 is much more damage resistant than ZnS.

It is difficult, however, to determine exactly the damage threshold for pure ZnS. Our small-spot data (and possibly also Turner's data) probably gives damage levels for ZnO on ZnS rather than for pure ZnS. However it is possible that crater damage levels give this information for ZnS. Since ThF_4 appears to have a high damage threshold, it is likely that intermediate layers of ZnS cause crater damage. If so, then pure ZnS damages at about 100 MW/cm^2 .

The Spectrum Systems coatings damaged at very low power densities, indicating that 1.08 micron absorption was occurring in one or both of the film materials. Perhaps the poor 1.08 micron transmission of Figs. 34 and 35 is partially due to absorption, as well as to reflection. The coatings damaged severely at 10 MW/cm^2 , which was the lowest power density which we tried. Unless this absorption can be reduced to very low levels by further work, this type of mirror will be of no use in our oscillator work.

Section VII

OPTICAL PARAMETRIC OSCILLATOR EXPERIMENTS

Experiments were performed in which internal optical parametric oscillation was obtained using crystals with various types of coatings. The purposes of these experiments were (1) to provide conclusive evidence that the coatings under study were indeed appropriate for oscillator work, and (2) to study the damage characteristics of the coatings in an operating oscillator. Oscillation was obtained near degeneracy (near 2.16 microns) using several different types of coatings, and in the 2.8 to 3.8 micron range using ZnS-ThF₄ coatings. The internal oscillator form is shown in Fig. 2; a photograph of the oscillator is shown in Fig. 42. The laser utilizes a Nd:YAlO₃ rod which is continuously pumped by two tungsten-iodide lamps. The laser is repetitively Q-switched by means of a fused quartz acousto-optic Q-switch. The lithium niobate crystals used were similar to that shown in Fig. 3. Each crystal was approximately 5 mm in length.

7.1 2.16 MICRON OSCILLATOR EXPERIMENTS

Degenerate optical parametric oscillation was obtained from crystals with the following coatings: (a) ZnS-ThF₄; (b) ZnS-ThF₄ overcoated with Al₂O₃; (c) ZnS-cryolite; and (d) ZnS-ThF₄ undercoated and overcoated with Al₂O₃. Oscillation was not achieved with two other crystals. The coatings for the first unsuccessful crystal were ZnS-cryolite overcoated with Al₂O₃. These coatings did not adhere well to the crystal; they began crazing and peeling immediately after they were received from Lambda. The second case in which oscillation could not be achieved was with the Spectrum Systems coatings. Here insertion of the coated crystal inside the laser extinguished it.

The following procedure was used on each of the oscillator tests. The oscillator was run continuously for a minimum of 10 hours. During this time the oscillator components were continually adjusted in order to (1) seek maximum output power, and (2) expose the entire coating area to damage. The crystal was translated a good deal in order to ensure that point (2) was met. The maximum output power was recorded in each case and is listed in Table 5.

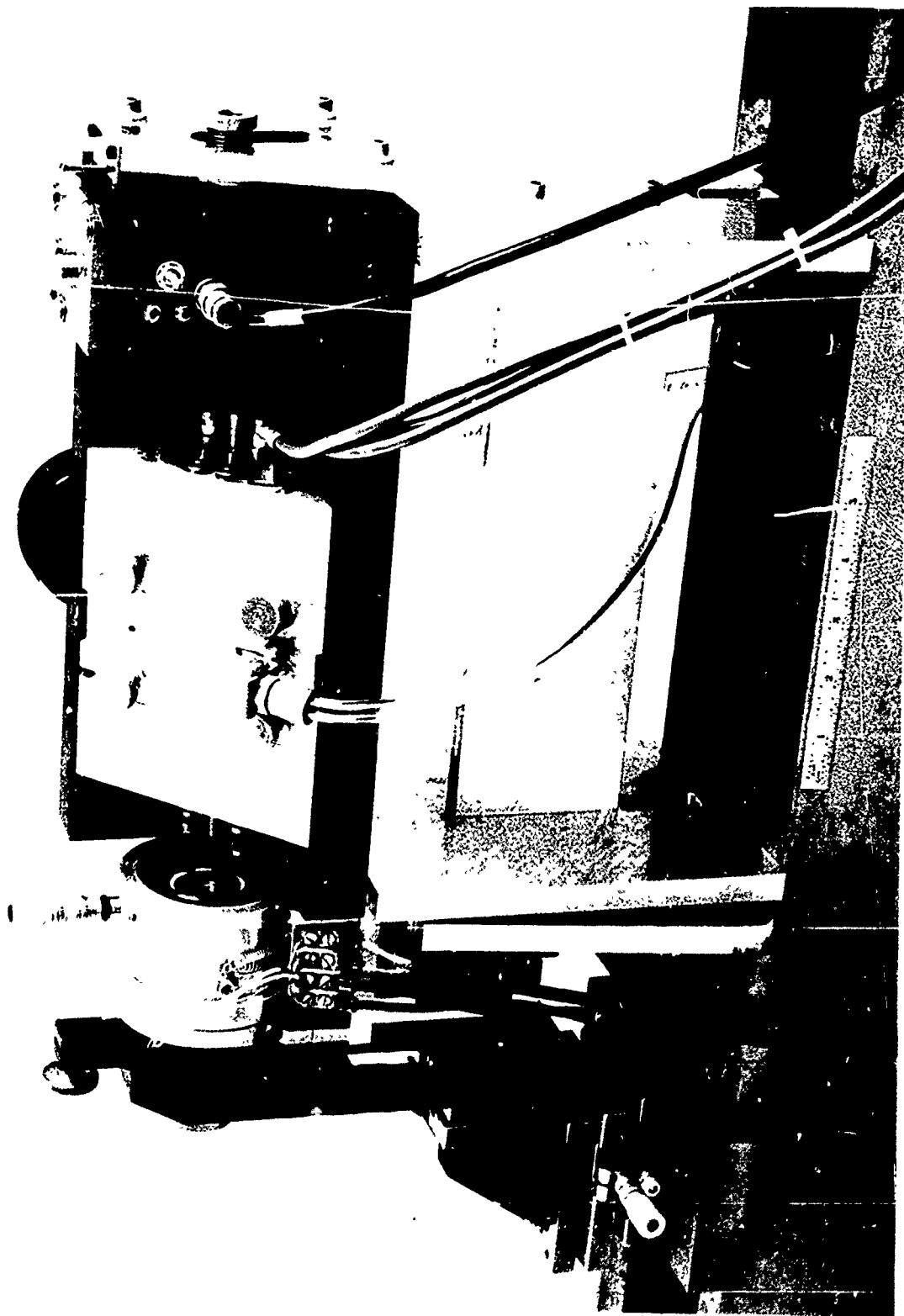


Figure 42 Internal Optical Parametric Oscillator

Table V

Average 2-Micron Oscillator Output Powers Obtained
using Crystals with Various Types of Coatings

Type of coating on crystal	Average 2 micron Output Power
ZnS-ThF ₄	450 mW
ZnS-ThF ₄ overcoated with Al ₂ O ₃	1 watt
ZnS-cryolite	900 mW
ZnS-ThF ₄ undercoated and overcoated with Al ₂ O ₃	940 mW

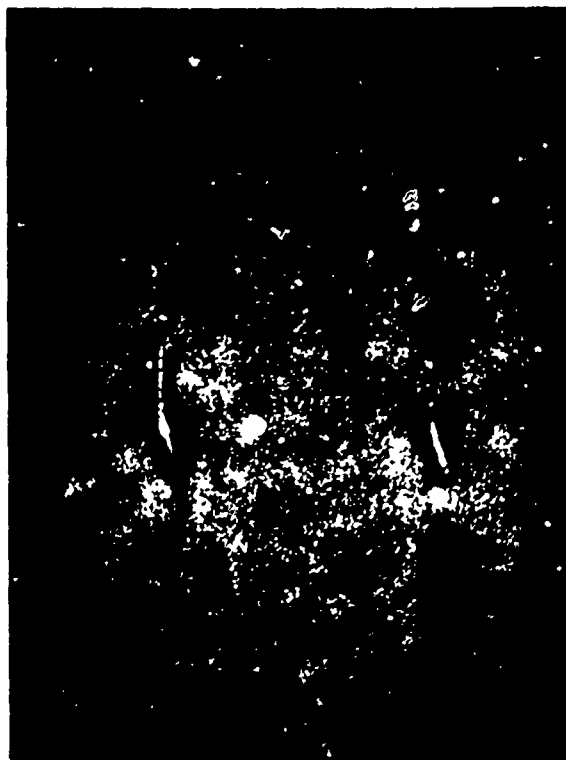
From Table 5 we see that substantial average output powers were obtained with each crystal. In order to establish some sort of reference, we note that 525 mW was the previous best output we had ever achieved under similar circumstances (5 mm long LiNbO_3 crystal, similar laser-cavity configuration). This was obtained about 1 year ago using ZnS-ThF_4 coatings on LiNbO_3 . This value was essentially matched or exceeded in each oscillator experiment of Table 5. The smallest value (450 mW) was obtained with ZnS-ThF_4 mirrors, but the "blame" cannot be ascribed entirely to the mirrors. It is quite possible that some variation in optical quality from crystal to crystal might exist, or simply that the ZnS-ThF_4 oscillator was never adjusted quite as well as the others.

The excellent power outputs of Table 5 attest to the low-scatter character and good spectral transmittances of the various coatings tested. We now discuss how well these coatings fared on the third criteria - resistance to optical damage. We first note that this damage test differed from that of Section 3.4 in at least three important ways. First, in this test signal and idler wavelengths, as well as the pump, were present and could contribute to damage. Secondly, laser operation was in a high-order transverse mode with its attendant hot spots rather than a TEM_{00} mode. A rough calculation shows that the peak 1.08 micron power density inside the laser is about 2 MW/cm^2 . This is undoubtedly low, however, since it considers neither hot spots due to the multimode nature of the beam nor etalon effects due to the presence of the crystal inside the laser. Thirdly, during oscillator tests the LiNbO_3 and its coatings are heated to 100 to 150°C . Damage levels may be somewhat different at these temperatures than at room temperature.

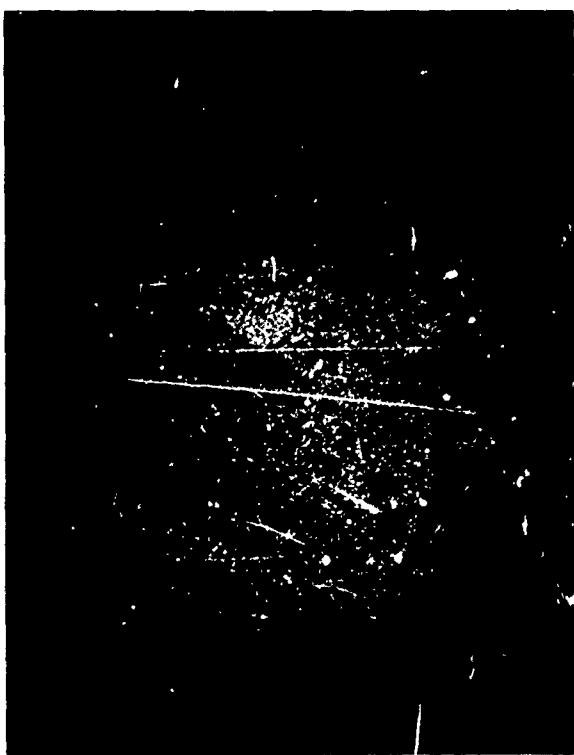
Figure 43a shows photos (28 times magnification) taken of the ZnS-ThF_4 HR coating before and after this oscillator test. It can be seen that extensive small-spot damage occurred over most of the coating area. Moderate crater damage also occurred to both coatings on this crystal. After running this oscillator for 15 hours, there was a fall-off in its output power which is probably due to the rather severe small-spot damage encountered.



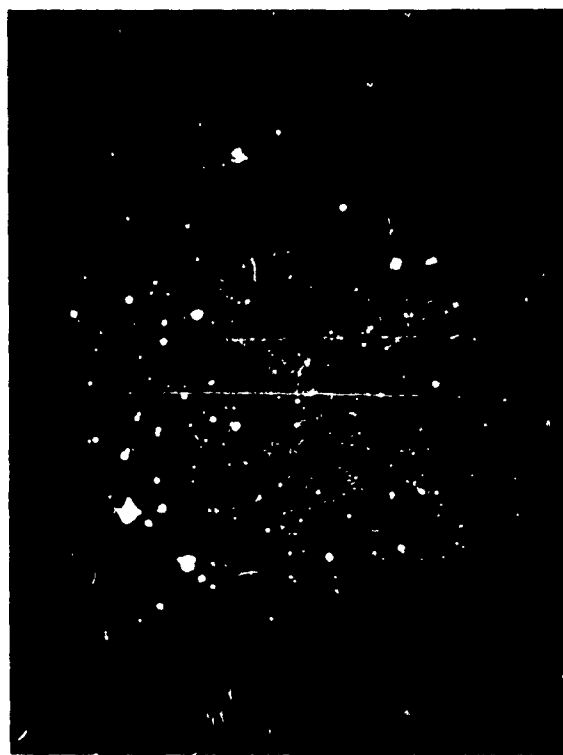
(a) before



(a) after

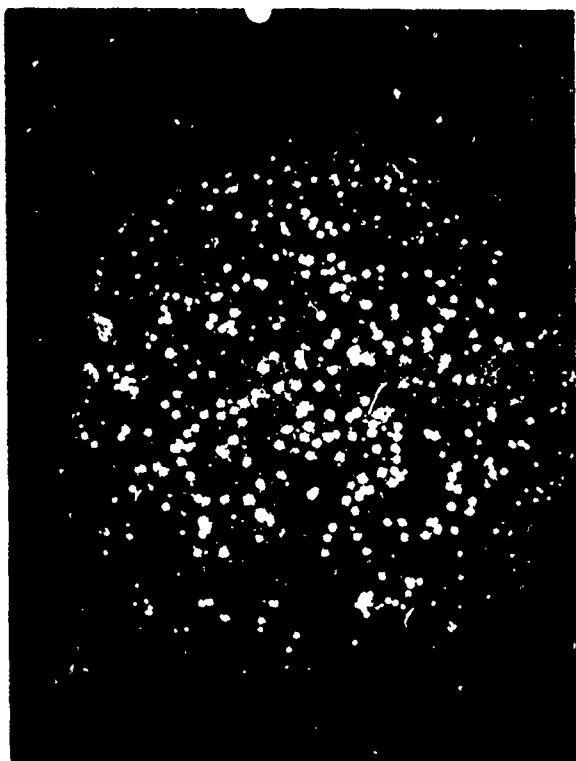


(b) before

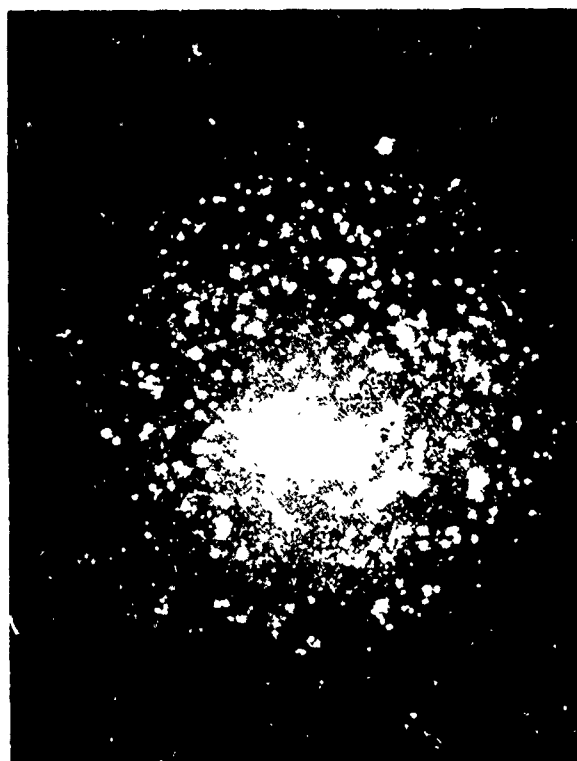


(b) after

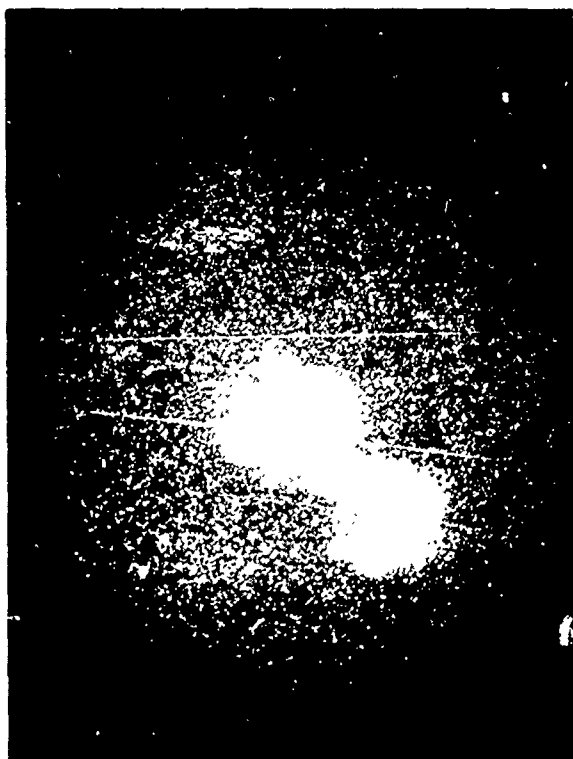
Figure 43 "Before" and "After" Damage photographs for 2-micron HR coatings
a and b of (a) ZnS-ThF_4 ; (b) ZnS-ThF_4 overcoated with Al_2O_3



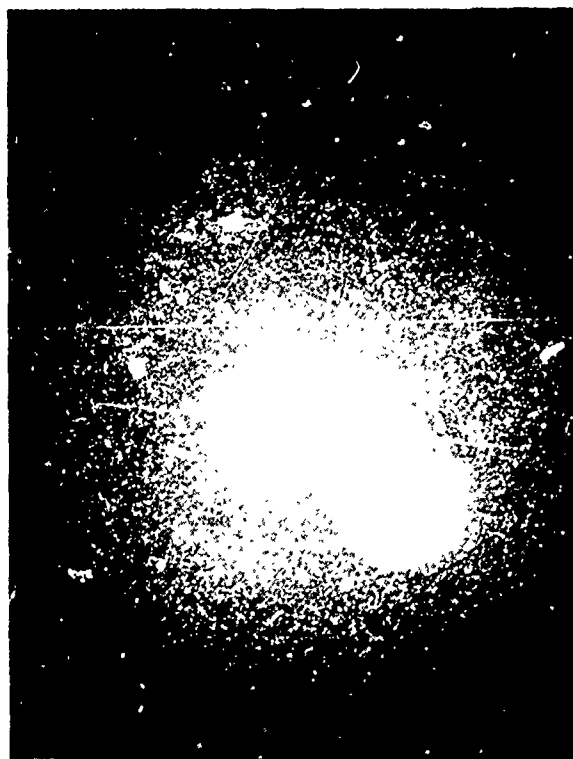
(c) before



(c) after



(d) before



(d) after

Figure 43 "Before" and "After" Damage photographs for 2-micron HR coatings of
 (c) ZnS-cryolite; and (d) ZnS-ThF₄ undercoated and overcoated with
 Al₂O₃.

Figure 43b shows photos taken of the ZnS-ThF_4 coating overcoated with Al_2O_3 before and after parametric oscillation. No small spot damage can be seen indicating that the Al_2O_3 overcoating successfully inhibits its formation. Moderate crater damage is again present, with many of the craters being quite small in size. This indicates that intermediate-layer damage occurred in one of the upper layers in these instances. No degradation in oscillator power output was noticeable during the course of this test.

Figure 43c shows photos taken of the ZnS-cryolite coating before and after oscillator tests. In the before photo, numerous blotches can be seen which appeared sometime during the 4 month period between the arrival of this coating from Lambda and its testing in an oscillator. These blotches were readily visible on the HR coating and very slightly visible on the transmitting coating. (The HR coating is pictured in Fig. 43c.) The blotches probably represent gradual deterioration of the ZnS-cryolite coating through absorption of moisture. We expected that the attainment of oscillation with the coating in this condition would not be possible. Surprisingly, however, the blotches did not adversely affect either the crystal insertion loss nor oscillator performance as evidenced by the 900 mW output which was obtained. The blotches do point up the frailty of this coating, however, compared to ZnS-ThF_4 coatings. Figure 43c shows that moderate small-spot damage occurred. The extent of this small-spot damage was probably reduced by the fact that we had scrubbed the coating prior to this test in an attempt to remove the blotches. Moderate crater damage is also apparent from Fig. 43c.

Before and after photos of the ZnS-ThF_4 undercoated and overcoated with Al_2O_3 are shown in Fig. 43d. From these photos, it can be seen that no small-spot damage occurred and that only minimal crater damage was present. This coating performed the best with respect to damage of the various coatings tried on this program. This type of coating is also satisfactory with respect to its other characteristics and thus appears to be a good choice for oscillator mirrors.

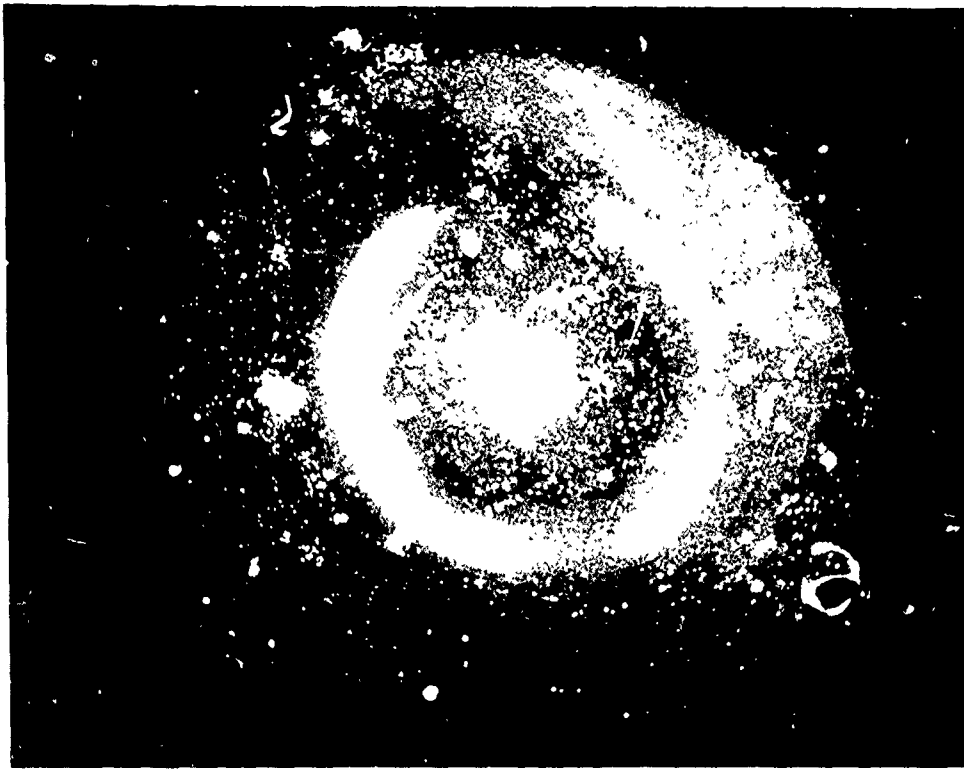
7.2 3 TO 4 MICRON OSCILLATOR EXPERIMENTS

Nondegenerate oscillator experiments were also performed using the setup of Fig. 42 and a 2.5 cm LiNbO_3 crystal with ZnS-ThF_4 singly-resonant coatings. Parametric oscillation was obtained from 2.8 to 3.8 microns, with average output powers ranging from 50 mW to 200 mW.

Before and after damage photos are shown in Fig. 44 for this coating. The coating was scrubbed with a Q-tip moistened with acetone just prior to this experiment in an attempt to minimize small spot damage. This undoubtedly helped, but as can be seen from Fig. 44 moderate small-spot damage and moderate crater damage were present. Thus the coating damage characteristics for the 3 to 4 micron oscillator are similar to those for the 2 micron oscillator. It is of interest to note that in all our oscillator coating-damage experiments, we did not encounter any LiNbO_3 damage. This is not too surprising for the Al_2O_3 over-coated coatings, but is rather surprising for the ZnS -cryolite and ZnS-ThF_4 coatings. It is likely that if somewhat greater pump powers were used, we would begin to encounter LiNbO_3 damage.



before



after

Figure 44 "Before" and "After" Damage photographs of ZnS-ThF_4 coating for 3-micron singly resonant oscillator.

Section VIII

SUMMARY AND RECOMMENDATIONS FOR FURTHER WORK

The goal of this one-year program has been to develop mirrors which are suitable for use with optical parametric oscillators having outputs in the 1.5 to 4.5 micron region. The properties which we have sought for these mirrors are that they (1) have the correct reflectances at signal, idler, and pump wavelengths; (2) have very little scatter; and (3) have high resistance to optical damage. The mirrors which were studied on this program have been designed to be used in a LiNbO_3 parametric oscillator which is pumped by 1.08 microns (Nd:YA10_3).

Several significant results were obtained on this program. These are:

- (1) Several different types of multilayer coatings for parametric oscillator mirrors were studied. These are listed and discussed in more detail below. The most satisfactory mirrors are composed of a ZnS-ThF_4 multilayer which is undercoated and overcoated with single Al_2O_3 layers. The scatter and damage properties of this type of mirror are superior to those of previously available oscillator mirrors. Damage threshold(at 1.08 microns) is approximately 110MW/cm^2 .
- (2) Surface damage studies were performed on coated and uncoated lithium niobate. It was found that the presence of mirrors having Al_2O_3 overcoatings raised the surface-damage threshold of lithium niobate by approximately a factor of three to a value of about 140MW/cm^2 .
- (3) A source of coating damage which occurs when ZnS is the top layer of the coating was identified and studied. Several different methods were found for avoiding this type of damage. This result is important because of the widespread use of ZnS as a coating material. Furthermore this has previously been the main source of damage to oscillator coatings.
- (4) An explanation has been proposed for the much greater scatter present in coatings on lithium niobate than in coatings on fused quartz. We believe that the pyro-electric effect in lithium niobate causes charged dust particles to be attracted to the crystal surface during coating. Electro-static measurements were carried out and techniques suggested for eliminating this source of scatter.

As indicated above, several different types of multilayer coatings were fabricated and tested. These types are listed below along with our comments on each. The tests which were performed on each type of coating included (1) microscopic inspection to determine scatter properties, (2) the running of spectrophotometer traces in order to check spectral transmittances, (3) 1.08 micron damage threshold tests, and (4) the use of the coatings in an optical parametric oscillator. Lambda Optics and Coating, Inc. performed most of the actual coating work on this program as a subcontractor.

ZnS-ThF₄

This is the type of mirror which has predominantly been used in past oscillator work. These mirrors have reasonably low scatter, but there is still some variation in scatter encountered from lot to lot. ThF₄ is believed to be primarily responsible for this scatter. Sections 4.1 and 4.3 describe methods of minimizing this scatter. ZnS and ThF₄ are both well behaved materials during deposition, and hence the spectral characteristics of this type of mirror can be controlled. The primary disadvantage of this type of mirror is its susceptibility to damage. Damage to the top ZnS layer (small-spot damage) is severe while damage to intermediate ZnS layers (crater damage) is moderate.

ZnS-ThF₄ overcoated with Al₂O₃

This type of mirror has the good scatter and spectral characteristics of ZnS-ThF₄ mirrors. Its damage properties are considerably better, however. Damage to the ZnS top layer is completely eliminated by the Al₂O₃ overcoating. Moderate damage to intermediate ZnS layers is still present however. This type of mirror shows all-around good performance.

ZnS-cryolite

This type of mirror has the least scatter of those types tested on this program. Its spectral characteristics are easy to control since ZnS and cryolite are both very well-behaved materials. The damage characteristics are similar to those of ZnS-ThF₄ mirrors; thus severe top-layer ZnS damage and moderate intermediate-layer ZnS damage occur. An additional problem with this coating is its lack of durability. Both constituents are soft and susceptible to moisture. The ZnS-cryolite coating on one end of a LiNbO₃ oscillator crystal had numerous white blotches appear (see Fig. 43c) after five months of storage in a laboratory environment.

ZnS-cryolite overcoated with Al₂O₃

This coating has the low scatter and good spectral properties of ZnS-cryolite coatings. The overcoating should produce improved damage properties, but has not done so yet because of coating adhesion problems. Reasonable adhesion of this coating has been achieved on fused quartz substrates, but very poor adhesion to LiNbO₃. If this adhesion problem were soluble, these coatings might be of some interest.

ZnS-ThF₄ undercoated and overcoated with Al₂O₃

This coating has produced the best performance of those coatings studied on this program. The scatter and spectral properties are good, being again comparable to those of ZnS-ThF₄ coatings. The damage performance is the best of all coatings tested. Top-layer ZnS damage is precluded by the presence of the overcoating, and only slight damage is encountered in intermediate ZnS layers. The presence of the undercoating and overcoating seems to somewhat reduce the intermediate layer ZnS damage compared to that obtained with the overcoating alone. It is recommended that this type of coating be employed with 1-micron-pumped parametric oscillators whenever possible.

Hard coating by Spectrum Systems

The coatings listed above (except for the Al₂O₃ overcoating) are all composed of low melting point materials. Numerous other materials exist which have considerably higher melting points and which are more durable, but they

are also more difficult to deposit. One set of "hard" coatings was tried on this program; this set was fabricated by Spectrum Systems, Inc., but they would not disclose the materials involved.

Several of the general problems which are known to exist with respect to the fabrication of hard coatings did indeed occur. The first was with respect to spectral transmittance of the coatings. Transmission at the pump wavelength of 1.08 microns was only about 50%, rather than the desired 80% or more. In addition, scatter is somewhat worse for this coating than for those coatings already discussed. This is partially because Spectrum Systems heats the substrate to about 260°C during coating; the scatter due to the pyroelectric effect of LiNbO_3 (see Section 4.3) is thus more severe than if the substrates were not heated (as with Lambda's coatings). Finally, 1.08 micron damage occurred at very low power densities in these coatings indicating that absorption was present. These problems are perhaps soluble if considerable additional work is done on this type of coating. Hard coatings such as these hold considerable promise for oscillator applications, but much development remains before this potential is realized.

Measurements were also performed to determine the damage threshold of uncoated and coated LiNbO_3 . It was found that uncoated LiNbO_3 damaged (1.08 microns) at about 45 MW/cm². The presence of ZnS-ThF₄ or ZnS-cryolite coatings raised this to about 60 MW/cm². The presence of a mirror overcoated with Al_2O_3 increased this even further to 120-150 MW/cm². Thus Al_2O_3 overcoatings give protection not only to the coatings, but to the LiNbO_3 substrate as well.

Let us now consider possible fruitful areas for further work in oscillator coatings. The coating which we found to be most suitable consists of ZnS-ThF₄ multilayers overcoated and undercoated with single Al_2O_3 layers. This type of coating works quite well for the present generation of infrared parametric oscillators. As oscillator output powers are increased still further, the limitation which will be reached with this coating will be damage to the intermediate layers of ZnS. There are two different approaches which can be tried in order to overcome this. (1) One can seek a (low-temperature) replacement material for ZnS. This material must be a high-index material and must have good scatter and spectral properties. Two possibilities are zinc selenide

(ZnSe) or ceric oxide (CeO_2). Both of these can be deposited using resistive-heating evaporation, and thus one avoids the various difficulties associated with high-temperature materials. (2) Employ high-temperature materials for the coating. This approach offers the possibility of eventually raising oscillator coating damage thresholds by a factor of 10 or more, whereas approach (1) would probably raise thresholds by a factor of 3 or so. The difficulties are also substantial, of course, but are not insurmountable. Possible thin-film combinations that could be tried with this approach include $\text{ZrO}_2\text{-SiO}_2$ and $\text{TiO}_2\text{-SiO}_2$. In both of these approaches, one would still strive to obtain coatings with low scatter, high damage thresholds, and controllable spectral transmittances.

REFERENCES

1. S. E. Harris, "Tunable Optical Parametric Oscillators," Proc. IEEE, vol. 57, pp. 2096-2113, December 1969.
2. V. R. Costich, "Coatings for 1, 2, Even 3 Wavelengths," Laser Focus, vol. 5, pp. 41-45, November 1969.
3. A. E. Ennos, "Stresses Developed in Optical Film Coatings," Appl. Optics, vol. 5, pp. 51-61, January 1966.
4. Military Standardization Handbook-Optical Design, MIL HDBK-141, Chapter 20, October 1962.
5. D. L. Perry, "Low-Loss Multilayer Dielectric Mirrors," Appl. Optics, vol. 4, pp. 987-991, August 1965.
6. N. Forbes and H. Fraser, "Research on Laser Mirrors," Final report on CVD research project RP1-43, (AD no. AD866277), November 1969.
7. G. D. Boyd and D. A. Kleinman, "Parametric Interaction of Focused Gaussian Light Beams," J. Appl. Phys., vol. 39, pps. 3597-3639, July 1968.
8. H. S. Bennett, "Absorbing Centers in Laser Materials," J. Appl. Phys., vol. 42, pp. 619-630, February 1971.
9. G. N. Steinberg, J. G. Atwood, P. H. Lee, and S. A. Ward, "Research into the Cause of Laser Damage to Optical Components," Perkin-Elmer Final Report PE-TR-7945, February 1965.
10. A. F. Turner, "Ruby Laser Damage Thresholds in Evaporated Thin Films and Multilayer Coatings," Proc. of 1971 Symposium on Damage in Laser Materials, pp. 119-123, November 1971.
11. See for example H. A. Macleod, "Thin-Film Optical Filters," Appendix I, American Elsevier Publishing Co., Inc., New York, N.Y., 1969.
12. W. Heitmann and E. Ritter, "Production and Properties of Vacuum Evaporated Films of Thorium Fluoride," Appl. Opt., vol. 7, pp. 307-309, February 1968.
13. G. Hass, "Filmed Surfaces for Reflecting Optics", J. Opt. Soc Am., vol. 45, pp. 945-952, November 1955.
14. Y. H. Hahn, "Optical Coating for High Power Lasers, "Electro-Optical System Design, pp. 18-19, January 1972.
15. R. Jacobsson and J. O. Martensson, "Evaporated Inhomogeneous Thin Films," Appl. Optics, vol. 5, pp. 29-34, January 1966.

16. S. Fujiwara, "Refractive Indices of Evaporated Cerium Dioxide-Cerium Fluoride Films," J. Opt. Soc. Am., vol. 53, p. 880, July 1963.
17. S. Fujiwara, "Refractive Indices of Evaporated Cerium Fluoride-Zinc Sulfide Films," J. Opt. Soc. Am., vol. 53, pp. 1317-1318, Nov. 1963.
18. H. A. Macleod, "Thin-Film Optical Filters," American Elsevier Publishing Co., Inc., New York, pp. 200-204, 1969.
19. M. Bass and H. H. Barrett, "Avalanche Breakdown and the Probabilistic Nature of Laser Induced Damage," IEEE J. Quant. Electr., vol. QE-8, pp. 338-352, March 1972.
20. K. V. Shalimova, V. A. Lmitriev, and N. M. Satybaev, "Crystal Structure of Zinc Oxide Made by Oxidizing Thin Films of ZnS," Soviet Physics - Crystallography, vol. 15, pp. 167-168, July-Aug. 1970.

UNCLASSIFIED

Security Classification

DOCUMENT CONTROL DATA - R&D		
(Security classification of title, body of abstract and indexing annotation must be entered when the overall report is classified)		
1. ORIGINATING ACTIVITY (Corporate Author) GTE Sylvania, Inc., Electro-Optics Organization Electronic Systems Group, Western Division P.O. Box 188, Mountain View, California 94040		2a. REPORT SECURITY CLASSIFICATION UNCLASSIFIED
		2b. GROUP
3. REPORT TITLE DICHROIC PARAMETRIC MIRROR TECHNIQUES		
4. DESCRIPTIVE NOTES (Type of report and inclusive dates) FINAL TECHNICAL REPORT April 1971 through March 1972		
5. AUTHOR(S) (Last name, first name, initial) Ammann, Eugene O.		
6. REPORT DATE May 1972	7a. TOTAL NO. OF PAGES 133	7b. NO. OF REFS 20
8a. CONTRACT OR GRANT NO. F33615-71-C-1403	8a. ORIGINATOR'S REPORT NUMBER(S)	
b. PROJECT NO. 6100		
c. Task No.: 610003	8b. OTHER REPORT NO(S) (Any other numbers that may be assigned this report) AFAL-TR-72-177	
10. AVAILABILITY/LIMITATION NOTICES Distribution limited to U. S. Government Agencies only, test and evaluation: May 1972. Other requests for this document must be referred to AFAL/TEL, Wright Patterson AFB, Ohio 45433		
11. SUPPLEMENTARY NOTES	12. SPONSORING MILITARY ACTIVITY Air Force Avionics Laboratory (AFAL/TEL) Wright-Patterson AFB, Ohio 45433	
13. ABSTRACT This report summarizes the results of a twelve-month program whose goal was to develop mirrors which are suitable for use with optical parametric oscillators having outputs in the 1.5 to 4.5 micron region. The properties which such mirrors must have are: (1) low scatter; (2) the correct spectral reflectances at signal, idler, and pump wavelengths; and (3) high resistance to optical damage. The mirrors which were studied on this program were designed for use with a lithium niobate parametric oscillator which is pumped by 1.08 microns. Several different types of multilayer coatings were fabricated and tested. These were ZnS-ThF ₄ , ZnS-ThF ₄ overcoated with Al ₂ O ₃ , ZnS-cryolite, ZnS-cryolite overcoated with Al ₂ O ₃ , ZnS-ThF ₄ undercoated and overcoated with Al ₂ O ₃ , and a "hard coating" of unknown composition. The tests which were performed on each coating included (1) microscopic inspection to determine scatter properties, (2) spectrophotometer traces to determine spectral transmittance, (3) 1.08 micron damage threshold tests, and (4) operation of an optical parametric oscillator using the coatings. Best overall results were obtained with mirrors composed of ZnS-ThF ₄ undercoated and overcoated with Al ₂ O ₃ . Measurements were also performed to determine the surface-damage thresholds of uncoated and coated lithium niobate; it was found both soft (e.g. ZnS, ThF ₄ , cryolite, etc.) and hard (e.g. Al ₂ O ₃) coatings raise this threshold, with the greatest improvement effected by the Al ₂ O ₃ coating.		

UNCLASSIFIED

Security Classification

14 KEY WORDS	LINK A		LINK B		LINK C	
	ROLE	WT	ROLE	WT	ROLE	WT
Optical Parametric Oscillator Mirrors 1.5 - 4.5μ region multilayer dielectric coatings ZnS, ThF ₄ , cryolite, Al ₂ O ₃						

INSTRUCTIONS

1. **ORIGINATING ACTIVITY:** Enter the name and address of the contractor, subcontractor, grantee, Department of Defense activity or other organization (*corporate author*) issuing the report.

2a. **REPORT SECURITY CLASSIFICATION:** Enter the overall security classification of the report. Indicate whether "Restricted Data" is included. Marking is to be in accordance with appropriate security regulations.

2b. **GROUP:** Automatic downgrading is specified in DoD Directive 5200.10 and Armed Forces Industrial Manual. Enter the group number. Also, when applicable, show that optional markings have been used for Group 3 and Group 4 as authorized.

3. **REPORT TITLE:** Enter the complete report title in all capital letters. Titles in all cases should be unclassified. If a meaningful title cannot be selected without classification, show title classification in all capitals in parenthesis immediately following the title.

4. **DESCRIPTIVE NOTES:** If appropriate, enter the type of report, e.g., interim, progress, summary, annual, or final. Give the inclusive dates when a specific reporting period is covered.

5. **AUTHOR(S):** Enter the name(s) of author(s) as shown on or in the report. Enter last name, first name, middle initial. If military, show rank and branch of service. The name of the principal author is an absolute minimum requirement.

6. **REPORT DATE:** Enter the date of the report as day, month, year, or month, year. If more than one date appears on the report, use date of publication.

7a. **TOTAL NUMBER OF PAGES:** The total page count should follow normal pagination procedures, i.e., enter the number of pages containing information.

7b. **NUMBER OF REFERENCES:** Enter the total number of references cited in the report.

8a. **CONTRACT OR GRANT NUMBER:** If appropriate, enter the applicable number of the contract or grant under which the report was written.

8b, 8c, & 8d. **PROJECT NUMBER:** Enter the appropriate military department identification, such as project number, subproject number, system numbers, task number, etc.

9a. **ORIGINATOR'S REPORT NUMBER(S):** Enter the official report number by which the document will be identified and controlled by the originating activity. This number must be unique to this report.

9b. **OTHER REPORT NUMBER(S):** If the report has been assigned any other report numbers (*either by the originator or by the sponsor*), also enter this number(s).

10. **AVAILABILITY/LIMITATION NOTICES:** Enter any limitations on further dissemination of the report, other than those

imposed by security classification, using standard statements such as:

- (1) "Qualified requesters may obtain copies of this report from DDC."
- (2) "Foreign announcement and dissemination of this report by DDC is not authorized."
- (3) "U. S. Government agencies may obtain copies of this report directly from DDC. Other qualified DDC users shall request through _____."
- (4) "U. S. military agencies may obtain copies of this report directly from DDC. Other qualified users shall request through _____."
- (5) "All distribution of this report is controlled. Qualified DDC users shall request through _____."

If the report has been furnished to the Office of Technical Services, Department of Commerce, for sale to the public, indicate this fact and enter the price, if known.

11. **SUPPLEMENTARY NOTES:** Use for additional explanatory notes.

12. **SPONSORING MILITARY ACTIVITY:** Enter the name of the departmental project office or laboratory sponsoring (*paying for*) the research and development. Include address.

13. **ABSTRACT:** Enter an abstract giving a brief and factual summary of the document indicative of the report, even though it may also appear elsewhere in the body of the technical report. If additional space is required, a continuation sheet shall be attached.

It is highly desirable that the abstract of classified reports be unclassified. Each paragraph of the abstract shall end with an indication of the military security classification of the information in the paragraph, represented as (TS), (S), (C), or (U).

There is no limitation on the length of the abstract. However, the suggested length is from 150 to 225 words.

14. **KEY WORDS:** Key words are technically meaningful terms or short phrases that characterize a report and may be used as index entries for cataloging the report. Key words must be selected so that no security classification is required. Identifiers, such as equipment model designation, trade name, military project code name, geographic location, may be used as key words but will be followed by an indication of technical context. The assignment of links, rules, and weights is optional.

DISTRIBUTION LIST - FINAL TECHNICAL REPORT

CONTRACT F33615-71-C-1403

<u>COPIES</u>	<u>ACTIVITIES AT WRIGHT-PATTERSON AFB, O 45433</u>
15	AFAL/TEO Attn: Elgene R. Nichols Wright-Patterson AFB, Ohio 45433
1	AFAL/TSR Wright-Patterson AFB, Ohio 45433
1	2750 ABWg/SSL Wright-Patterson AFB, Ohio 45433
1	AFIT/LD (Library) Wright-Patterson AFB, Ohio 45433
1	ASD/OIP Attn: Robert Quayle Wright-Patterson AFB, Ohio 45433
1	AFAL/WRW Attn: Lawrence Baumgardner Wright-Patterson AFB, Ohio 45433
1	AFAL/WRW Attn: John D. MacAulay Wright-Patterson AFB, Ohio 45433
1	ASD/GTG Attn: Richard Durig Wright-Patterson AFB, Ohio 45433
1	ASD/QDF Attn: Craig Bauman Wright-Patterson AFB, Ohio 45433
1	AFML/LPT Wright-Patterson AFB, Ohio 45433
1	AFML/LTE Wright-Patterson AFB, Ohio 45433
1	ASD/QDS Attn: LT Col Joe B. Tyra Wright-Patterson AFB, Ohio 45433

COPIES

ACTIVITIES AT WRIGHT-PATTERSON AFB, OHIO (Cont)

1 AFAL/WRW
Attn: Stan Herr
Wright-Patterson AFB, Ohio 45433

1 AFAL/RSO
Attn: Lt Col Rudzki
Wright-Patterson AFB, Ohio 45433

1 AFAL/WRW
Attn: Charles Hoey
Wright-Patterson AFB, Ohio 45433

OTHER DEPARTMENT OF DEFENSE AGENCIES

COPIES

AIR FORCE

1 AUL (AUL 3T-64-519)
Maxwell AFB, Ala 36112

1 Hq, USAF (SAMID)
Wash, DC 20330

1 DAD (ATT)
Attn: V. L. Reiersen
Eglin AFB, FL 32542

1 AFCRL (OPL)
Attn: Mr. Bradbury
LG Hanscom Field
Bedford, MA 01731

1 Hq, USAFSS (ORL)
San Antonio, TX 78241

1 AFCRL (LP)
Attn: Dr. Howard Schlossburg
LG Hanscom Field
Bedford, MA 01731

1 AFWL (WLZXI)
Attn: Dr. Arthur H. Guenther
Kirtland AFB, NMEX 87117

COPIES

NAVY

- 1 Naval Research Laboratory
Attn: Dr. Herbert Rabin (Code 6510)
Wash, DC 20390
- 1 Director, Office of Naval Research
Department of the Navy
Attn: Dr. W. J. Condell (Code 421)
Arlington, VA 22217
- 1 Commanding Officer and Director
U. S. Navy Electronics Laboratory
Attn: Mr. David K. Forbes (Code 3295)
San Diego, CA 92152
- 1 Naval Research Laboratory
Code 6503 (LTPO)
Attn: Dr. Walter R. Sooy
Wash, DC 20390
- 1 Naval Air Systems Command
Attn: Commander Dennis Glover (AIR 52022)
Wash, DC 20360
- 1 Naval Research Laboratory
Optical Sciences Division
Attn: R. A. Andrews
Wash, DC 20390

COPIES

ARMY

- 1 Office of Chief, Army Research and Development
Department of the Army
3D-442, The Pentagon
Attn: Dr. Robert B. Watson
Wash, DC 20310
- 1 Director
USAEL
HQS USAECOM
Attn: AMSEL-RD-PR
Ft. Monmouth, NJ 07703
- 1 Director
USAEL
HQS USAECOM
Attn: AMSEL-KL-S (Dr. H. Jacobs)
Ft. Monmouth, NJ 07703

COPIESARMY

(Cont)

- 1 Director
USAEL
HQS USAECOM
Attn: AMSEL-RD-PR (Mr. Al Giambalro)
Ft. Monmouth, NJ 07703
- 1 Army Research Office - Durham
Physics Division
Attn: Dr. Robert J. Lontz
Box CM, Duke Station
Durham, NC 27706
- 1 Commanding Officer
Frankford Arsenal
Attn: Mr. M. Schoenfeld (SMUFA-N5300)
Philadelphia, Pa 19137

COPIESOTHER U.S. GOVERNMENT AGENCIES

- 4 Advisory Group on Electron Devices
201 Varick St., 9th Floor
New York, NY 10014
- 1 Director, National Security Agency
Attn: Mr. R. T. Thompson, Jr (R-42)
Fort George G. Mead, MD 20755
- 1 ARPA
Attn: Dr. C. M. Stickley
Wash, DC 20301
- 2 DDC (TISIA-1)
Cameron Station
5010 Duke St
Alexandria, VA 22314

COPIESNON-GOVERNMENT INDIVIDUALS AND ORGANIZATIONS

- 1 California Institute of Technology
Department of Electrical Engineering
Attn: PROFESSOR Ammon Yariv
Pasadena, CA 91103

COPIES NON-GOVERNMENT INDIVIDUALS AND ORGANIZATIONS (Cont)

1	Sanders Associates, Inc Electro-Optics Division Attn: Dr. Charles Naiman 95 Canal St Nashua, NH 03060
1	Hughes Research Laboratories Attn: Dr. Victor Evtuhov 3011 Malibu Canyon Road Malibu, CA 90265
1	Hughes Research Laboratories Attn: Mr. Bernie Soffer 3011 Maliby Canyon Road Maliby, Calif 90265
1	Hughes Aircraft Company Attn: Dr. William Krupke Centinela & Teale St Culver City, CA 90230
1	Chromatix, Inc Attn: Dr. Dick Wallace 1145 Terra Bela Ave Mountain View, CA 94040
1	Stanford University Microwave Laboratory Attn: Professor Robert Byer Stanford, CA 94305
1	Stanford University Microwave Laboratory Attn: Orofessor Steve Harris Stanford, CA 94305
1	Stanford University Microwave Laboratory Attn: Professor Anthony Siegman Stanford, CA 94305
1	Spectra-Physics 1250 W. Middlefield Road Mountain View, CA 94040
1	Martin-Marietta Corp Post Office Box 5837 Orlando, FL 32805

COPIES NON-GOVERNMENT INDIVIDUALS AND ORGANIZATIONS (Cont)

1	Perkin-Elmer Corp Main Avenue Norwalk, CT 06852
1	Honeywell, Inc 2701 4th Ave, South Minneaspais, MN 55408
1	Optical Coating Laboratory, Inc 2789 Giffen Ave Santa Rosa, CA 95403
1	Westinghouse Electric Corp R&D Center Churchill Boroughs Pittsburgh, PA 15235
1	LTV Aerospace Corporation Missile and Space Division Attn: Bob Anderson P.O. Box 6267 Dallas, TX 75222
1	ITEK Corporation Attn: Don Wilmot 10 Maguire Road Lexington, MA 02173
1	Stanford Research Institute Attn: Mgr, Electromagnetic Techniques Lab 333 Ravenswood Ave Menlo Park, CA 94025
1	University of Minnesota Department of Electrical Engineering Attn: Dr. Robert J. Collins Minneapolis, MN 55455
1	University of Michigan Physics Department Attn: Professor Peter A. Franken Ann Arbor, MI 48107
1	Bell Telephone Laboratories Murray Hill, NJ 07971

COPIES

NON-GOVERNMENT INDIVIDUALS & ORGANIZATIONS (Cont)

- 1 Massachusetts Institute of Technology
 Department of Electrical Engineering
 Attn: Dr. Robert H. Rediker
 Lincoln LABORATORIES, Room B286
 Lexington, MA 02173

- 1 Raytheon Company
 Research Division Library
 28 Seyon St
 Waltham, MA 02154

- 1 Coherent Radiation
 Attn: Vern Costich
 3210 Porter Drive
 Palo Alto, CA 94303